GOING OFF THE DEEP END
FISHERY RESERVES AND CONSIDERATIONS FOR THE MANAGEMENT OF DEEP-WATER DEMERSAL FISHES

A DISSERTATION SUBMITTED TO THE GRADUATE DIVISION OF THE UNIVERSITY OF HAWAIʻI AT MĀNOA IN PARTIAL FULFILLMENT OF THE REQUIREMENTS FOR THE DEGREE OF

DOCTOR OF PHILOSOPHY

IN

MARINE BIOLOGY

DECEMBER 2019

BY

Stephen R. Scherrer

Dissertation Committee:

Kevin Weng - Chairperson
Jeffrey Drazen
Anna Neuheimer
Erik Franklin
Eva-Marie Nosal

Keywords: *Pristipomoides filamentosus,* Fishery reserve, Acoustic Telemetry, Tagging, BACIP, Growth

ACKNOWLEDGEMENTS

Thank you to all of the teachers that have inspired, encouraged, and fostered my curiosity.

I would like to thank Dr. Kevin Weng for serving as my advisor on the projects that would ultimately become this dissertation. I am grateful for the opportunities under your tutelage, and for continuing to support my research in spite of the obstacles and challenges involved. I also owe a debt of gratitude to my committee members, Drs. Anna Neuheimer, Jeff Drazen, Erik Franklin, and Eva-Marie Nosal for being generous with their knowledge, experience, and time so that I could succeed in the endeavors this document represents. I am also grateful to Dr. Taylor Chappel for his mentorship and guidance which ultimately lead me to pursue this work.

I am appreciative of Brendan Rideout, Giacomo Giorli, and Donald Kobayashi for their inspiration, insights, and contributions to this work. I am indebted to the captains that assisted in the field components of this research including Jeremy Harden, Kidd Pollock, Craig Yamada, Tom Swenarton, Gary Shirikata, and Mike Abe. In addition to their crew, there was a small army of volunteers including but not limited to Alex Filous, Nick Ciuffetelli, Christian Squire, Keith Kamikawa, Lauren VanWoudenberg, and Astrid Leitner that deserve acknowledgement for their help in the field. Whitlow Au provided access to equipment and facilities used in tank experiments and Ross Barnes and the UH Marine Center assisted with field logistics.

Mahalo to the administrative staffs of the Oceanography department and Marine Biology graduate program, in particular, Anne Lawyer, Phil Repoza and his crew, Catalpa Kong, Kristin Momohara, Lindsay Root, Xuan Tran, Mark Nakamoto, Dodie Lau, Stan Yoshida, and Alexander Shor. Thank you each for your hard work and dedication to our community.

Thanks to the past and present members and associates of the Weng lab, including Gen DelReye, Gadea Perez, Christina Comfort, Andrew Grey, Martin Pedersen, Greg Burgess, and

Dan Crear, for their help in the lab and at sea. Also, thanks to the Franklin and Drazen labs for adopting me and holding me accountable during my orphaned student phase.

Thank you to the State of Hawaii's Division of Aquatic Resources, the Fernando Leonida Memorial Scholarship and the University of Hawaii Graduate Student Organization for funding much of this research and to the department of Oceanography for the opportunity to teach to fill in the gaps.

Finally, thank you to my family and friends for their love and support over the years. To the 2013 graduate cohorts in Marine Biology and Oceanography, the TGs gang, those on the sixth floor of MSB past and present, I am grateful for the friendships forged on this roller coaster. For those friends met outside the University, on kickball fields, at dog parks, in the lineup, and elsewhere, thank you for keeping me grounded and reminding me that the world is greater than graduate school. To Krissy and Lucas Remple, thank you for always being on my team. To my parents, Joann and Fred Scherrer, I am grateful for your endless support and encouragement.

ABSTRACT

Deep-living demersal fishes are an important resource throughout the tropical Indo-Pacific supporting commercial, recreational, and subsistence fisheries. Many of these species are long-living, slow growing, and late to mature making them particularly susceptible to over-exploitation. Effective management of these stocks are imperative to their long-term sustainability. This dissertation addresses the effectiveness of no-take fishery reserves in Hawaii as a strategy for managing these resources. I explore the ways in which we evaluate the appropriate spatial scale for reserves using acoustic telemetry and how these methods differ in deep-water environments. Applying this method to *Pristipomoides filamentosus*, a key species component of Hawaii's bottomfish stock complex, I compare the range of their observed movements to a reserve off of Oahu's eastern shore, finding the scale of movement to be less than a coarse estimate of the available habitat in this, and other reserve areas. Using a database of landings for the commercial fishery, I quantify changes in catch, effort, and fisher participation that have occurred since these areas were enacted and explore how these metrics changed disproportionately in areas where habitat has been protected compared to unrestricted areas of the fishery. Finally, I apply an integrative method for estimating growth, a key parameter for understanding stock dynamics, to *P. filamentosus* using existing datasets and mark-recapture data collected in the early 1990s. Parameters obtained using this method are then compared to previous estimates of growth for this species.

TABLE OF CONTENTS

LIST OF TABLES

Chapter 2

Chapter 3

Chapter 4

Chapter 5

LIST OF CHARTS, GRAPHS, FIGURES, ILLUSTRATIONS, PLATES, AND MAPS

Chapter 2

Chapter 3

Chapter 4

Chapter 5

CHAPTER 1: INTRODUCTION

Fishery reserves as an Instrument of Management Policy

Over the last 60 years, the global fishing fleet has expanded to keep pace with the growing demand for seafood. The harvest of deep-water demersal fish along ocean seafloor slopes are one of several major habitats for fishery exploitation that has fulfilled that demand (Haedrich, Merrett, and Dea, 2001; Morato et al., 2006). Though accounting for less than 9% of the seafloor, the slopes where these fish are found are some of the most dynamic ocean habitats (Gordon, Merrett, and Haedrich, 1995). The rugged complexity of these environments support highly diverse communities of fish (Haedrich, Merrett, and Dea, 2001). While species associated with these habitats may have a broad horizontal distribution, fauna is often stratified vertically and regional assemblages can vary dramatically with changes in depth of a few hundred meters (Haedrich, Merrett, and Dea, 2001).

Many deep-water species are particularly vulnerable to over-exploitation. Deep-living fishes are often characterized by slow growth, delayed maturity, and greater longevity than their shallow-water counterparts (Haight, Kobayashi, and Kawamoto, 1993; Fry, Brewer, and Venables, 2006; Morato et al., 2006; Brodziak et al., 2011; Drazen and Haedrich, 2012; Stephen J. Newman et al., 2016a). Deep-water populations are also often less resilient to exploitation. Stocks with these attributes are often slow to reach compensation with changes in fishing pressure and may require years or decades to recover from over-harvesting (Clark, 2001; Haedrich, Merrett, and Dea, 2001; Norse et al., 2012).

The management of deep-water resources has been criticized for a tendency to lag behind commercial exploitation (Haedrich, Merrett, and Dea, 2001). Methods to directly observe these stocks and verify management outcomes are often costly, labor intensive, and require the use of specialized and expensive equipment (Murphy and Jenkins, 2010). Therefore management decisions and their outcomes often rely on proxies derived from fishery dependent data (ex:

abundance estimated from catch-per-unit-effort (CPUE), size structure determined from landing data, etc.) which may introduce additional uncertainties about the status of the overall population (Haedrich, Merrett, and Dea, 2001; Murphy and Jenkins, 2010; Merritt et al., 2011; Langseth et al., 2018).

Fishery reserves are areas where fishing activities are prohibited. These areas are increasingly being used to manage deep-water fishes and can serve as buffer against management uncertainty (Lauck et al., 1998; Mangel, 2000; A. Williams et al., 2009; Gaines et al., 2010; Alan M. Friedlander et al., 2014; Huvenne et al., 2016; Uehara et al., 2019). Fishery reserves are a subcategory of marine protected area that restrict fishing activities with the explicit goal of reducing fishing pressure on resident fish allowing individuals to live longer and grow larger resulting in increased fecundity (Bohnsack, 1998; Gell and Roberts, 2003; M. A. Hixon, Johnson, and Sogard, 2014). Reserves areas benefit the fishery through increased larval output and the spillover of larger fish to adjacent areas of the fishery (Hilborn et al., 2004; Vandeperre et al., 2011), insulation from fishery-induced evolutionary effects (Hard et al. 2008), and by maintaining the ecosystem roles of targeted species (Leenhardt et al. 2015).

The size of a fishery reserve is critical to achieving desired management outcomes. Successful reserves balance biological, political, and socioeconomic factors (Lundquist and Granek, 2005). Reserves of insufficient size may fail to adequately protect vulnerable populations for the fishery to benefit, while protection at scales too large may negatively impact those fishing communities reliant on the resources, either financially or for sustenance (Kramer and Chapman, 1999; Botsford, Micheli, and Hastings, 2003; Sale et al., 2005, Stewart and Possingham, 2005, Charles and Wilson, 2009). Regular assessment of reserve areas on the fish

and fishing community is therefore key to their success as a management strategy (Pomeroy et al., 2005).

Tagging studies are a popular method for determining the spatial requirements of fishery reserves by resolving the scale over which fish move (M. Heupel, Simpfendorfer, and Lowe, 2005; Murphy and Jenkins, 2010; Crossin et al., 2017). These studies come in two varieties, conventional mark-recapture and telemetry-based studies. Conventional mark-recapture studies require individual fish to be captured at least twice, once where they are marked with a unique identifier and then one or more subsequent times. This provides a coarse estimate of movement potential as well as information on growth and population size (Stickel, 1954; Fabens, 1965; Otis et al., 1978). By contrast, telemetry-based systems can provide detailed long-term movement records without requiring individuals to be recaptured but cannot resolve growth or population size. Passive acoustic telemetry systems consist of a transmitting tag attached to or implanted within an animal and one or more stationary receiver units. Each tag emits a unique acoustic signal into the environment at semi-regular intervals. When a tagged individual is within the detection range of a receiver, the receiver decodes the acoustic signal and logs the tag's unique identifier and the time of detection. By constructing an array from multiple receiver stations, detailed movement histories of multiple tagged individuals can be resolved including movements into or out of fishery reserves (Heupel et al., 2006; Heupel and Webber, 2012).

While acoustic tagging has an established history for evaluating fishery reserves, application of this technology to the depths required for tracking deep-water fish is relatively new and presents novel challenges (Edwards et al., 2019). Methods for designing passive tracking arrays and understanding their performance under these conditions remain underdeveloped (Arnold and Dewar 2001; Heupel et al. 2006a; Grothues 2009; Farmer et al.

2013; Pedersen et al. 2014). Evaluation of this technology as part of this dissertation has revealed unique performance characteristics when deploying these systems to the deeper depths required for tracking bottomfish and other species that dwell in the deep.

The effect of fishery reserves on those that are economically dependent on the fishery is also an important consideration. If the goal of a fishery reserve is to reduce or eliminate fishing mortality, then by definition these areas affect both the stock and the fishing community (Hannesson, 1998; Hilborn et al., 2004). Understanding fisher behavior has been shown to dramatically improve the success of these areas (Wilen et al., 2002). It is therefore important that both fish and fishers are considered when planning and evaluating these areas.

Hawaii's Commercial Deep-Water Handline Fishery

The fishery that has developed around deep-water demersal resources in Hawaii is the region's second largest commercial fishery by value. During the 2017 federal fishing year, Hawaii's commercial fleet landed over 114 tons of bottomfish with an ex-vessel value in excess of $1.65 million (Division of Aquatic Resources, 2019). In addition to being economically important, the fishery also preserves a cultural heritage that predates European contact (Spalding, 2006).

In Hawaii and the U.S. Pacific Territories, management of bottomfish resources is conducted by a partnership of federal and state agencies (Anonymous 2009). The Hawaiian fishery is managed with reference to the "Deep 7", the seven species primarily concentrated on by the fishing industry and representing the highest economic value. The Deep 7 consists of six species of snapper, *Etelis coruscans* (local name: onaga), *Etelis carbunculus* (local name: ehu), *Pristipomoides filamentosus* (local name: opakapaka), *Pristipomoides sieboldii* (local name: kalekale), *Aphareus rutilans* (local name: lehi) *Pristipomoides zonatus* (local name: gindai), and

one endemic grouper, *Epinephelus querns* (local name: hapuupuu) (Hawaii Administrative Rules §13-74-20 - Commercial marine license, 1998).

The use of fishery reserves in this fishery dates back over two and a half decades. Starting with the establishment of the Kahoolawe Island Reserve in 1993, bottomfishing was prohibited up to two miles from the island's shores (Hawaii Administrative Rules §13-261 - Kaho`olawe Island Reserve, 2002). In 1998 managers introduced a network of 19 reserve areas, known as the bottomfish restricted fishing areas (BRFAs), along with annual catch limits to curb the overfishing of bottomfish stock components which had been occurring since at least the late 1980s (Ikehara, 2006). The Northwestern Hawaiian Islands were closed to bottomfishing in 2006 when the Papahānaumokuākea Marine National Monument was established by Presidential Proclamation 8031. Around this time it was determined that the Main Hawaiian Island bottomfish stock remained overfished so in 2007 the BRFAs were restructured to incorporate improved knowledge of preferred bottomfish habitat with a goal of further reducing fishing mortality rates (Moffitt, Kobayashi, and Dinardo, 2006; Western Pacific Regional Fishery Management Council, 2007). In the years that followed, the outlook for Main Hawaiian Island bottomfish improved; since 2010, stock assessments have indicated that the Deep 7 are neither overfished nor is overfishing occurring (Brodziak et al., 2011; Brodziak, Yau, O'Malley, Andrews, Humphreys, DeMartini, et al., 2014a; Langseth et al., 2018). However, little work was done to assess the contribution of the BRFAs to this recovery or address the role of these areas moving forward. This September (2019), four of the BRFAs were reopened to fishing leaving eight areas remaining (Harding, 2019).

Researchers have been tasked by state and federal agencies to assess the effects of the BRFA management system. To date, these efforts have largely taken two approaches, direct

observations and tagging studies. The first has investigated changes in the size and abundance of individuals within the BRFAs since area closures were enacted. The BOTCAM project obtained size measurements using underwater baited stereo video cameras to provide a snapshot of fish present at a given location at the time of sampling. This study found positive changes in the relative size and abundance of bottomfish species within some BRFAs and that these effects declined as distance from reserve boundaries increased (Sackett, Kelley, and Drazen, 2017). These observations are consistent with the BRFAs having a positive effect on bottomfish populations inside the areas.

The second approach has been to quantify the BRFA's ability to retain and thus protect individual fish. The earliest efforts to track bottomfish are represented by The Opakapaka Tagging Project (OTP). Using conventional mark-recapture methods, 4,179 *P. filamentosus* were surgically implanted with streamer tags and released over a 5-year period (1989 – 1995). Over the following 15 years, 439 of the tagged fish were recaptured by OTP researchers, and recreational and commercial fishers, providing the first insight on the scale of movement for the species. Approximately 4.9% of tagged individuals were detected moving between island groups, requiring movement across ocean channels significantly deeper than the depths described by the species' essential fish habitat (EFH), however the majority of fish tagged during this project were recaptured within 1 nautical mile of its tagging location (Oishi, 1994, 1995; Kobayashi, Okamoto, and Oishi, 2008).

Observations from an ongoing mark-recapture tagging study conducted by PIFSC and the Pacific Islands Fishery Group (PIFG) closely resemble those of the OTP study. A preliminary report stated that PIFG fishers had tagged and released 4,571 *P. filamentosus* between 2008 and the 2013. Of those individuals recaptured, 81 fish had records sutable for conducting movement

analysis. Ninety percent of these individuals were recaptured within 10 km of their tagging location. Two individuals were recaptured after having moved inter-island across deep water channels. The greatest movement detected was 61 km over a period of 44 days. While large distance movements are notable, their frequency appears to be rare (O'Malley, 2015).

A handful of acoustic tagging studies have provided insights to the movement behavior of Deep 7 species in Hawaii. Two juvenile *P. filamentosus* tracked in Kaneohe Bay were observed making short-range crepuscular migrations, returning to sites on a daily basis even when displaced after tagging. The purpose of these movements was unknown as they occurred within an environment described as uniform and featureless (Moffitt and Parrish, 1996a). Similar methods were used to assess the movement potential of adult *P. filamentosus* in reference to the Kahoolawe Island Reserve. Movements between protected and non-protected waters and diurnal movement patterns were reported for 32 *P. filamentosus* over 3 years. However the ability to track these fish was limited by the size of the receiver array (3-7 acoustic receivers depending on the year) and by the very short track lengths of tagged fish (0.21 – 5.8 days on average depending on the year) (Ziemann and Kelley, 2004, 2007, 2008). In a separate study, acoustic tracking of *E. carbunculus* (n = 6) and *E. coruscans* (n = 12) found that most individuals spent the majority of their time within the protective boundaries of the BRFA south of the island of Niihau (Weng, 2013).

Fundamental questions regarding the use of BRFAs by bottomfish and bottomfishers remain unanswered. The fine scale movement patterns of commercially exploited species relative to closed area boundaries, and thus the degree of protection provided by these areas to local bottomfish populations, are poorly understood. Of critical importance is to understand if these fish stay within the BRFAs. The effect of the BRFAs on the fishery's catch and effort also

remains largely unquantified. Members of the bottomfish fishing community generally view these areas as ineffective with illegal fishing occurring within the BRFAs (Hospital and Beavers, 2011). Members of this community have stated anecdotally that area closures have forced experienced fishers out of the fishery and required those that remain to fish farther from port and in unfamiliar areas leading to reduced catch while increasing operational costs (Minutes of the 158th meeting of the Western Pacific Regional Fishery Management council, 2013). The primary data used by NOAA to assess the status of the Deep 7 stock are the records of commercial landings reported by fishers as required by the State of Hawaii (Brodziak, Yau, O'Malley, Andrews, Humphreys, DeMartini, et al., 2014a). However, fisher reported catch data may also provide insight on the long-term effects of spatial management both on stock structure and the distribution of fisher catch and effort.

Commercial fisheries targeting deep-water demersal resources have expanded in recent years throughout the Indo-Pacific. Many of these regional fisheries lack the resources and infrastructure to collect important biological information and conduct formal stock assessments (A. J. Williams et al., 2012). A "Robin Hood" approach has been suggested where information from data-rich regions is used to guide the development of research priorities and management strategies for data-limited fisheries (A. J. Williams et al., 2012; Stephen J. Newman et al., 2016b). Extensive work has been done to understand Hawaii's bottomfish resources and many of Hawaii's species are represented in the stock complexes that make up many the resources of these smaller regional fisheries (J J Polovina et al., 1987; Moffitt, 1993; Gaither et al., 2011; Gillett, 2011). Therefore, an improved understanding of the biology, ecology, and management of bottomfish in Hawaii can benefit deep-water demersal fisheries elsewhere in the Indo-Pacific region.

Research Objectives and Dissertation Structure

The overall objective of my dissertation research is to increase our understanding of deep-water fishery reserves as an instrument for managing bottomfish resources. Examining the frequency and scale of movements of *P. filamentosus* relative to the BRFAs will provide decision makers with a clearer understanding of how Hawaiian bottomfish interact with these areas. In the process, the performance of acoustic telemetry systems will be evaluated to show how tag detection differs when these systems are applied in deep-water settings. I will also use fisher reported trip records to quantify changes within the Deep 7 fishery and look for evidence that the BRFAs contributed to these changes through fisher participation and by redistributing patterns of catch and effort.

A secondary objective of my research is to improve parameter estimates available for managers to assess and predict stock trends. While the current stock assessment of this fishery relies on a surplus production model for all Deep 7 bottomfish, there is interest in the use of species-specific, age-structured assessments (Langseth et al., 2018). Holistic growth parameters obtained using integrative methods that more accurately describe observations from mark-recapture work and incorporate them with traditional age and growth studies will improve these data for future stock assessments.

This dissertation comprises six chapters in total, with 4 chapters addressing specific questions to better understand the spatial ecology, biology, and management of bottomfish. **Chapter 1** (this chapter) serves as an introduction and guide to the material that follows. **Chapter 2** addresses the question, “Does acoustic telemetry work in deep water?” The chapter focuses on the performance of passive acoustic telemetry systems in deep-water environments. Prior work suggests that the performance of these systems differs in some environments. In order to properly interpret results from deep-water acoustic tracking experiments, performance under

these conditions must first be quantified. As fishery researchers extend their studies to greater depths, this question will be of increasing interest to this community.

In this chapter, deep-water performance of acoustic telemetry is evaluated with controlled ranging experiments. These experiments are conducted at depths representative of the array design described in Chapter 3 and analysis of detection characteristics are compared between different depth conditions. During deep-water ranging experiments, acoustic receivers reliably fail to detect transmissions from tags co-located or positioned at close range. A geometric spreading model is presented to interpret these results and predict the outcome of a series of validation experiments.

Chapter 3 addresses the questions, "Are fishery reserves an appropriate fisheries management tool for *P. filamentosus?*" and "Are the current BRFAs spatially appropriate in scale for *P. filamentosus*?" I address these questions by analyzing the movements of tagged *P. filamentosus* in and around the BRFA located within the Makapuu region of Oahu, Hawaii. The detection patterns of individual fish observed across the receiver network provide data on the scale of their movement and are used to calculate their home range and the frequency at which they transit between protected and unprotected regions. Metrics for the spatial requirements of the population are compared to the size of the present reserve network. These results provide valuable information regarding the efficacy of spatial protections provided by the BRFA.

Chapter 4 investigates "How have the BRFAs changed fishing patterns and fisher participation?" and looks at how landings of Deep 7 species and patterns of fisher behavior have changed with the introduction and subsequent restructuring of the BRFA network. Using records of commercial landings collected for use in stock assessment, changes in fishing effort, fisher participation, average catch per trip, and total harvest were evaluated for differences

corresponding to changes in management strategy. These metrics are also compared between reporting areas that contain protected habitat and those that did not to understand if and how the fishery responded to the introduction of the BRFAs.

Chapter 5 addresses the questions, "Can we improve growth estimates, a key input to stock assessment?" as well as "Which previous growth parameter estimates are most credible?" This chapter synthesizes prior efforts to quantify growth for *P. filamentosus* across the Hawaiian archipelago and develops an improved set of growth parameters using available data. Von Bertalanffy growth curves are fit to data collected from a mark-recapture experiment conducted by a research team from Hawaii's Division of Aquatic Resources. This data is combined with direct-aging and length-frequency datasets previously used to estimate regional growth for the species. The integrative growth parameters obtained using this method result in smaller variation between expected and observed growth than previously reported parameters.

Finally, **Chapter 6** summarizes and synthesizes the content and implications of the chapters which proceed it. In it, I discuss the successes, failures, and limitations of this collection of work as well as discuss potential directions for future research to further explore and quantify the ideas and themes that have been presented.

CHAPTER 2: DEPTH- AND RANGE-DEPENDENT VARIATION IN THE PERFORMANCE OF AQUATIC TELEMETRY SYSTEMS: UNDERSTANDING AND PREDICTING THE SUCCEPTIBILITY OF ACOUSTIC TAG-RECEIVER PAIRS TO CLOSE PROXIMITY DETECTION INTERFERENCE

Published as Scherrer SR., Rideout BP., Giorli G., Nosal E-M., Weng KC. 2018. Depth- and range-dependent variation in the performance of aquatic telemetry systems: understanding and predicting the susceptibility of acoustic tag–receiver pairs to close proximity detection interference. *PeerJ* 6:e4249. DOI: 10.7717/peerj.4249.

Abstract

Background: Passive acoustic telemetry using coded transmitter tags and stationary receivers is a popular method for tracking movements of aquatic animals. Understanding the performance of these systems is important in array design and in analysis. Close proximity detection interference (CPDI) is a condition where receivers fail to reliably detect tag transmissions. CPDI generally occurs when the tag and receiver are near one another in acoustically reverberant settings. Here we confirm transmission multipaths reflected off the environment arriving at a receiver with sufficient delay relative to the direct signal cause CPDI. We propose a ray-propagation based model to estimate the arrival of energy via multipaths to predict CPDI occurrence, and we show how deeper deployments are particularly susceptible.

Methods: A series of experiments were designed to develop and validate our model. Deep (300 m) and shallow (25 m) ranging experiments were conducted using Vemco V13 acoustic tags and VR2-W receivers. Probabilistic modeling of hourly detections was used to estimate the average distance a tag could be detected. A mechanistic model for predicting the arrival time of multipaths was developed using parameters from these experiments to calculate the direct and multipath path lengths. This model was retroactively applied to the previous ranging experiments to validate CPDI observations. Two additional experiments were designed to validate predictions of CPDI with respect to combinations of deployment depth and distance. Playback of recorded tags in a tank environment was used to confirm multipaths arriving after the receiver's blanking interval cause CPDI effects.

Results: Analysis of empirical data estimated the average maximum detection radius (AMDR), the farthest distance at which 95% of tag transmissions went undetected by receivers, was between 840 and 846 m for the deep ranging experiment across all factor permutations. From these results, CPDI was estimated within a 276.5 m radius of the receiver. These empirical

estimations were consistent with mechanistic model predictions. CPDI affected detection at distances closer than 259–326 m from receivers. AMDR determined from the shallow ranging experiment was between 278 and 290 m with CPDI neither predicted nor observed. Results of validation experiments were consistent with mechanistic model predictions. Finally, we were able to predict detection/nondetection with 95.7% accuracy using the mechanistic model's criterion when simulating transmissions with and without multipaths.

Discussion: Close proximity detection interference results from combinations of depth and distance that produce reflected signals arriving after a receiver's blanking interval has ended. Deployment scenarios resulting in CPDI can be predicted with the proposed mechanistic model. For deeper deployments, sea-surface reflections can produce CPDI conditions, resulting in transmission rejection, regardless of the reflective properties of the seafloor.

Introduction

The past three decades have seen an increase in the popularity of passive tracking of aquatic animals using acoustic telemetry systems (Heupel &Webber, 2012). Due in part to the relatively low cost to acquire large amounts of data, adaptability to a range of taxa, and ease of use by a global community of researchers, these systems are useful for answering a host of ecological questions including those concerning spatial use and management, home range size, migratory behaviors, and mortality rates (Heupel &Webber, 2012; Kessel et al., 2015). Established in 1979, Vemco Ltd. is the market-leading manufacturer of aquatic passive acoustic tracking systems (VEMCO, 2015). Their systems consist of two primary components; a transmitter tag attached to the study organism and a stationary receiver unit which detects coded acoustic transmissions from the tag, indicating the presence of a tagged individual in the detection region of the receiver.

Interpretation of the results of a telemetry study requires knowledge of the receiver's detection region to understand the probability of a transmission's detection across a range of potential depths and distances which a tagged individual may occupy. The passive sonar equation provides a framework for understanding factors affecting detection of transmissions.

$$SL - TL - NL > DT$$

A transmission is likely to be detected when the signal-to-noise ratio of the arriving ping exceeds the receiver's detection threshold (DT). The received level (RL) depends on the source level (SL) and transmission loss (TL), including geometric spreading and attenuation via scattering and absorption. A signal can be detected when the RL exceeds the background noise level (NL) by a level greater than the DT in the frequency range of interest (Urick, 1967). The NL of an environment fluctuates over time, with abiotic, biotic, and anthropogenic sources contributing to environmental background noise. Abiotic sources affecting passive acoustic

telemetry systems include ocean tides and waves, stratification, weather events, and the absorptive and reflective acoustical properties of the environment. Sources of biotic noise include snapping shrimp, mantis shrimp, urchins, some reef fish, and cetaceans (Cagua, Berumen & Tyler, 2013; Gjelland & Hedger, 2013; Kessel et al., 2013; Mathies et al., 2014). For a given signal level, detection probability is generally improved in cases with lower TL and lower NLs.

Propagation conditions, TLs, and NLs differ across sites; therefore, determining the detection characteristics of receivers for every study is critical. A 2013 meta-analysis of321 acoustic tracking studies called for more comprehensive detection range testing and reporting in acoustic tagging studies, finding that only 48.6% of studies reviewed included results from equipment ranging experiments (Kessel et al., 2013). Some of the ways a receiver's effective detection range has been determined include citing previously published studies (Kessel et al., 2013), modeling the effects of environmental parameters based on the study site using tools provided by the manufacturer (Parrish et al., 2015), and empirical range testing involving measurement of tag detections at receivers in conditions similar to the proposed study site (Simpfendorfer, Heupel & Collins, 2008).

A common finding of range testing experiments is that the probability of detecting a transmission decreases with increasing range between a tag and receiver, with the highest probability of detection occurring when tags are at distances closest to the receiver (Simpfendorfer, Heupel & Collins, 2008). However, under some circumstances, detection probabilities for tags in close proximity to the receiver unit can be low, with the peak probability of detection occurring at some intermediate distance from the receiver unit. Kessel et al. (2015) termed this phenomenon "close proximity detection interference," CPDI. The study identified

acoustically reflective environments with strong echoes as particularly susceptible to these effects.

Observations of CPDI have been noted in other acoustic ranging experiments (Beveridge et al., 2012). A cruise report from the Ocean Tracking Network in the Sea of Gibraltar from 2005 describes the effects of CPDI in ranging experiments conducted in the Mediterranean Sea. Six moorings with VR2-Wand VR4 receivers were deployed at depths between 270 and 280 m. Affixed to additional mooring lines placed at various distance from the receiver were Vemco V9, V13, and V16 acoustic tags with output power ranging between 158 and 165 dB. While the depths of tags and receivers are unclear, figures indicate a radial increase in the size of the region impacted by CPDI corresponding to tags with higher power outputs (Beveridge et al., 2012). The positive relationship between the signal strength of tag output and the size of the area affected by CPDI is consistent with expectations from the passive sonar equation.

To understand when and how CPDI occurs, it is helpful to understand the way Vemco tags encode and transmit data and how receivers decode and interpret those transmissions. Each transmission consists of a train of 7-10 rapid high frequency acoustic pings with data encoded in the timing of the intervals between successive pings. The interval between the first two pings, known as the synchronization interval, defines a narrow range of possible coding schemes indicating the tag's model, a range of potential identification numbers, and other associated data. The last interval acts as a checksum used to confirm that a series of detected pings are from a single train of a valid tag. The remainder of the inter-ping intervals encode the tag's unique identifier and any sensor data. Each complete transmission lasts roughly 3 to 5 seconds (Pincock, 2008). On receipt of each ping, the receiver enters a short "blanking interval" period during

which it does not detect additional pings. A blanking interval can have a maximum duration of 260 milliseconds and can be selected by the user during receiver initialization (Figure 2.1). When a receiver unit successfully detects the full ping train, including valid synchronization and checksum intervals, it stores the date, time, tag identification, and data from the tag's environmental sensors (Simpfendorfer, Heupel & Collins, 2008). Acoustic energy in the same operational frequency as the tag that arrives at the receiver after the blanking interval and before

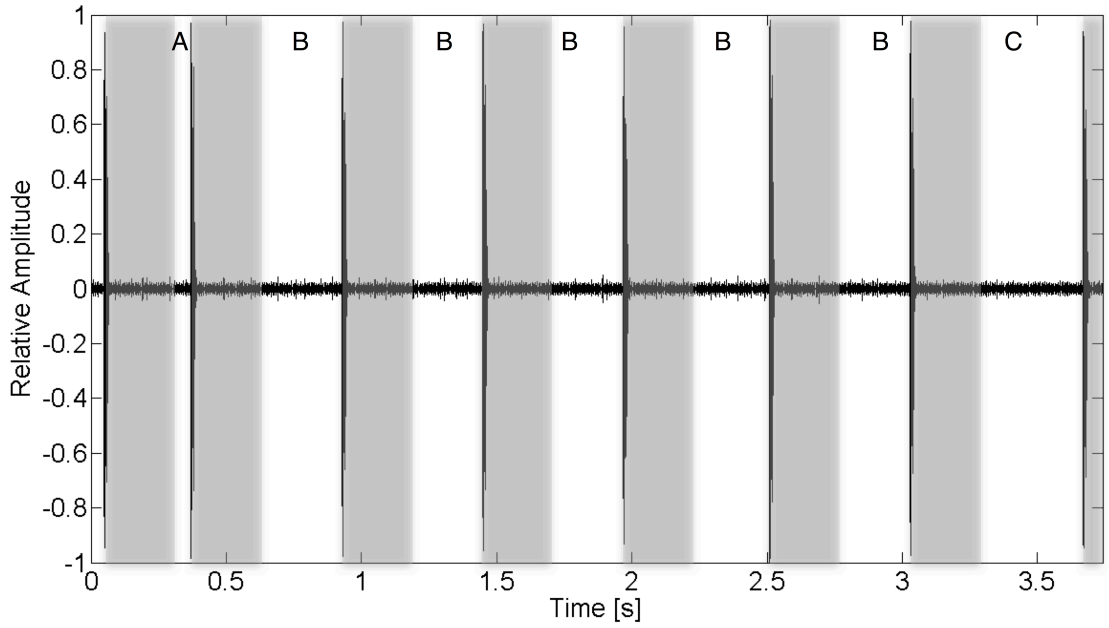

Figure 2.1. Recorded Acoustic Waveform of V13 Tag Transmission Indicating the Function of Various Inter-Ping Interval Regions.

For this tag, a full transmission train is composed of 8 pings. The inter-ping region (A) is the transmission's synchronization interval. (B) regions encode the transmitter's ID. The final interval, (C), is the check sum validation. Grey bars overlaid on the wave form represent a 260 ms blanking interval following the arrival of a ping during which additional acoustic energy arriving at the receiver is ignored. Acoustic energy arriving at the receiver outside of these blanking periods may result in CPDI if the arriving intensity exceeds the detection threshold.

the subsequent ping may result in failure of the receiver to log the detection or accurately record the tag's identifier (Simpfendorfer, Heupel & Collins, 2008; Pincock, 2012).

In this manuscript, we will use the term "multipath" in place of "echo" to refer to arrivals of the signal that have been reflected off the sea surface and/or seafloor, for reasons of clarity and consistency with acoustic terminology. CPDI occurs when a ping's multipath arrives at a receiver during the tag's transmission sequence, outside of a prescribed blanking interval. If the received level of the multipath is sufficiently high, the receiver may misinterpret the multipath as the arrival of the subsequent ping, resulting in rejection of the transmission (Pincock, 2012, Kessel et al., 2015). The arrival time of each multipath can be calculated from the geometry of the relative position of the tag and receiver in an environment, and the sound speed of that environment. As acoustic energy radiates outward from the tag during each transmission, it can arrive at a receiver via the shortest and most direct path as well as by reflecting off one or more surfaces before arriving at the receiver. The paths of the reflected acoustic energy are termed multipaths. The length of multipaths intersecting the position of a receiver are by definition longer than the direct path, having had to reflect off of some interface during propagation. The relative arrival time of each multipath is therefore a function of the length of the direct path, the multipath propagation distance, and the speed of sound, which itself is dependent on the water's pressure, salinity, and temperature (Medwin & Clay, 1998).

Broadly, reflections result when acoustic energy encounters sharp acoustic impedance contrasts such as those occurring between the water and air and (often to a lesser degree) between water and the seafloor. Acoustic energy may arrive at a receiver having been reflected one or more times off such interfaces. For fixed tag-receiver pair depths, the path length difference (hence relative multipath arrival time difference) between direct and multipath arrivals

decreases as the range between tag and receiver increases (Figure 2.2). Consequently, increasing tag-receiver separation decreases the number of multipaths arriving after the receiver's blanking interval, decreasing the likelihood of transmission rejection. Furthermore, the intensity of the reflected signal is attenuated during propagation, with signal strength inversely related to multipath length, resulting in such a point that the intensity of the received signal is no longer exceeds the receiver's detection threshold. This explains why effects of CPDI are most pronounced at close ranges and only under certain (e.g. reverberant environment) deployment conditions. The goal of the present study is to construct and validate a mechanistic model for CPDI which simulates multipath arrival under various deployment scenarios and can be used to understand and predict when transmission detection may be affected by CPDI. Prior models have been developed to explain the inverse relationship of detection probability and distance (How & de Lestang, 2012; Gjelland & Hedger, 2013) but no other model has considered CPDI. We propose a simple position-based mechanistic CPDI model based on the time delay between direct path transmission and reflected (multipath) arrivals. Our model is based on the hypothesis that a multipath from a tag ping reflected off the sea surface and/or seafloor, arriving after the receiver's blanking interval with sufficient energy for detection, will cause the receiver to reject the transmission. The purpose of our proposed mechanistic model is to predict when CPDI may result in the rejection of tag transmissions for a given environment and receiver position using parameters commonly derived during equipment ranging experiments. This will allow future studies to use their own range test results to select deployment configurations that mitigate CPDI conditions.

Our model identifies deployment depth as an important factor contributing to CPDI. Consider the simplest case of the arrival of transmission energy along the direct path and the first

multipath reflected off the sea surface in an environment with a uniform sound speed (sound speed is constant across all water depths) where arrival time is directly related to propagation distance of the direct and multipath. When the water surface is smooth, the sea-surface acts as a near perfect reflector with virtually no transmission loss (Urick, 1967). In the case of a sufficiently shallow receiver and tag, the difference in the arrival time of acoustic energy along the direct and surface reflected multipath is less than the receiver's blanking interval (Figure 2.3A). The multipath arrives during the receiver's blanking interval and does not interfere with

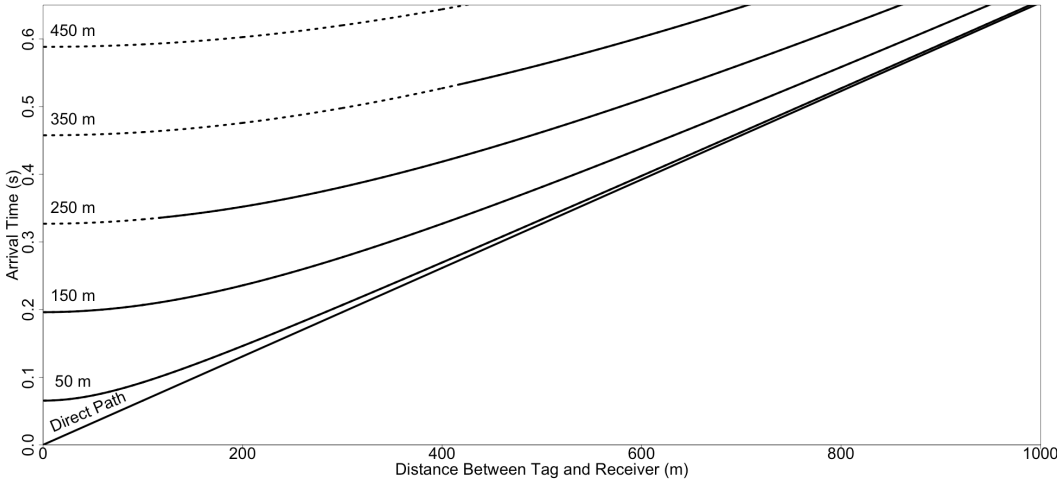

Figure 2.2. Simulated Arrival Times for a Transmission Between a Tag and Receiver as a Function of Depth and Distance.

Arrival time of the direct and first surface reflected multipath. Arrival times were simulated in 100 m increments for depths between 50 and 450 m, with both tag and receiver positioned at the same depth, a fixed sound speed of 1,530 m/s, and an unconstrained (infinite) average maximum detection distance. Dashed lines represent positions of tags and receivers where the arrival of the first surface reflected multipath is predicted to result in CPDI for a receiver with a blanking interval lasting 260 ms. For each depth, as the distance between the receiver and tag increases, the relative arrival time of acoustic energy along the direct path and the first surface reflected multipath converge. CPDI occurs until the point at which the relative arrival time no longer exceeds the blanking interval.

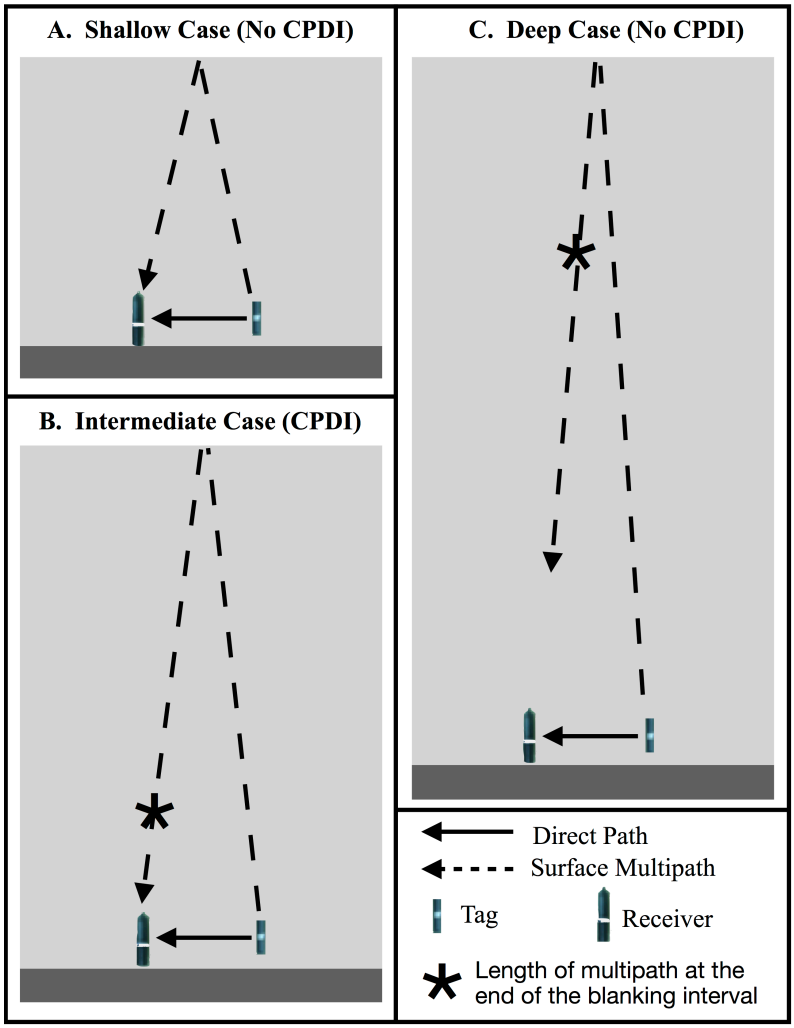

Figure 2.3. Schematic Showing the CPDI Outcome of Direct and Surface Reflected Multipath Arrivals as a Function of Depth.

In the simplified scenario considering only the direct and surface reflected multipath, (A) when receiver and tag are sufficiently shallow that the multipath arrives before the conclusion of the blanking interval, the multipath does not result in CPDI. (B) At intermediate depths, the multipath arrives at the receiver following the end of the receiver's blanking interval, producing CPDI. (C) In environments of sufficiently deep depth, where the path length of the surface reflected multipath is greater than the maximum distance the receiver can detect a tag, the reflected multipath does not arrive with sufficient intensity, and does not result in CPDI.

the transmission. Holding the horizontal distance between receiver and tag fixed while increasing their depth increases the arrival time difference between the direct and surface-reflected arrival. At sufficient tag/receiver depths, the surface reflection will arrive after the blanking interval (Figure 2.3B). When this happens, the receiver may conflate the reflection for the next ping in the transmission resulting in CPDI. Further increasing the depth of the tag and receiver will eventually lead to the point at which the propagation distance for the surface reflection is long enough (i.e. transmission losses are high enough) that the surface reflection is no longer detectable (Figure 2.3C). When this occurs, the reflected ping is not detected by the receiver and CPDI does not occur. This needs to be a consideration as the number of acoustic tracking studies taking place in deeper environments grows.

With this study we conducted a series of sequential experiments building on the results of one another to answer the following questions: How does the shape of the detection function differ between receivers that experience CPDI and those that do not? What causes CPDI? Can we accurately predict where CPDI will occur? How does depth contribute to the CPDI phenomena and what depths are most susceptible?

Materials and Methods

Summary

We performed a series of five experiments which incrementally build on the results of the prior to construct and validate our mechanistic CPDI model. The goal of the first experiment was to determine the range of distances from a receiver at which tags could be detected in a deep-water environment (300 m). The observation of CPDI in the results of this experiment led us to conduct a second range test in a shallow water setting (25 m) to determine if CPDI effects persisted. From observations of the presence/absence of CPDI in experiments 1 and 2, we developed the mechanistic model for predicting CPDI using a simplified straight-line ray-

propagation model where direct and multipath arrivals are modeled as a function of sound speed, water depth, and relative receiver and tag positions. We initialized our mechanistic model with similar conditions from the results of experiments 1 and 2 and compared the respective presence

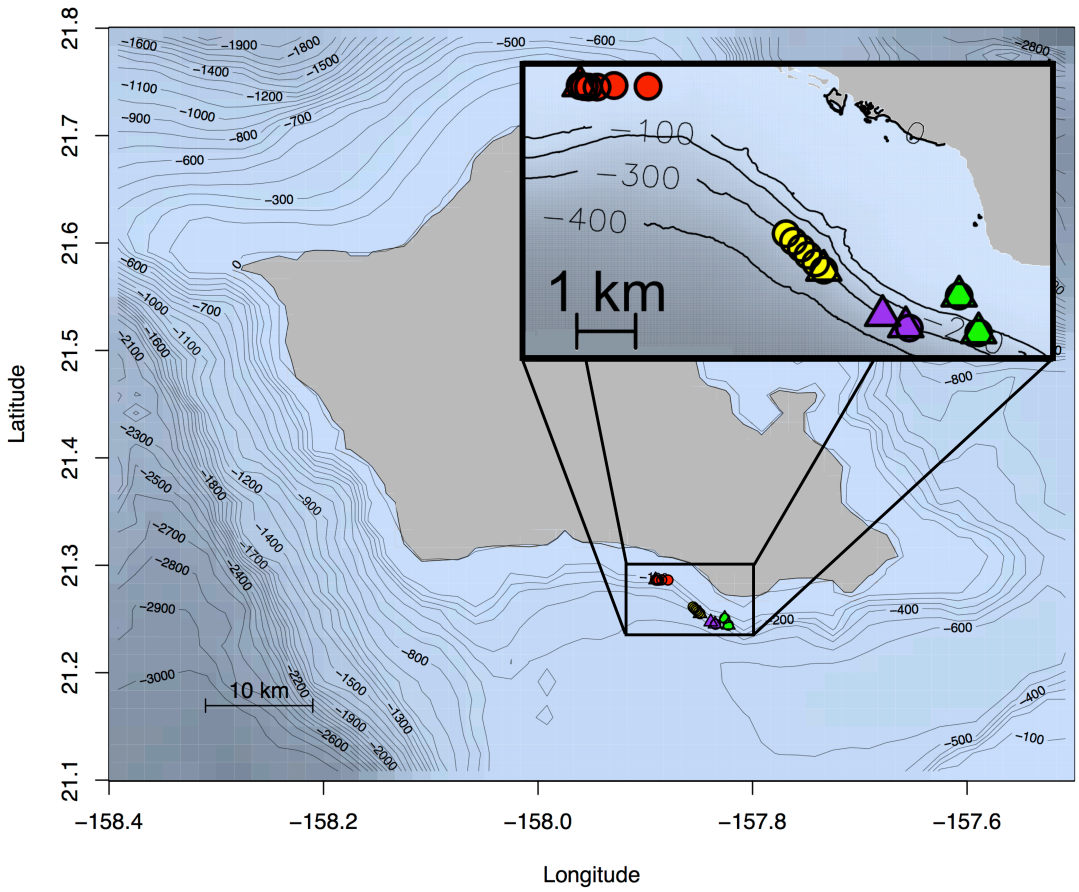

Figure 2.4. Map of Oahu, Hawai`i Depicting the Location of Experiments 1-4.

The location of each of the four field experiments conducted off the south shore of the island of Oahu, Hawaii. Receiver locations are indicated by triangles and tag locations with circles. Color corresponds to 1 of the 4 experiments with yellow showing the location of the deep water ranging experiment (experiment 1), red showing the location of the shallow water ranging experiment (experiment 2), the depth dependent model validation experiment (experiment 3) in green, and the depth and distance validation experiment (experiment 4) in purple.

and absence of CPDI during these experiments to the mechanistic model's predictions. We then developed two further field experiments comparing CPDI observations with the mechanistic model's predictions. Finally, we used playback of a recorded acoustic tag transmission in a controlled tank setting to confirm the hypothesis that arrivals occurring after the blanking interval result in missed detections (hence CPDI). The location of each of the four field experiments is shown in figure 2.4. Each experiment is described individually in greater detail in the sections that follow.

Acoustic Telemetry System and Generalized Performance Analysis

Following the work outlined by Kessel et al (2015), Vemco VR2-W acoustic receivers were used for all experiments. After each experiment, detection logs (with detection time and tag id for all ping train transmissions detections) were downloaded from each receiver using Vemco's VUE database application and exported as CSV files for further analysis in R (R Core Team, 2014). Except where noted, all experiments used Vemco V13 acoustic tags (69 kHz, 153 dB re 1 uPa @ 1 m) with a variable transmission interval (the time between subsequent ping train transmissions) ranging between 30 and 90 seconds (60 second nominal transmission interval).

At a glance, the number of detected tag transmissions is significantly lower than would be expected during the first two ranging experiments. This is due to the number of tags used during these experiments and their transmission interval. As the number of tags with variable transmission intervals which are detectable by a receiver increases, so too does the probability that individual transmissions from two or more tags will overlap. When this occurs, the receiver will reject both transmissions. Therefore, when multiple tags are within the detection range of a receiver, even when transmissions were theoretically detectable on their own, the realized number of detections will be less than the total number of transmissions sent by all tags. This

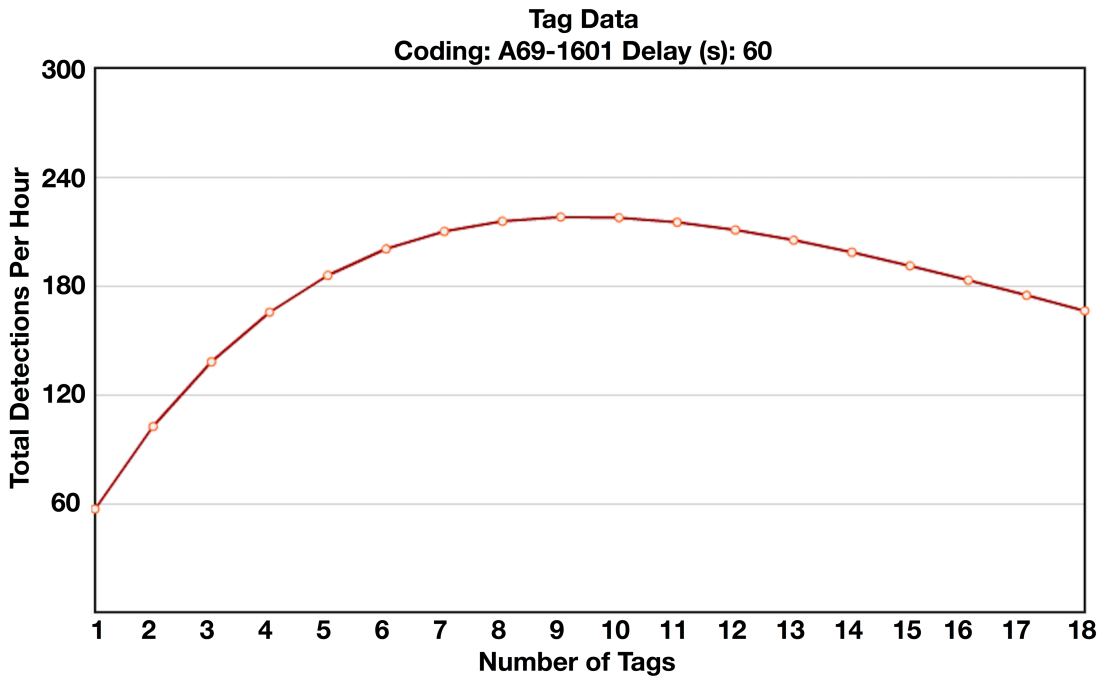

Figure 2.5. Vemco Collision Calculator Results.

Vemco Collision Calculator results showing the expected number of total detections recorded by a receiver per hour as a function of the number of tags present (Vemco, 2017). As the number of tags detectable by the receiver increases, the probability of overlapping transmissions from multiple tags increases, leading to the rejection of both transmissions. Results shown are for tags with A69-1601 coding scheme and a 60 second nominal delay, the same parameters used in experiments 1-3.

problem is exacerbated when the transmission interval of tags is short, further depressing the number of transmissions detected. For this reason, we present the number of total detections logged by receivers during each hour of the experiment without standardizing values by average number of detections sent per hour as this would be dependent on the exact detection characteristics during each transmission. Vemco's website provides a collision calculator for estimating the expected number of detectable transmissions when a number of tags with similar

transmission parameters are within detection range of a receiver, the results of which we have provided for reference (Figure 2.5).

Experiment 1: Quantifying Detection Range in Deep Water: ***7 June – 16 June 2014***

A ranging experiment was initially conducted to quantify detection probability at various distances from a receiver for a tracking study investigating the movements of a Hawaiian deep-water demersal snapper. The experiment occurred offshore of the Diamond Head crater on the south shore of Oahu. This area was selected as a study site for its accessibility, moderate slope, and similarity to a nearby site involved in other ongoing passive telemetry work. It features a protruding flat shallow shelf between 0 and 100 m extending approximately 1.8 km offshore and terminating with a moderate slope to 700 m over a distance of 5 km into the Kaiwi channel between the islands of Oahu and Molokai (Johnson & Potemra, 2011).

Three receivers were deployed from the R/V Ho'okele in 300 m depth. Receivers were suspended 1, 15 and 30 m from the seafloor on a single mooring using trawling floats, 80 kg of concrete, a polypropylene line, and an acoustic release (LRT, Sonardyne, Yateley, UK). Acoustic tags were moored in a similar manner at 1 and 15 m above the seafloor at ranges spaced by approximately 200 m from 0 to 1000 m (Figure 2.6A). Equipment was recovered 13 days after deployment by activating the acoustic releases. Due to a battery failure in the receiver positioned 15 m off the seafloor, only data from the receivers positioned 1 m and 30 m above the seafloor was recovered.

A transmission's detection probability across the full range of the study was estimated using a generalized additive model (GAM) to explain the number of hourly transmissions detected for each tag and receiver pair as a function of the distance between tags and receivers

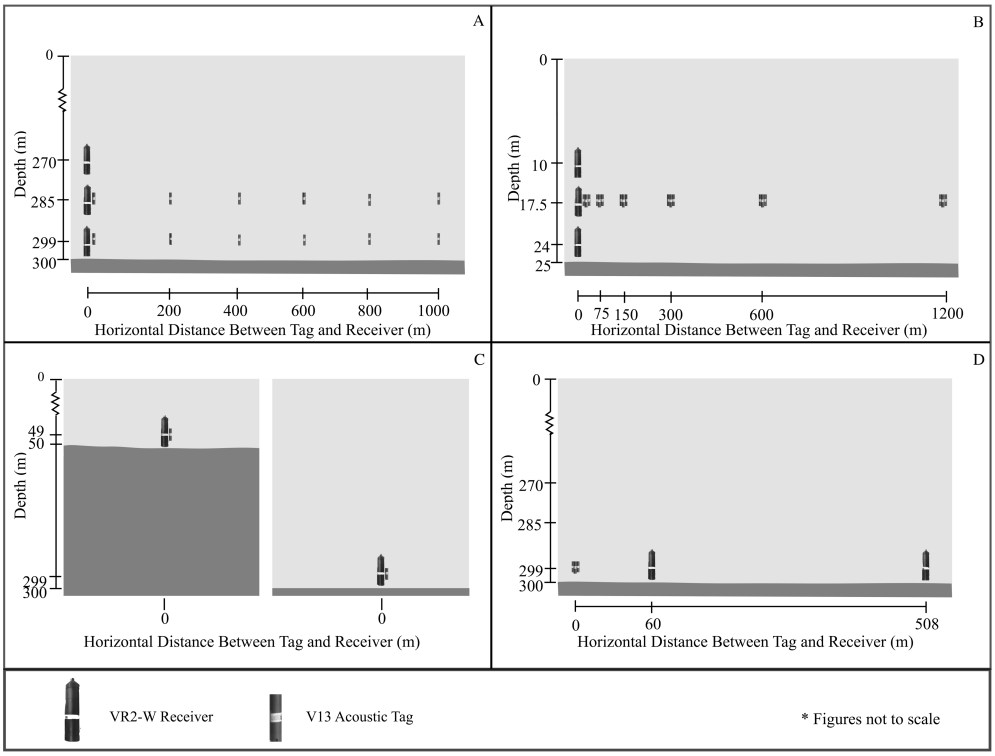

Figure 2.6. Design of Experiments 1-4.

(A) Setup of the first component's deep-water ranging experiment was designed to determine AMDR and CPDI extent for a deep-water environment. The battery for the receiver positioned 15 m above the seafloor failed resulting in detection records from the receivers 1 and 30 m above the seafloor only. (B) Setup of the second component's shallow water ranging experiment, designed to determine AMDR and investigate CPDI in a shallow water setting. (C) The third component's depth dependent validation experiment was conceived to validate the predictions of CPDI provided by the mechanistic model with two receiver and tag pairs at different depths. The mechanistic model predicted the effects of CPDI observed by the deeper receiver while no CPDI was predicted for the shallower receiver. (D) The third component's depth and distance validation experiment was again designed to test the predictive capabilities of the mechanistic model. Two VR2-W receivers were deployed at distances from three acoustic tags. The mechanistic model predicted the receiver closer to the tags but within range of the CPDI affected region would detect fewer transmissions than a receiver farther away and outside the CPDI affected region.

and the height of the receiver relative to the seafloor, as well as a number of random factors identified by other studies to affect detection distance, using a Poisson distribution to model the error distribution. Random effect variables included mean hourly wind speed and mean hourly wind gust (from NOAA buoy #161234), hourly tide height and hourly tide direction data (from NOAA tide station #1612340), and diurnal period, with periods divided into day (6 am to 6 pm) or night (6 pm to 6 am). GAMs were fit using the Mixed GAM Computational Vehicle (mgcv) package in R (Wood, 2011). From GAM results, the number of transmissions detected was predicted for all distances up to the maximum tag range in 1 m increments and then used to determine AMDR and the extent of the area from the receiver affected by CPDI. The distance variable was fit with a penalized regression spline smoother, selected to reduce the potential of overfitting the data when estimating the number of detections between sampled ranges. The largest appropriate basis dimension, 6, was selected for the smoother argument to minimize the underfitting bias of the region closest to the receiver, where CPDI has the potential to occur, by detections from tags at ranges unaffected by CPDI. All random effects were fit with a ridge penalized smoother and the value of the basis term for each was assessed for statistical appropriateness.

From the resulting global GAM, candidate GAMs consisting of all possible permutations of independent explanatory variables were compared to determine the best fit models using Akaike's information criterion (AIC). Candidate models within two AIC units of the best fit GAM were used to estimate AMDR and CPDI extent. The number of expected hourly detections across the range of potential tag locations for each combination of explanatory factors were predicted using each GAM using median values for wind speed, wind gust, water level, and incoming/outgoing tides during both day and night periods. Predicted hourly detections were

then used to determine AMDR and presence/extent of CPDI. AMDR was defined as the distance at which the number of predicted detections fell below a threshold of 5% of detections sent. In practice, this occurred when there were fewer than three predicted detections per hour. We then constructed a range including standard error around this value by also predicting the standard error values at each predicted distance and then adding and subtracting the error from our model fit. We then calculated a range inclusive of the standard error as the distance where each of our predictions incorporating the error term fell below our 5% threshold as a measure of the model's fit. CPDI was said to affect the range from the receiver to the distance at which the predicted number of detections and their standard error first overlapped the maximum predicted value and its standard error. At this point we could be 95% confident the predicted values no longer statistically differed.

Experiment 2: Quantifying Detection Range in Shallow Water: ***22 November – 2 December 2014***

A second experiment was designed to determine the relationship between detection probability and horizontal distance in a shallow setting, and to explore whether CPDI is present in this setting. A field site was selected off Sand Island, immediately west of the Honolulu Harbor channel. Characterized by a loose sand substrate and sparse coral rubble, this location was selected for accessibility to a relatively linear swath of 25 m isobath, water properties presumed similar to the deep water ranging experiment site due to their geographic proximity, and a standing agreement between the University of Hawaii and Hawaii's Department of Aquatic Resources for use of the area for research purposes.

Nine Vemco VR2-W units were deployed on a single mooring from the R/V Ho'oponopono. The mooring design used was similar to the one employed in the deep-water ranging experiment except that the polypropylene line was reinforced with a 1/8" braided steel

cable and acoustic releases were not used. The nine receivers were suspended in groups of three at 1 m, 7.5 m, and 15 m above the seafloor. Eighteen acoustic tags were affixed 7.5 m from the seafloor, in groups of three, spaced at approximate horizontal distances of 0, 75, 150, 300, 600 and 1200 m from the receivers, as measured by GPS during each mooring deployment (Figure 2.6B).

Following deployment, divers descended on the receiver mooring to assess equipment condition and measure the bottom depth which was found to be 25 m using a dive computer (Zoop, Suunto, Vantaa, Finland). Bottom depth was measured using the same dive computer during recovery of the tag moorings which ranged between 23.8 m and 25.3 m. The same process for determining AMDR and CPDI extent was performed for data from this shallow water ranging experiment as was done during the deep-water ranging experiment.

Development of a Mechanistic Model for Predicting CPDI

The proposed mechanistic CPDI model uses a depth and range-independent sound speed (i.e. straight-line acoustic propagation), relative positions of the receiver and tag, water depth at the receiver, the duration of the receiver's blanking interval, and AMDR determined from ranging experiments to calculate the path length of direct and multipath arrivals for a grid of potential tag position (Figure 2.7). All direct and multipath arrivals with a path length less than or equal to the AMDR are considered by the model. Our model assumes that the only factor affecting detection of acoustic energy by the receiver is the length of the propagation path. Our model does not account for scattering and reflective losses at the surface and seafloor (i.e., we assume transmission losses are equal for equal path lengths regardless of propagation path). Since some energy loss is always suffered on reflection, this approach considers the multipath arrivals that in practice may not be detectable by the receiver. This results in the potential for falsely predicting

CPDI observations where they may not be present in an experimental setting, resulting in a more conservative model with predictions of a "worst-case scenario" situation. However, when surface conditions are calm, transmission losses at the sea surface are nominal (Urick, 1967). Our model also cannot account for minor variation in tag output as a result of tolerances in Vemco's manufacturing process. Implementations of our model, in both R and Matlab, are provided as supplemental material.

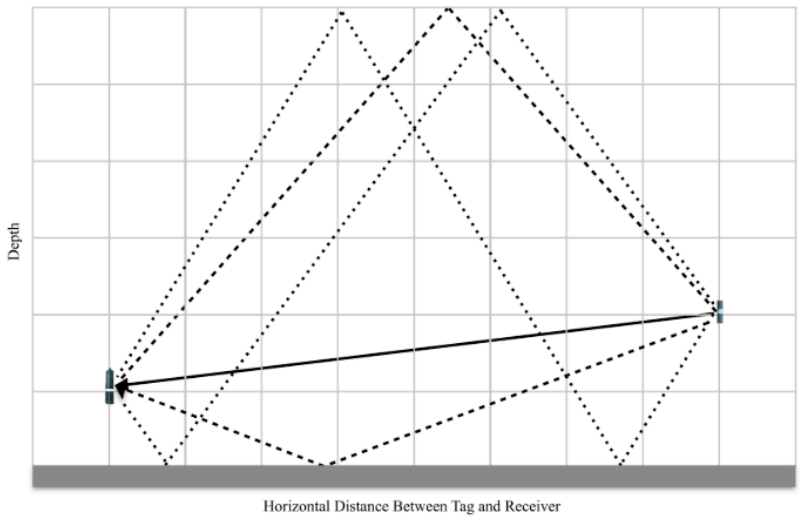

Figure 2.7. Sketch of the Mechanistic CPDI Model Applied to a Hypothetical Environment.

The direct transmission path from source to receiver is represented by solid arrow and the first four multipath arrivals reflecting off the surface and seafloor are illustrated with dotted arrows. With the assumption of a uniform sound speed, the arrival time of the direct arrival and each multipath is a function of their respective path length. When the difference in path length between any multipath and the direct path is greater than the product of the speed of sound and the receiver's blanking interval, CPDI is predicted to occur.

The first step of the proposed mechanistic model is to grid the study area by range and depth, with each grid point representing a potential tag position and the receiver fixed at 0 m range. A resolution parameter allows the user to select an appropriate grid spacing. A ray tracer

calculates both direct and multipaths lengths at each grid point using an ideal model of multipath propagation (Lurton, 2010). This is repeated for each multipath until a set of all multipath lengths less than the AMDR is compiled. Our model then predicts the occurrence of CPDI by evaluating the propagation path lengths of the direct and multipath arrivals by two criteria. The direct path length is subtracted from the length of each multipath and multiplied by a sound speed constant to determine a relative arrival time for each multipath. The set of relative arrival times for each grid point is then assessed using our two criteria: Do any multipath arrivals have a path length less than AMDR? If so, do these path lengths have relative arrival times greater than the receiver's blanking interval? The reasoning behind the criteria is as follows: The direct path arrival of the first ping in the tag's ping train, arriving before any multipath arrivals, should trigger the receiver to begin the blanking interval. Once the blanking interval ends, any detectable multipath arriving (e.g. the surface reflected bounce of the first ping) may cause the receiver to reject the ping train since the receiver is expecting the direct path arrival of the second ping in the train. Rejection is not predicted for multipaths with lengths longer than the AMDR as we assume transmission losses incurred during propagation will be equal to or in excess of the direct path and will therefore be undetectable to the receiver.

Therefore, each multipath arriving at a receiver may fall into one of three categories. 1. If the relative arrival time is less than or equal to the blanking interval and the total path length is less than or equal to the AMDR, the multipath is not predicted to interfere with detection of the direct signal. 2. If the relative arrival time is greater than the blanking interval and the total path length is less than or equal to the AMDR, the multipath is predicted to interfere with the direct signal resulting in failure of the receiver to detect the transmission. 3. If the path length is in excess of the AMDR, no interference is predicted, as the multipath has experienced transmission

losses during propagation such that it is below the threshold for detection. At each grid point, each multipath is categorized. Grid points with at least one multipath falling into the second category are predicted to experience CPDI based on our criteria; grid points where all transmission multipath are of the first and third type are predicted not to experience CPDI.

Following the development of the mechanistic CPDI model, we input parameters from both deep water and shallow water ranging field experiments to compare the range affected by CPDI to predictions from the mechanistic CPDI model. We used a 260 ms blanking interval (by default the largest blanking interval available when initializing a VR2-W), a sound speed of 1530 m/s (typical of the environment in which testing was performed (Tsuchiya et al., 2015)), and a grid resolution of 1 m. For the deep-water ranging experiment (experiment 1), transmission detection was predicted by simulating receivers at 270 and 299 m depth in a water column depth of 300 m across horizontal distances up to 1,000 m from the receiver with the mechanistic CPDI model. For the shallow water range experiment (experiment 2), receivers were simulated at 24, 17.5, and 10 m depth in a 25 m environment over the 1,200 m range tags were deployed. The AMDR variable was defined as the distance at which the number of transmissions detected by receivers, estimated from the median of all considered candidate GAM estimations, fell below 5%. With a nominal transmission interval of 60 seconds, this threshold was 3 detections per hour for the tags used in these two experiments.

Experiment 3: Depth Dependent Model Validation: *17 March – 25 March 2015*

The first of two validation experiments was designed to test predictions of CPDI related to deployment depth. In this experiment, the mechanistic CPDI model was used to identify two depth conditions: One in which multipaths were predicted to arrive outside the receiver's blanking interval, producing CPDI, and a second, where no detectable multipaths arrived outside

the receiver's blanking interval, and thus no CPDI effects were present. The mechanistic model's AMDR parameter was set to 843 m, the closest whole number to the median value determined during the deep-water ranging experiment (experiment 1), due to similarities in depth and deployment location. The model's blanking interval was initialized at 260 ms and sound speed was 1,530 m/s. The mechanistic model predicted CPDI for receiver and tags on the same mooring line (a horizontal distance of 0 m), when both receiver and tag were positioned 1 m above the seafloor in 215 m bottom depth. No CPDI was predicted for a similar tag and receiver pair in 50 m water depth. Latitude and longitude coordinates were selected for locations matching these depths in proximity to the location where the deep-water ranging experiment was conducted using bathymetry charts (Johnson & Potemra, 2011). One mooring was deployed at each site from the RV Ho'okele. Each of the moorings consisted of a tag and receiver positioned 1m from the seafloor. The vessel's depth sounder indicated that the unit intended for deployment at 50 m was deployed at its target depth, while the receiver intended for 215 m was deployed just off target in 212 m water depth (Figure 2.6C). The experiment ended prematurely when the 50 m unit broke free of its mooring and was recovered by State of Hawaii Division of Aquatic Resources enforcement officers nine days after deployment. Logistics and strong trade wind conditions prevented recovery of the remaining unit for a further eight weeks.

The number of tag transmissions detected hourly by each receiver was assessed for normality using Shapiro-Wilks' test and were compared between receivers using a Wilcoxon Sign-Rank test due to the non-parametric distribution of data collected. To account for the independence in the number of transmissions sent by each tag, daily meta-logs for each receiver were downloaded from the VUE database. These provided the number of valid detections, valid synchronization intervals, total detected pings, and the number of detections rejected due to

invalid checksums logged by each receiver. Daily performance metrics, including code detection efficiency (CDE) and the rejection coefficient (RC) were determined for each receiver from meta-logs using methods previously established (Simpfendorfer et al 2008). CDE is defined as the fraction of detected transmissions to the number of detected first inter-ping intervals (synchronization intervals). CDE ranges between 0 and 1 and is a measure of the receiver's ability to successfully record a detected transmission. RC is the fraction of transmissions rejected for failure to validate the checksum relative detected synchronization intervals (Simpfendorfer et al 2008).

These metrics allowed receiver logs to be normalized for comparison independently of the total number of tag transmissions sent. This is important when comparing detection logs in which variations in transmission interval may have resulted in each receiver being exposed to a different number of transmission ping trains. However, both CDE and RC use the number of detected valid syncs as a proxy for the number of transmissions sent. For a receiver to recognize a synchronization interval, the time between the arrival of two pings must be of a strictly defined length. We suspect multipath arrivals of the first ping of the synchronization interval may occur before the subsequent ping, resulting in failure of the receiver to categorize these pings as defining a valid synchronization interval. If this occurred, the number of synchronization intervals would be an underestimate of the number of transmissions for a receiver experiencing the effects of CPDI. To decouple our CDE and RC receiver metrics from the number of synchronization intervals, we created adjusted CDE and RC metrics replacing the number of detected syncs with number of pings detected reduced by a factor corresponding to the number of pings composing a complete transmission train. For our tags, a complete transmission train consisted of 8 pings.

Experiment 4: Depth and Distance Model Validation: ***25 May – 30 May 2015***

The second of the validation experiments was designed to test the mechanistic CPDI model with respect to depth and distance. Simulations using the mechanistic CPDI model indicated that in 300 m water depth, multipath arrivals producing CPDI conditions would persist to distances of 255 m when receivers and tags were positioned 1 m above the seafloor using a sound speed of 1,530 m/s and an 843 m estimate for AMDR. Therefore, it was predicted a receiver positioned 500 m from a group of tags would be more likely to detect a greater number of transmissions than a receiver positioned 50 m from the same tags, within the range CPDI was predicted. Three acoustic tags with 15-minute fixed transmission intervals were activated 5 minutes offset from one another to prevent transmission overlap and moored off Diamond Head in 300 m of water. Two separate VR2-W moorings were deployed at target distances of 50 and 500 m from the transmitter tags along the 300 m isobath. GPS marks taken during deployment indicated the receiver targeted for 50 m was deployed 10 m off mark, 60 m from the tags, and that the receiver targeted for 500 m was deployed 8 m off mark, 508 m from the tags (Figure 2.6D). The normality of hourly recovery rate data was again assessed for each condition using Shapiro-Wilks' test and then between conditions using a Wilcoxon Sign-Rank test.

Experiment 5: Multipath Confirmation: ***13 July 2016***

A controlled tank experiment was designed to test the underlying hypothesis behind our CPDI model, that the primary driver of CPDI is spurious ping multipaths arriving after the blanking interval. A laptop running Matlab's Data Acquisition Toolbox (MathWorks 2015) was used to playback a waveform signal recorded from a V13 acoustic tag using a digital-to-analogue converter, amplifier, and two ITC 1042 transducers (one transmitting and one recording the sound) with a relatively flat sensitivity of -200 dB re 1V/µPa between 1 and 100 kHz and a sampling frequency of 192 kHz (we refer to the transmitting and recording transducers as the

“transmitter” and the "hydrophone", respectively). The transmitter was suspended in the tank about 1 m away from a VR2-W receiver unit and the hydrophone. The output level of the transmitter was calibrated to match the output of a tag by incrementally increasing amplifier output until the peak-to-peak voltage measured by the hydrophone matched the output level produced by the acoustic tag placed in the tank at the same position as the transmitter.

Recordings of the acoustic tag were processed to create a simulated tag transmission. Transmission loss for each simulated multipath was calculated using a straight-line acoustic propagation model to calculate the path length (I_{Arr}) for each of the first 20 acoustic arrivals (direct arrival and interface-reflected multipath arrivals). Then, the received level factor (RL) for each arrival path was calculated using the formula:

$$RL = 10^{-1*log_{10}(I_{Arr})}$$

This yielded 20 sets of scalars by which the simulated transmission wave form was multiplied to get the simulated received level of each multipath determined from its arrival path. These scalars were turned into the impulse response by placing them at the appropriate time delay relative to the direct path arrival time (base on the time of arrival info from the mechanistic model for predicting CPDI. A waveform containing the direct transmission signal, and when appropriate, simulated multipath arrivals, was then constructed by convolving the simulated source waveform with this impulse response. Further reductions in signal intensity for multipath arrivals to mimic transmission losses incurred during reflection and scattering at surface and seafloor interfaces were not considered. Reflections from the walls of the tank were not expected to produce CPDI as preliminary testing indicated the tank had an impulse response length shorter than the receiver’s 260 ms blanking interval. In other words, the noise level in the tank returned to ambient levels within the 260 ms window of the blanking interval.

All permutations of tag and receiver placement from field experiments were simulated with and without multipath arrivals. This led to two conditions: A control condition in which only the direct arrival was emitted into the tank (and thus CPDI not predicted), and an experimental condition which included both the direct path and simulated multipaths. Scenarios in the experimental condition were further categorized into those in which CPDI was predicted and those in which CPDI was not predicted (according to the CPDI model). All simulated transmissions were repeated five times.

Each simulated transmission was assigned an event identification based on the experiment simulated and the placement of the receiver in the water column. One of three predictive classifications were assigned to each transmission: 1) No multipath (control), 2) With multipath, no CPDI predicted, and 3) With multipath, CPDI predicted, leading to 4 possible outcomes 1) detection predicted, detection occurred, 2) detection predicted, no detection occurred, 3) no detection predicted, no detection occurred, and 4) no detection predicted, detection occurred. A transmission was coded 1 if it was detected by the receiver and 0 if it was not detected. A logistic regression was fit using a generalized linear model (GLM) with transmission detection/non-detection as the binary response variable. Predictor variables included the predictive classification (control, with multipath, no CPDI Predicted, with multipath CPDI predicted), and the event ID representing the analogous experiment and condition simulated. Terms representing the interaction between predicted/observed and each event ID, which would identify any simulated experimental analogues where observations varied from predictions, were also considered. Model selection was used to identify the best GLM. A pseudo R^2 was calculated for the GLM (McFadden, 1973) and hierarchical partitioning was performed to

determine the percentage each term contributed to the GLM's overall explanation of observed variance.

Results

Summary

The shape of the detection functions for the deep-water ranging experiment (experiment 1) differed from that of the shallow water ranging experiment (experiment 2) (Figure 2.8). The presence of CPDI in the deep-water experiment created an area of low detection probability surrounding the receiver, with the highest number of observed detections coming from tags at an intermediate distance from the receivers. In contrast, the highest observed number of detections during the shallow water ranging experiment, where no CPDI was observed, came from the tags positioned closest to the receivers. Our mechanistic model for predicting CPDI was largely congruent with field observations from ranging and validation tests, accurately predicting when the effects of CPDI were observed. For both validation experiments, detection of transmissions from tag-receiver pairs where no CPDI was predicted surpassed those where CPDI was predicted by our mechanistic model. In controlled tank experiments, we were able to accurately predict the detection/non-detection of 460 simulated transmissions with 95.7% accuracy using our multipath arrival prediction criterion.

Experiment 1: Quantifying Detection Range in Deep Water: *7 June – 16 June 2014*

During the deep-water ranging experiment, on average, the range at which tag transmissions were detected ranged between 840 and 846 m (Range including standard error: 839 – 847 m)

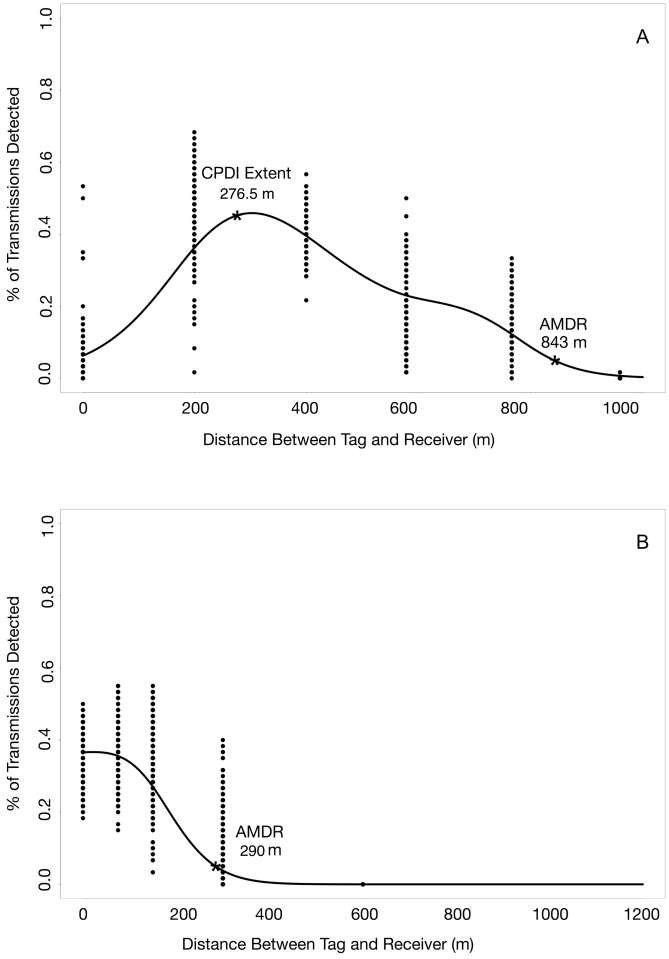

Fig. 2.8 Detection probability profiles from deep and shallow water ranging experiments.

(A) Effects of CPDI are clearly present in the results of the deep-water ranging experiment, as indicated by low detection probabilities at ranges close to the receiver increasing to a maximum detection probability at an intermediate range. (B) Effects of CPDI are not present in detection probabilities of the shallow water ranging experiment, with the maximum detection probability occurring at distances nearest the receiver.

with some variation arising from different factor levels of random predictor variables (Figure 2.8A). The range affected by CPDI extended 276.5 m (Range including standard error: 276 – 277 m) from the receiver for all permutations of predictor variables. The influence of each combination of predictor variables on GAM estimates of AMDR and CPDI range are presented in Table 2.1.

There were 8 GAMs with AIC values equal to or within 2 AIC values of the lowest, and thus best fit, model. Each of these explained 64.6% of variation in the number of transmissions per hour detected by the receivers (Adjusted R2 = 0.647). The predictor variables included in the GAM with the lowest AIC were distance, receiver height, tag height, mean hourly wind speed, mean hourly wind gust, and diurnal period.

Table 2.1. Deep-water Ranging Experiment Results.

Median predictions of AMDR and CPDI from all candidate GAMs and, in parenthesis, the minimum and maximum value predicted by any one candidate GAM inclusive of standard error. Also presented are estimates for CPDI range from the proposed mechanistic model, fit with the median AMDR value for each combination of factors.

Receiver Height (m)	Tag Height (m)	Tidal Phase	Diurnal Period	GAM Estimated AMDR (m)	GAM Estimated CPDI (m)	Model Predicted CPDI (m)
1	1	In	Day	843 (839-847)	276.5 (276-277)	259
1	1	Out	Day	843 (839-847)	276.5 (276-277)	259
1	1	In	Night	843 (839-847)	276.5 (276-277)	259
1	1	Out	Night	843 (839-847)	276.5 (276-277)	259
1	15	In	Day	844 (839-847)	276.5 (276-277)	279
1	15	Out	Day	843.5 (839-847)	276.5 (276-277)	279
1	15	In	Night	844 (839-847)	276.5 (276-277)	279
1	15	Out	Night	843.5 (839-847)	276.5 (276-277)	279
30	1	In	Day	844 (842-847)	276.5 (276-277)	301
30	1	Out	Day	845 (842-847)	276.5 (276-277)	301
30	1	In	Night	844 (839-847)	276.5 (276-277)	301
30	1	Out	Night	844 (839-847)	276.5 (276-277)	301
30	15	In	Day	843.5 (842-845)	276.5 (276-277)	326
30	15	Out	Day	843.5 (842-845)	276.5 (276-277)	326
30	15	In	Night	843 (839-847)	276.5 (276-277)	326
30	15	Out	Night	843.5 (839-847)	276.5 (276-277)	326

Experiment 2: Quantifying Detection Range in Shallow Water: ***22 November – 2 December 2014***

During the shallow water ranging experiment, on average, tag transmissions were detected to a distance of 278 and 290 m (Range including standard error: 277 – 290 m) from the receiver (Figure 2.8B). CPDI was not observed during this experiment; that is, the GAM estimated CPDI was 0. The influence of each combination of predictor variables on GAM estimates of AMDR and CPDI range are presented in Table 2.2.

There were 4 GAMs with AIC scores equal to or within 2 values of the lowest, and thus best fit, AIC value. Each of these 4 candidate GAMs explained approximately 72.7% of the variation in the number of detected transmissions per hour (Adjusted R2 = 0.684). Predictor variables for the GAM with the lowest AIC score included distance, receiver height, diurnal period, mean hourly wind gust, mean hourly wind speed, and mean hourly water level.

Table 2.2: Shallow Water Ranging Experiment Results.

Five number summaries (minimum, first quantile, median, third quantile, and maximum values) for predictions of AMDR and CPDI range over all candidate GAMs and CPDI model estimates for CPDI range, fit with the median value for each combination of factors.

Receiver Height (m)	Tidal Phase	Diurnal Period	GAM Estimated AMDR (m)	GAM Estimated CPDI (m)	Predicted CPDI (m)
1	In	Day	290 (289-290)	0 (0-0)	0
1	Out	Day	290 (289-290)	0 (0-0)	0
1	In	Night	285 (284-285)	0 (0-0)	0
1	Out	Night	285 (284-285)	0 (0-0)	0
7.5	In	Day	283 (282-283)	0 (0-0)	0
7.5	Out	Day	283 (282-283)	0 (0-0)	0
7.5	In	Night	278 (277-278)	0 (0-0)	0
7.5	Out	Night	278 (277-278)	0 (0-0)	0
15	In	Day	284 (283-284)	0 (0-0)	0
15	Out	Day	284 (283-284)	0 (0-0)	0
15	In	Night	278 (278-279)	0 (0-0)	0
15	Out	Night	278 (278-279)	0 (0-0)	0

A Mechanistic Model for Predicting CPDI

We input environment parameters from the deep and shallow water ranging experiments (experiments 1 and 2) and their median AMDR estimates into our mechanistic model for CPDI. CPDI estimates from range test results were compared to the mechanistic model's predictions (Tables 2.1 and 2.2). For the deep-water ranging experiment, the mechanistic model predicted CPDI extending from the receiver to distances between 259 and 326 m while GAM predictions estimated CPDI extent to 276.5 m from the receiver (Table 2.1). Predictions of the CPDI ranges using the mechanistic predictive CPDI model were within 52 m of the median estimations from the GAM models for the deep-water ranging experiment (experiment 1), differing by an average of 14.75 ± 9.44 m. For the shallow water ranging experiment, CPDI was neither predicted nor observed by either method (Table 2.2).

As the mechanistic CPDI model does not consider transmission losses from reflection and absorption, it was not unexpected that the CPDI model predicted a slightly larger CPDI range than that estimated by the GAMs results. Only the combination of receiver and tag both positioned 1 m above the seafloor produced GAM estimated CPDI ranges larger than those predicted by the CPDI model.

Experiment 3: Depth Dependent Model Validation Experiment: 17 March – 25 March 2015

During this experiment, observed detections of tag transmission by each receiver were consistent with predictions made by the mechanistic model. Shapiro-Wilks' tests indicated that distributions for the number of hourly detections by each receiver were non-normal ($p < 0.05$ for the 50 m case and $p < 0.001$ for the 212 m case). The number of detections recorded by the two receivers differed significantly as determined by using a Wilcoxon sign-rank test ($p < 0.001$). The 50 m tag/receiver pair experienced mean detection rates over 5.5 times greater than that of the 212 m

tag/receiver pair (56.6 detections per hour vs. 10.0 detections per hour, respectively). There were no periods in which the deeper receiver, where CPDI producing multipaths were predicted, detected more transmissions than the shallow receiver where CPDI producing multipaths were not predicted.

Assessment of performance data for each receiver from meta-logs was done using conventional CDE and RC metrics with the number of detected syncs serving as a proxy for total transmissions as well as adjusted metrics substituting the syncs for the number of pings detected divided by the number of pings composing a full transmission. For both metrics, non-parametric methods were required due to non-equivalent variances between receivers and a non-normal distribution of both CDE and adjusted CDE from the receiver in 50 m depth. The 50 m depth receiver had median CDE and adjusted CDEs of 1.00 (meaning virtually no detections were missed) while the 212 m receiver had a significantly lower median CDE of 0.0865 ($p < 0.01$; paired Wilcoxon sign-rank tests). When compared using the adjusted CDE metric, the difference between receivers remained significant ($p < 0.05$). The 50 m depth receiver had a median adjusted CDE of 1.00 while the receiver at 212 m depth had an adjusted CDE of 0.214 (Figure 2.9).

Median RC values for each receiver were not significantly different, with a median value of 0 for the receiver at 50 m depth (no detections were rejected) and a median value of 0.0138 for the receiver at 212 m depth ($p > 0.05$). When adjusted as described above, the difference was significant ($p < 0.05$). The median daily adjusted RC was 0 for the receiver at 50 m depth and 0.110 for the receiver at 212 m. These daily results, which make no assumptions about the number of transmissions sent during the study period, are similarly consistent with our hourly

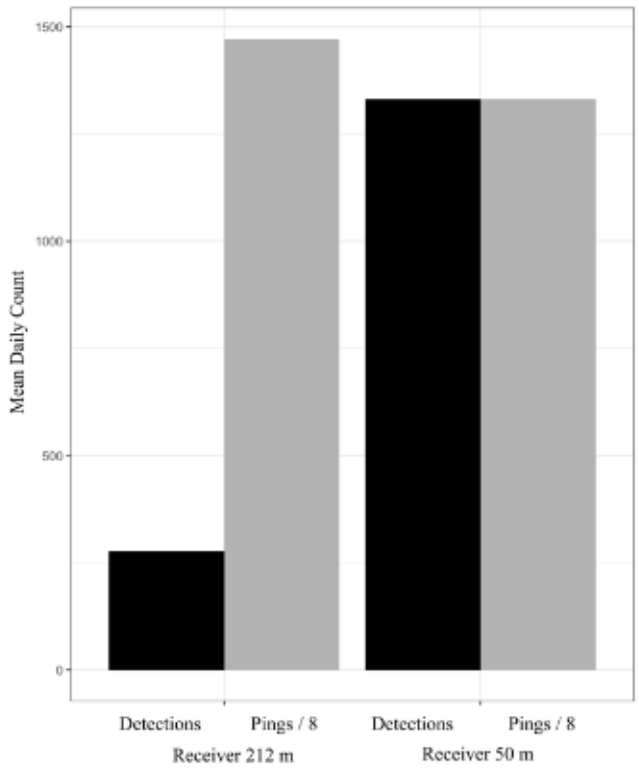

Figure 2.9. Comparing the Mean Daily Components of the Adjusted CDE Between Receivers in the Depth Dependent Model Validation Experiment (Experiment 3). *The number of pings detected has been standardized by a factor of 8, the number of pings comprising a transmission as a proxy of total transmissions sent. The receiver affected by CPDI (212 m depth) detected a greater number of transmission pings but detected substantially fewer transmissions than the receiver not affected by CPDI (50 m depth).*

analyses and the mechanistic model's predictions, supporting the use of our adjusted metrics when CPDI effects are present.

Experiment 4: Depth and Distance Model Validation Experiment: 25 May – 30 May 2015

Consistent with the mechanistic model's predictions, the receiver 60 m from the tags detected fewer transmissions than the receiver 508 m from the tags. Shapiro-Wilks' testing indicated that detection probability distributions were non-normal ($p < 0.01$ and $p < 0.001$ for the receivers at 60 m and 508 m from the tags respectively). A Wilcoxon sign-rank test used to compare hourly

detection counts between the receivers found that the receiver at 508 m recorded significantly more detections per hour than the receiver at 60 m, logging on average over 1.5 more detections per hour (7.67 transmissions per hour compared to 4.88) than its shallow water counterpart ($p < 0.001$), despite the greater distance. The receiver at 508 m range outperformed the receiver at 60 m range in 120 of the 133-hour intervals and recorded the same number of transmissions during 4 of the 133-hour intervals. In the 9 remaining cases, the receiver at 60 m detected more transmissions than the receiver at 508 m. Although the specific explanation for these 9 cases is unknown, it is possible that it was due to fluctuating noise levels.

In support of the hypothesis that fewer transmissions detected by the receiver closest to the tag were caused by invalidated ping trains, meta-logs showed that the receiver located 60 m from the tags recorded more individual pings than the receiver at 508 m over the duration of the study (11,277 pings compared to 9,731 pings). Despite this, the 60 m range receiver logged fewer detections of completed transmissions during the same period (674 detections compared to 1050). These results compare favorably to the mechanistic model, which predicts a CPDI range of 276.5 m.

Experiment 5: Multipath Confirmation: 13 July 2016

Of the 900 simulated tag transmissions, only 20 measured outcomes differed from CPDI predictions. Of these, there were 4 detections where transmissions included simulated multipaths predicted to interfere with detection. The remaining 16 discrepancies occurred when the model predicted detection, but no detection was logged by the receiver.

The binomial GLM compared detection or non-detection of a transmission logged by the VR2-W during tank testing to predictions of the CPDI model. Initially, a GLM was fit with predictive CPDI classification, event ID, and their interaction as independent variables. The

interaction term was found to be statistically insignificant ($p > 0.05$) so the GLM was refit with just predictive classification and event ID variables (Table 2.3). In addition to the intercept term, representing the control prediction while simulating the receiver closest to the seafloor during the deep-water ranging experiment (experiment 1), two model terms were significant. The most significant term was the predictive classification "with multipath, CPDI predicted" ($p < 0.001$). There was no statistical difference in the number of detections between the control group and the 'with multipath, no CPDI predicted' group. These results indicated that the detection of transmissions with simulated multipaths where no CPDI was predicted did not differ from the control group without multipaths, for which detection was also predicted. Conversely, there were significantly fewer detections when the arrival times of simulated multipaths predicted CPDI

Table 2.3: Component 4 GLM Results.

Summarized results for the controlled tank experiments fit with a binomial GLM.

Model Term	Est.	Std. Error	z-value	p-value
Intercept (Control/Deep Water Ranging: Receiver 1 m)	4.159	0.634	6.559	0
Multipath CPDI Predicted	-8.319	0.712	-11.676	0
Multipath No CPDI Predicted	1.447	0.803	1.802	0.072
Exp Analogue - Deep Water Ranging: Receiver 30 m	0	0.742	0	1
Exp Analogue - Shallow Water Ranging: Receiver 1 m	-1.883	0.766	-2.458	0.014
Exp Analogue - Shallow Water Ranging: Receiver 7.5 m	15.871	1575.438	0.01	0.992
Exp Analogue - Shallow Water Ranging: Receiver 15 m	-0.987	0.879	-1.123	0.261
Exp Analogue - Depth Dependent Validation: Depth 50 m	-23.299	2746.956	-0.008	0.993
Exp Analogue - Depth Dependent Validation: Depth 212 m	-4.565	0.905	-5.047	0
Exp Analogue - Depth and Distance Validation: Depth 60 m	0	1.891	0	1
Exp Analogue - Depth and Distance Validation: Depth 508 m	0	1.891	0	1
Residual deviance: 109.28 on 449 degrees of freedom				
Null deviance: 583.73 on 459 degrees of freedom				

conditions. Of the factor levels for the event ID model terms, only the condition corresponding to results of the 212 m water depth scenario from the depth dependent model validation experiment (experiment 3) were significant ($p < 0.001$). Overall, the model explained approximately 81.5% of the observed variance (pseudo $R^2 = 0.815$) with 81.8% of that total explained variance coming from our predictive CPDI classification.

Discussion

Predicting conditions under which CPDI may occur is important for optimal implementation of acoustic networks and interpretation of study results. The present study demonstrates that relative positions (in both depth and distance) of a receiver and tag can lead to conditions where acoustic energy reflected from the surface and/or seafloor may interfere with detection of the transmission's pulse train. Implementation of a ray tracing mechanistic CPDI model was able to predict when this interference occurred in multiple experiments with a high degree of accuracy.

It has been noted that CPDI may be present in environments particularly amenable to acoustic reflection (Kessel et al., 2015). This stands to reason as transmission losses incurred during reflection in these environments are low, producing multipaths that are relatively loud. However, particularly for receivers deployed in deep water settings, surface reflections may be enough to produce observable CDPI effects regardless of the reflective properties of the seafloor. Compared to their shallower receiver counterparts, for deeper receivers, reflected acoustic energy has the potential to arrive following the end of the blanking interval with fewer reflections off the surface and/or seafloor. These signals incur fewer transmission losses due to scattering and reflection than signal energy reflected multiple times. In relatively low noise environments also prone to acoustic reflections, multipath acoustic energy reflected off the surface, seafloor, or some combination of each, may also arrive with sufficient intensity for

detection by the receiver, invalidating the tag identification and event recording, and exacerbating the problem of detection under CPDI conditions.

During our deep and shallow ranging experiments (experiments 1 and 2), some variability in the presence and observed magnitude of CPDI effects can likely be attributed to the number of high output tags used and their variable transmission intervals. The maximum transmissions detected by a receiver of a single tag was 40 of 60 expected hourly transmissions. We believe this was partially a result of the large number of tags used during each ranging experiment (12 in the deep water experiment and 18 in the shallow water experiment), with relatively short transmission intervals (averaging 60 s) resulting in failure to detect transmissions during periods of transmission overlap, reducing the overall number of transmissions detected each hour.

Selecting an appropriate transmission interval and power output of study tags is often a tradeoff. The tags used in experiments 1-3 were selected for use in a deep-water snapper study with receivers positioned so their detection ranges would overlap in fence/gate configurations. A relatively short transmission interval was selected so multiple transmissions would be emitted by tagged fish swimming between receivers, improving the probability of detecting the presence of an individual. For similar reasons, tags were also high output. This allowed us to maximize the distance from a receiver that transmissions could be detected and construct a fence from a minimum number of receivers. However, increasing the output level of a tag also increased the received signal level of transmission multipaths which, under sufficient conditions, produce CPDI.

Some hourly variation in the number of total transmissions sent by each tag was expected and may have contributed further variability to the observed hourly data. However, it is

unlikely the variable transmission interval accounts for the magnitude of observed CPDI effects as each transmitter has the same variability in transmission interval; thus, all tags were expected to have a similar number of hourly transmissions.

Standardizing test results of the depth dependent model validation experiment using data from receiver meta-logs allowed us to control for discrepancies in variable transmission intervals. The number of synchronization intervals and pings detected are likely underestimates of the true values due to the receiver's inability to detect transmissions during blanking intervals (Simpfendorfer, Heupel & Collins, 2008). Both synchronization interval and ping data were used to compare between the two depth conditions in the depth dependent model validation experiment (experiment 3). These may have led to underestimation of the number of transmissions undetected at the deeper receiver, but we do not think this had an effect on the overall outcome of the experiment. Relative to the receiver at 50 m water depth, the receiver at 212 m depth showed the effects of CPDI while having comparatively higher daily values for both synchronization intervals detected (3658 median daily synchronization intervals compared to 1355.5 median daily synchronization intervals) and daily pings detected (11,777.5 median daily pings compared to 10,844.5 median daily pings). Despite greater detection of individual syncs and pings, this receiver logged 1039 fewer transmissions per day on average (316.5 median daily detections compared to 1355.5 mean daily detections). This indicates that the deeper receiver detected more individual pings but failed to detect the transmissions. This observation is consistent with transmissions being affected by CPDI. The remaining experiments were not subject to these concerns as each used a design in which all transmissions were detectable by each receiver.

Environmental and anthropogenic factors have been implicated as external sources of variability affecting receiver detection performance (Cagua, 2012; Cagua, Berumen & Tyler, 2013; Gjelland & Hedger, 2013; Mathies et al., 2014). While our mechanistic model does not directly account for background noise level, in practice, increased background noise leads to a reduction of the AMDR term and decreases CPDI range. Similarly, lower background noise levels may increase both AMDR and CPDI range. Thus, background noise levels are accounted for indirectly in the model through the AMDR term. Parameters for the AMDR used in the mechanistic CPDI model were estimated from ranging results by fit of the candidate GAMs. During periods of increased background noise within the receiver's detection frequency bandwidth, greater acoustic energy is required to get a signal-to-noise ratio greater than the detection threshold. We suspect that this accounts for the large discrepancy between the AMDR values for the deep-water ranging experiment (experiment 1) which took place in deeper and presumably quieter waters than the shallow water ranging experiment (experiment 2) where equipment was positioned near a patchy coral reef and harbor entrance.

Low background noise levels in the tank and artificially high signal levels for simulated multipath arrivals produced CPDI at simulated distances far surpassing those observed during shallow and deep-water ranging experiments. There was a higher number of detected transmissions in the tank environment for simulated tag transmissions which mimicked distances between tag and receiver where a low number of detections were observed in field experiments and for which CPDI was not expected. Low background noise levels in the tank environment meant that signals of weaker intensity were detected by the receiver. In several instances, CPDI was not observed in field results, but was present in the tank experiment analogue. Multipath arrivals in the ocean undergo additional attenuation when reflecting off the sea surface and

seafloor interfaces. These losses were not accounted for in the calculation for reducing signal intensity of multipath arrivals in tank simulations. When coupled with the tank's favorable low noise conditions, we would expect more simulated multipath arrivals to arrive at the receiver with sufficient intensity for detection to produce CPDI in the tank than in the field.

There are a number of study designs and analysis methods that would benefit from the consideration of CPDI. When paired with knowledge of an organism's swimming speed, this model can be helpful in the selection of an appropriate interval for tag transmissions. An ideal transmission interval will ensure tagged individuals traveling through the detection range of the receiver have a likelihood of detection equal to or greater than some acceptable probability. This is particularly relevant to passive acoustic network arrays where the detection footprints of receivers overlap, such as full coverage, gate, and curtain designs (Heupel, Semmens & Hobday, 2006). When applied post-hoc, the mechanistic model for predicting CPDI described here can give some indication of overall network performance and estimate the permeability of overlapping receiver detection footprints. In studies using depth sensor tags to investigate the depth distribution of an organism, detection logs may under-represent depths where CPDI conditions are prevalent, given that the incidence of CPDI is sensitive to tag depth. Studies where receivers are attached to dynamic platforms such as vessels, gliders, autonomous underwater vehicles, and marine animals, should also consider the effect that changes in receiver position and environment depth can have on CPDI and transmission detection. It is also important to understand a receiver's susceptibility to CPDI when choosing to analyze telemetry data using space state models. In their current implementations to marine animal telemetry, these models rely on both detection and non-detection probabilities to estimate the distance of tagged individuals from a receiver (Pedersen & Weng, 2013; Alós et al., 2016). CPDI may confound

position estimates if not accounted for as equivalent detection probabilities can occur at multiple distances from the receiver. Paired with appropriate range testing and knowledge of the study organism's habitat preferences, the model for CPDI proposed in this study can be used to suggest optimal vertical receiver positioning within the water column. If preferred depth of the study species is unknown, the model can be run over the full depth range or a subset of ranges with only a small increase in computational runtime.

Conclusion

CPDI results in the failure to detect tag transmissions when reflected acoustic energy arrives at a receiver with intensity and timing sufficient to be mistaken for a unique signal. Our results show that when CPDI conditions are present, the shape of a receiver's detection function includes an area of low detection probability near the receiver. Conditions leading to CPDI can be reasonably predicted by incorporating knowledge of the study environment and a receiver's detection parameters. Depth is also a key factor in the occurrence of CPDI. Assuming a constant sound speed of 1,530 m/s, CPDI may occur when relative path lengths exceed 400 m. In this example scenario, CPDI arising from the first surface reflection occurs for receivers at depths greater than 200 m. In cases where reflection off both the surface and seafloor are important, the receiver depth for which CPDI occurs will decrease relative to this surface-reflection only case. Relatively quiet and/or highly reflective environments (e.g. hard bottoms) lead to higher signal-to-noise ratios which result in a greater number of multipath arrivals that can be detected at the receiver. These signals potentially interfere with transmission detection, increase the CPDI range, and result in fewer (or potentially no) detections from tagged individuals near receivers.

Modeling for CPDI, therefore, is an important step for designing and interpreting acoustic tagging studies, particularly when working at greater depths. This is particularly a concern as

acoustic tracking studies occurring in deeper waters becomes more common (Starr, Heine & Johnson, 2000; Afonso et al., 2012, 2014; Weng, 2013; Comfort & Weng, 2014; Gray, 2016). Prior to deployment of acoustic hardware, CPDI modeling over known depth distributions, consistent with a study species, can recommend deployment configurations to potentially mitigate CPDI effects. When the depth distribution for a species of interest is unknown, or a receiver network is being used to monitor multiple species with differing depth distributions, modeling over the entire water column can still provide researchers with valuable suggestions for deployment depth with little extra computation time.

CHAPTER 3: EVALUATING MOVEMENTS OF THE DEEP-WATER SNAPPER *PRISTIPOMOIDES FILAMENTOSUS* RELATIVE TO A FISHERY RESERVE USING A PASSIVE ARRAY AND CONSTRAINED LINEAR HOME RANGE ESTIMATOR

Submitted as: Scherrer, SR., Weng, KC. Evaluating movements of the deep-water snapper *Pristipomoides filamentosus* relative to a restricted fishing area using a passive array and constrained linear home range estimator. *Fishery Bulletin.* September 2019.

Abstract

Networks of no-take reserves have emerged as a tool for managing stocks of deep-water fishes. In Hawaii and elsewhere, these areas are being used to manage deep-water snappers. However, there is a paucity of information regarding the movements and home range size of these fishes relative to these reserves. We used passive acoustic telemetry to track opakapaka (*Pristipomoides filamentosus)* relative to one of Hawaii's bottomfish restricted fishery areas (BRFAs) to assess its suitability for this species.

From January 2017 to January 2018, we tagged 179 fish. A decision tree method used to classify track status categorized 10 fish as "alive". Of the 10 fish categorized alive, the median track duration was 415 days with 28,321 detections/individual. Individual home range estimates averaged 6.0 km, smaller than the median length of Hawaii's BRFAs. Half of the fish were detected crossing reserve boundaries on average once every 5.8 days. Fish that left the reserve were detected within the reserve on 97% of the days they were tracked. These results suggest that this species is likely to benefit from reserve networks, and Hawaii's current BRFAs are likely sufficient in scale to confer positive benefits to *P. filamentosus* residing within their borders.

Introduction

Deep-water fishes are typically characterized by slow-growth and late maturity, leaving them vulnerable to overexploitation (Cailliet et al., 2001; Drazen and Haedrich, 2012). Deep-water fishery reserves have emerged as a tool for rebuilding and maintaining these stocks (Williams et al., 2009; Friedlander et al., 2014; Huvenne et al., 2016; Uehara et al., 2019). Key to understanding the benefits of these reserves is quantifying their ability to retain and protect fish during critical life stages to confer positive, beneficial effects (Roberts et al., 2014). However, biological considerations are often unknown or neglected when reserve areas are designed which can lead to uncertain outcomes (Halpern, 2003). Understanding the spatial ecology and movement dynamics of these fishes relative to proposed or implemented areas is therefore critical to both the planning and evaluation processes (Stephen R. Palumbi, 2004). Passive tracking using acoustic telemetry is a popular and versatile tool for quantifying fish movements relative to fishery reserves (Crossin et al., 2017). However, deep-water fishes are particularly susceptible to post-release mortality compared to shallow-water species due to barotrauma and other stressors (Edwards et al., 2019).

Deep-water demersal fish are a valuable resource throughout the Indo-Pacific (Kami, 1972). These multi-species complexes are both economically and culturally important; supporting commercial, recreational, and subsistence fishing (Craig et al., 1993; Pooley, 1993). In the Hawaiian Archipelago, management of bottomfish resources is a partnership of federal and state agencies and focuses on six species of eteline snapper and one endemic grouper that inhabit island slopes and banks at depths that typically range between 100 and 400 m (Kelley and Ikehara, 2006; Oyafuso et al., 2017). Locally these species are referred to as the Deep-7 with *Pristipomoides filamentosus* (local name ‘opakapaka’) accounting for the largest fraction of the commercial and recreational harvest. During the 2017-2018 fishing year, the ex-vessel value of

these species was in excess of $1.6 million with *P. filamentosus* accounting for just over half of this figure[1].

In response to the declining spawning potential ratio for *Etelis coruscans* and *Etelis carbunculus,* the second and third most abundant species harvested, respectively, an annual catch limit and a network of restricted fishing reserves were introduced in 1998. These control measures were meant to facilitate the recovery of Deep-7 stocks. The Bottomfish Restricted Fishing Areas, or BRFAs as they are known, are a network of fishery reserves designed to recover stocks by protecting 20% of bottomfish habitat in the Main Hawaiian Islands (Friedlander et al., 2014). In 2008 the BRFAs were restructured, with a goal of further reducing fishing pressure. The number of reserve areas was also reduced from 19 to 12. Incorporated in this revision process was improved knowledge of preferred bottomfish habitat (Parke, 2007). Since this process, several studies have further documented the habitat associations of bottomfishes in the Hawaiian Islands (Misa et al., 2013; Cordelia Moore et al., 2016; Oyafuso et al., 2017). In August 2019, four reserves were reopened leaving 8 closed areas.

The BRFAs are controversial among fishery stakeholders (Hospital and Beavers, 2011). Studies have shown that within several of the BRFAs fish size and abundance has increased (Sackett et al 2014) and there is some evidence that spillover has occurred to neighboring fished areas (Sackett et al 2017). Despite these conservation benefits, in recent years some bottomfish fishers have lobbied managers to do away with some or all of the areas (Minutes of the 158th meeting of the Western Pacific Regional Fishery Management council, 2013). They argue that

[1] Harding, K. 2018. Personal Commun. State of Hawaii Department of Land and Natural Resources, Division of Aquatic Resources, Honolulu, HI

they do not adequately balance economic effects experienced by the fishers with conservation benefits to the fish stocks (Oyafuso, Leung, and Franklin, 2018). NOAA, The State of Hawaii's Department of Land and Natural Resources, and the federal Western Pacific Regional Fishery Management Council, who jointly manage bottomfish resources in Hawaii, require information on the home range size and movement of bottomfishes to inform the future of these management strategies (Western Pacific Regional Fishery Management Council, 2014).

There has previously been little empirical data to assess how the spatial scale of the BRFAs compares to the routine movements of *P. filamentosus* and other bottomfish species they are intended to protect (Western Pacific Regional Fishery Management Council, 2014). Coarse estimates of movement potential *for P. filamentosus* in the Hawaiian archipelago were obtained through a mark-release-recapture tagging study (O'Malley, 2015). In the study, *P. filamentosus* (*n* [number of fish] = 111, median time at liberty = 325 days) were recaptured up to 61 km from their tagging location, however most individuals appeared to move at more limited scales with 86% of recaptured fish recovered less than 10 km from their tagging site.

A handful of studies have used acoustic tracking to study the Hawaiian deep-water snappers. An active tracking study followed 2 juvenile *P. filamentosus* over 5 and 6 day periods and described crepuscular movements between day and night habitat with movements occurring over areas 0.4 km^2 in size (Moffitt and Parrish, 1996a). Passive acoustic telemetry was used to track *P. filamentosus* in 2004 (*n* = 12, median time at liberty = 5.80 days, 5 receiver array), 2006 (*n* = 5, median time at liberty = 0.21 days, 3 receiver array), and again in 2007 (*n* = 10, median time at liberty = 0.58 days, 7 receiver array) as they moved over the boundary demarking the Kahoolawe Island Reserve (Ziemann and Kelley, 2004, 2007, 2008). Fish were observed

undertaking diurnal movements leaving the area at night and returning in the morning, however the size and position of the acoustic array was insufficient to determine movement extent.

Only one tagging study has described bottomfish movements in relation to the BRFAs. Weng (2013) passively tracked *E. coruscans* (n = 12, median time at liberty = 40.83 days, 8 receiver array) and *E. carbunculus* (n = 6, median time at liberty = 28.44 days, 8 receiver array) in BRFA-B off of Niihau, Hawaii. The majority of tagged fish spent most of their time within the protected area of the BRFA, suggesting that the BRFA was a reasonable management measure for these species of bottomfish.

Previous studies of Hawaiian bottomfish movement used small tracking arrays, tagged small numbers of fish, tracked fish over short durations, or were limited to observations during marking and recapture. Therefore, the usefulness of the BRFAs to decrease fishing mortality on the Deep-7 stocks is unclear. The goal of this study was to determine if the movements of *P. filamentosus* were confined to reserves or extended beyond the area boundaries. Passive acoustic telemetry was used to track individuals within and outside the boundaries of one reserve area. Home range requirements were then estimated and compared to the scale of protection provided by the current reserve network. Finally, we looked at how individual fish allocated time between reserve and non-reserve areas to understand how frequently fish move between protected and non-protected waters.

Materials and Methods

Study Area

The Makapuu region (21° 33.5 N, 157° 52.5 W) was selected as the study site for this project because it contains both protected (BRFA-E) and non-protected habitat with sufficient area to capture the scale of bottomfish movements observed during a previous multi-island pilot study.

The area is important to the commercial fishery and in close proximity to the population center of Honolulu.

The area is located off Oahu's windward side, and extends outward from Makapuu Point, the south east tip of the island of Oahu, north to the Lanikai Peninsula. A flat broad shelf protrudes east from the island's southern edge before terminating in a deep slope that forms the western side of the Kaiwi Channel. The shelf narrows to the north joining with a series of deeper shelves and forms submarine canyons. BRFA-E extends from 1.5 miles offshore westward across the shelf in line with Koko Head crater to the south and Kailua to the north (Figure 3.1). Within BRFA-E, habitat between the 100 and 400 m depth contours encompasses approximately 49 km^2.

Fish Capture and Tagging

Fish in this study were captured with the assistance of local fishers using vertical deep drop hook and line gear and hydraulic or electric line pullers. We used kaka line and mak-e dog rigs, which are the most common method of bottomfishing in the Hawaiian archipelago (Glazier, 2007). Hooks were baited with squid, anchovies, sardines, and/or saury for bait. Kaka line rigs were fished with no more than 6 baited hooks at a time. Palu is used to attract bottomfish while fishing and consists of finely chopped bait (and sometimes a filler material such wheat chaff, rice, or oats). Palu was released when the rig was at depth to attract and aggregate bottomfish. To reduce barotrauma, when possible, the rate at which the mainline was pulled when a fish was hooked was slowed to facilitate some compensative off gassing of the swim bladder during ascent while still pulled at a rate fast enough to limit predation by sharks.

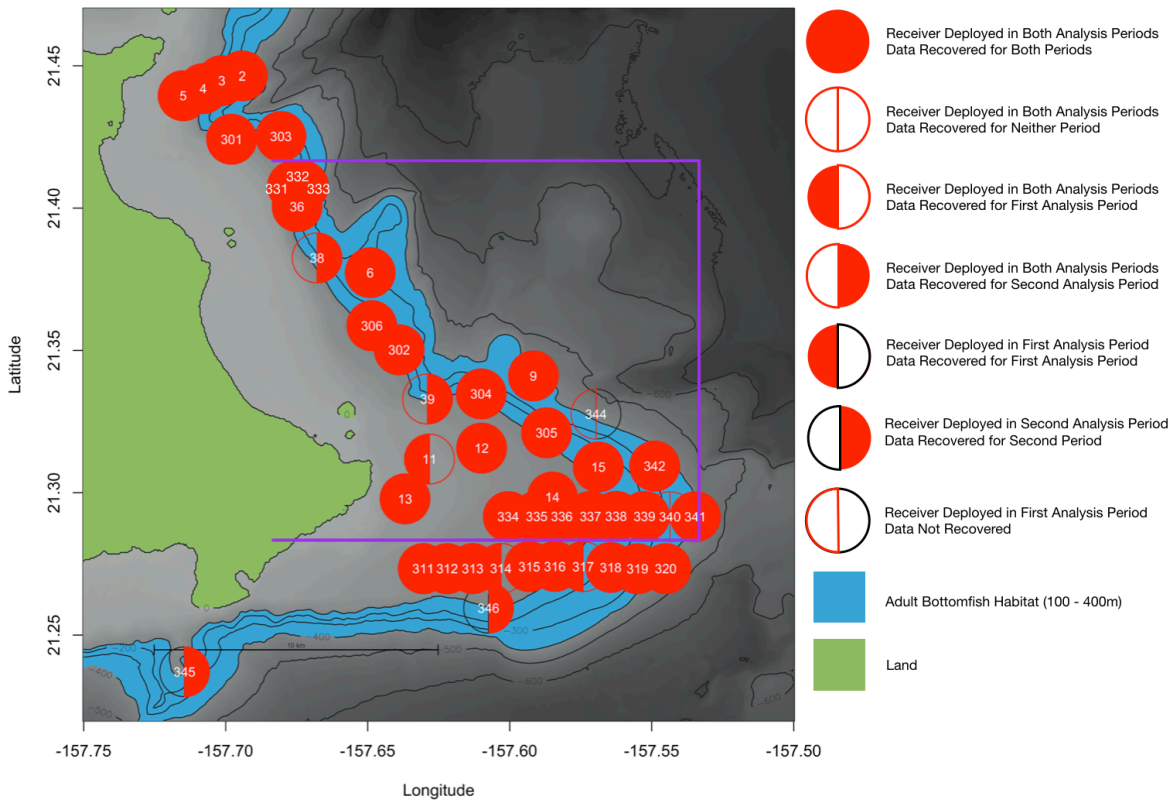

Figure 3.1. Chart Showing the Station Array Deployed During Analysis Periods 1 and 2. *The boundaries of BRFA-E are shown by the purple bounding box. Solid red circles show receiver stations that were successfully deployed, recovered, and downloaded. Open red circles show stations that could not be recovered or downloaded (station loss, data failure). Adult bottomfish habitat (100-400 m) is highlighted in blue while green represents land.*

Fish were brought aboard the vessel for surgical tagging and then immediately released back to the wild. Once the hook was removed, fish that were deemed acceptable for tagging were placed ventral side up in a padded v-board cradle. Sea water was pumped over the gill surface using a saltwater hose or a recirculating pump to provide the fish oxygen. Routine venting of the swim bladder is not recommended for this species (O'Malley, 2015) so venting was only performed if symptoms of barotrauma were severe and was conducted by puncturing the swim bladder or protruding stomach with an 18-gauge hypodermic needle stored in disinfectant. An incision between 1.5 and 2.5 cm in length was made with a sterile scalpel along the fish's ventral

centerline anterior to the urogenital pore. An acoustic tag was inserted into the peritoneal cavity through this opening along with triple antibiotic cream. The incision was closed using sutures (Ethicon PDS&Plus antibacterial monofilament, Ethicon US LLC) and secured with a surgeon's knot. When conventional dart tags were available (4-inch PDS-2, Hallprint PTY Inc, Hindmarsh Valley, South Australia), fish were tagged externally between the lateral line and the dorsal fin. Dart tags were provided by the Pacific Islands Fisheries Group as part of a long-term mark-recapture program. On-deck handling times were typically less than 5 minutes.

Two types of acoustic tag were used in the study, one with a depth sensor and one without. Each acoustic tag transmitted a unique ultrasonic identifier once every 90 to 200 seconds (nominal transmission interval 145 seconds). V13 transmitters had an expected battery life of 2.25 years and provided only presence data, while V13P tags had an expected battery life of 1.63 years and provided both records of both presence and depth.

To determine the size range of fish suitable for tagging, V13 (non-depth recording) and V13P (depth recording) tags were weighed. The minimum size of *P. filamentosus* eligible for tagging with each type of tag was calculated using a conservative 2% of bodyweight threshold and a species specific allometric relationship between fork length and weight (Uchiyama and Kazama, 2003). The minimum fork length suitable for tagging was 31 cm for V13 tags and 33 cm for V13P tags.

Four main strategies for release were used in an attempt to balance rapid recompression and predator avoidance: (1) Release at the seafloor using a drop shot device (Blacktip Brand, n = 74), (2) midwater release (30 – 60 m) using a drop shot device (Seaqualizer Brand, n = 70), (3) surface/near surface release (n = 18), and (4) driving the vessel rapidly away from the fishing

location before release, either at the surface (n = 8) or using the drop shot device (n = 2). The method of release was not recorded for 3 individuals.

To directly assess the impact of barotrauma and surgery on *P. filamentosus*, we built a mid-water net-pen (approximately 1.5 m high, 2.5 m diameter) and used it to hold a tagged fish at 20 m depth following capture and surgery. After 30 - 60 minutes we descended to the net-pen using SCUBA and observed the fish, noting condition and ability to orient and maintain neutral buoyancy. We then opened the net pen, allowing the fish to swim free and observed its swimming ability. This was conducted for 4 individuals.

Acoustic Monitoring

The location of fish in the study area was inferred from patterns of presence and absence at receiver stations. Each receiver station consisted of an acoustic receiver (VR2-W or VR2-AR, Vemco Ltd, Halifax, Nova Scotia, Canada) and acoustic release (VR2-AR, Vemco Ltd, Halifax, Nova Scotia, Canada or LRT, Sonardyne International Ltd, Yateley, Hampshire, UK) buoyed by three or four trawl floats and anchored to the seafloor with approximately 80 kg of concrete. Each mooring line was sheathed within a 1.5-inch diameter PVC tube to minimize the potential for entanglement or fraying.

Individual receiver stations formed a larger tracking array that monitored the movement of tagged fish in the study area. The tracking array was made up of five sub-arrays representing either fence or sparse configurations (Figure 3.1). A ‘fence’ sub-array is a line of receivers deployed with overlapping detection regions so that a tagged fish transiting the ‘fence’ will be detected. The fences were designed to detect individuals crossing BRFA borders. Because a fence placed on the border would detect fish located inside or outside the BRFA, it was necessary to have two fences – one outside the BRFA at a distance from the border greater than

the receiver's detection range, and another located inside the BRFA's border by a similar distance. Four fences were deployed with one pair monitoring the northern border and the other at the southern border. Placement of each fence was optimized with respect to the probability of detecting a tag transmission at a receiver across a range of depths, the bathymetry along the fence's transect, the height of the receiver from the seafloor, the desired height of the water column to be monitored, the swimming speed of the species, and a minimum 25% probability of detecting any given transmission from a tag.

The probabilities of detecting transmissions from tags across a range of distances were determined through range testing experiments. Results of range experiments showed that 5% of tag transmissions could be heard at a distance of 847 m from the receiver. One quarter of tag transmissions were detectable at a distance of 545 m and 12.5% of tag transmissions were detectable at a distance of 765 m (Scherrer et al, 2018). Therefore, to achieve a 25% detection rate, spacing between adjacent receivers in a fence configuration could not exceed 1,530 m. To be conservative, the fence algorithm was initialized with a 12.5% detection range of 600 m and a 25% detection range of 500 m. Receiver stations were deployed from the vessel over the target location and were allowed to sink freely to the seafloor. Using the position of the vessel at the time of deployment as the station's position, the largest distance between two receivers in any of the fence configurations was 1,232 m, within the minimum 1,530 m spacing requirement.

A 'sparse' sub-array is a group of receivers with non-overlapping detections regions, used to detect movements around a region, but with much of the region unmonitored. In this study, the sparse sub-array area was used to monitor individual movements between areas within the BRFA. Individual receiver positions within the spar se sub-array were determined in iterative stages using the Acoustic Web App telemetry optimization algorithm (Pedersen, Burgess, and

Weng, 2014) and 50 m and 1 km bathymetry of the Hawaiian Archipelago (Johnson and Potemra, 2011). Sparse sub-array deployment locations were selected within the bounds of BRFA-E after constraining depth between 75 and 475 m. Aggregations of up to 100 *P. filamentosus* have been observed from manned submersibles 2–10 m above the seafloor in the Penguin Banks region (Haight, 1989; Haight, Kobayashi, and Kawamoto, 1993; Kelley and Moriwake, 2012), so a preferred depth above the seafloor of 6 m was selected. A maximum receiver detection range of 847 m was specified using results from deep-water range tests we have previously reported (Scherrer et al., 2018).

Receivers in relatively deep water are particularly susceptible to close proximity detection interference (CPDI), a phenomenon where a receiver may fail to detect transmissions from tags at close distances (Kessel et al., 2015a; Scherrer et al., 2018). Results from predictive modeling indicate that CPDI occurs for receivers in depths exceeding 200 m. However, CPDI is not believed to have affected the detection of fish transiting through receiver fence sub-arrays as multiple transmissions would be sent by a tagged fish while within the detection range of the receiver before and after encountering the region affected by CPDI.

Data Analysis

Categorizing Fish Status

An algorithmic process was developed to sort fish detected on the receiver based on features of their tracks using a decision tree (Figure 3.2). High post-release mortality and moderate to high rates of single station residency made determining fish status non-trivial. Simply, it is difficult to distinguish a fish with a small home range near a single receiver, from a tag laying on the bottom near a receiver. Our algorithm assigned tracks to one of three categories: expired tracks from fish that are dead, valid tracks from fish believed to be alive, and uncertain tracks in which a track

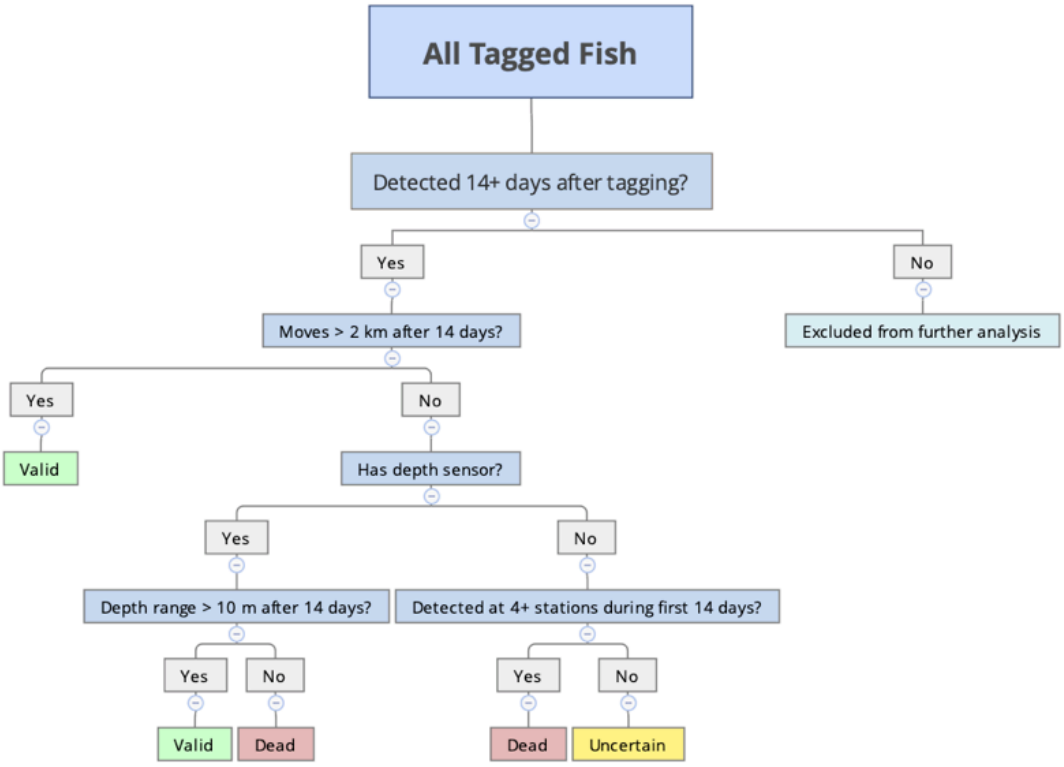

Figure 3.2. Mortality Decision Tree.

A flowchart outlining the algorithm used to classify the fate each tagged fish from features of their detection record.

could not be determined. Following classification, we reviewed records of each tag and made adjustments to status where appropriate.

It is similarly difficult to distinguish a rapidly moving tagged fish from a shark that has eaten a tagged fish, so we tagged several predator species to assist in parameterizing the classification algorithm. We tagged 8 sandbar sharks (*Carcharhinus plumbeus*), one silky shark (*Carcharhinus falciformis*), and one Galapagos shark (*Carcharhinus galapagensis*). All tagged sharks were detected on the receiver array during the analysis period. Their behavior patterns were characterized by frequent movement between stations (mean movements per day = 8.94, standard deviation [SD] = 10.7 movements per day), detection at multiple stations in a single day (mean stations detected per day: 3.5, SD = 1.6 stations per day), and movement over large

distances (mean linear home range = 18.1 km, SD = 5.7 km). Since a meal eaten by a predator is likely to be digested and the tag regurgitated within about one week (Medved, 1985), we doubled this time period to be conservative, and defined 'shark-like' movement as detection at 4 or more stations during the first 14 days of the track. Tags exhibiting 'shark-like' qualities followed by cessation of movement were used as indication of a predation event. Tracks shorter than 14 days were discarded (as these might be *P. filamentosus* that are inside a shark's stomach).

Further classification was based on horizontal movement. Range testing indicated that under the optimal conditions, tag transmissions could be detected by receivers up to a distance of 1,000 m, so detections on two receivers less than 2 km apart could be from a stationary tag laying between them. Therefore, fish with tracks that moved between two stations separated by more than 2,200 m after the 14th day post-tagging were considered valid.

If no movements were observed for a given individual, their status could still be classified if their tags were capable of reporting depth. Following the 14th day, a valid status was assigned to tracks from individuals with depth-sensing tags where vertical movement range exceeded 10 m. This threshold was selected as it is greater than the maximum fluctuation in depth that could be explained by tidal changes alone.

Tags lacking depth sensors that did not move after 14 days were classified as dead if they had a strong shark-like movement pattern at the beginning of the track. The status of a fish detected at fewer than 4 stations during the first 2 weeks of the track was uncertain. Visual inspection of tracks belonging to these fish were indistinguishable from stationary tags belonging to fish that were known to be dead while also resembling highly resident fish that were known to be alive from depth records. The group tags with an uncertain status likely includes a mixture of

both valid tracks from highly resident fish that were detected consistently at a single receiver and detections of stationary tags belonging to fish that died after they were tagged.

Testing for Size-selective Survivorship Bias

Correlation between body size and survivorship outcome for tagged *P. filamentosus* was tested by comparing the distribution of fork lengths from fish with valid tracks to the total population of tagged fish. A subset of fork lengths equal in number to the fish with valid tracks was selected at random from the total population of fork lengths without replacement. The mean and standard deviation of this subset of fork lengths were calculated, and the process was repeated 10,000 times. These summary statistics were used to calculate 95% confidence intervals to compare the size of surviving *P. filamentosus* with all *P. filamentosus* that were tagged.

Analysis Periods

Data were split into two analysis periods because receiver losses caused the tracking array to change, making early and late data not comparable. Five stations were lost midway through the study and replaced, meaning data for these stations exists only for the later period. Three receiver stations were lost later in the study, such that data for these sites exists only for the early period. Because the stations lost during redeployment and recovery differed, the realized tracking arrays during these two periods are of non-comparable shapes (Figure 3.1). The first analysis period began on 26 May 2017 and lasted until 15 April 2018. The second analysis period began 6 May 2018 and lasted until 6 January 2019.

Calculating Individual Home Range

A number of methods for quantifying home range have been proposed with application varying depending on the technology and method used (Stickel, 1954; Stumpf and Mohr, 1962; Schadt et al., 2002; Börger et al., 2006; Dwyer et al., 2015). Since adult *P. filamentosus* are associated with

a narrow depth band, their habitat can be thought of as a river winding along island slopes and flanked by areas where individuals are unlikely to occur. In similar systems, a constrained linear home range estimator has been shown to provide a more robust estimate of space-use when compared to minimum convex polygon, kernel utilization, and other common methods used to quantify home range (Dwyer et al., 2015). A constrained linear home range estimator was used to calculate the home range size for each individual based on their known locations from detection records.

The home range distance for each individual was calculated as the least cost path between receivers at which a given individual was detected. Paths between receivers were constrained to depths between 100 and 400 m using a least-cost path algorithm from the marmap package, vers. 1. 0.3, in R, vers. 3.5.0 (Pante and Simon-Bouhet, 2013; R Core Team, 2014). In effect, if the linear path between two stations crossed a depth falling outside this range, the pathfinding algorithm would shift to the nearest point with a depth inside the acceptable range, resulting in a longer path consistent with present knowledge of bottomfish habitat use.

Comparing Home Range Distance to BRFA Size

Least cost home range estimates for *P. filamentosus* were compared to a metric of the linear habitat available within each of the 8 BRFAs. Since BRFAs include both preferred and non-preferred habitat, we quantified a linear habitat dimension for each BRFA using the same depth-constrained least-cost path algorithm that was used to calculate individual fish home ranges. For the 7 BRFAs located along slopes, a path was calculated between the two sides of the BRFA's boundary intersecting bottomfish habitat using 50 m resolution bathymetry. The start and end points for each path were 120 m, the preferred depth of *P. filamentosus*. The East-West distance

across the rectangular area was used to define its linear habitat dimension of the BRFA containing depths exclusively within defined bottomfish habitat.

Quantifying Movement Frequency and Site Fidelity

Detections from fish on receiver fences were used to determine the proportion of time individuals spent within protected areas of the study site and the frequency of movements across reserve boundaries. A fish would move into the reserve when a tag was detected at a receiver outside of the reserve followed by a detection at a receiver inside the reserve and similarly a fish moved out of the reserve if it was detected first at a receiver inside the reserve followed by a receiver located outside. The fraction of time an individual was within the reserve was standardized by the total time that individual was tracked to calculate their proportional time of protection. The number of movements across reserve boundaries was then standardized by the track duration, defined as the number of days elapsed between the first and the final detection of a tag on the array during the analysis period to estimate the frequency at which they moved between protected and non-protected areas.

Results

Fish Capture and Tagging

Between 9 January 2017 and 11 January 2018, 179 *P. filamentosus* were tagged and released within the Makapuu study area. One hundred twenty five of the 179 fish were also tagged with conventional dart tags. All fish tagged were larger than the 15 cm minimum size requirement. Tagged fish ranged in size from 34 to 76 cm (median = 45.5 cm, IQR: 41 - 53 cm). Tag IDs of 168 fish were detected at least once on the receiver array between 26 June 2017 and 6 January 2019. Sixty-eight of the detected tags were depth sensing and transmitted pressure data in addition to the unique ID.

None of the fish held in the net pen showed symptoms of severe barotrauma, with all four individuals maintaining neutral buoyancy and proper orientation. Each swam away once the net pen was opened. However, between 2 and 5 sharks were observed in near proximity within 10 minutes of each deployment of the pen.

Categorizing Fish Status

Of the 168 tracks from tagged *P. filamentosus* detected on the array between 26 June 2017 and 6 January 2019, 10 were classified valid, 35 classified as uncertain and 83 classified as dead. Tracks of 40 individuals with track durations less than 14 days were excluded from analysis and 11 tags were not detected on the array during the analysis period (Table 3.1). The classification algorithm initially assigned 30 tracks a valid status, however 20 of these tracks were reclassified post-facto with 12 tracks reclassified uncertain while 8 appeared dead. These tracks were reclassified due to faulty depth sensors, detection patterns that could be otherwise explained by a tag on the seafloor detected only under optimal acoustic conditions, or diurnal depth patterns that closely resemble those of the six-gill shark (*Hexanchus griseus)* (Comfort and Weng, 2014). The following analyses are for the 10 fish with valid tracks. Because the group of uncertain tags likely contained a mixture of tags from fish that are dead and alive, a less conservative analysis that includes these additional tracks is included as supplemental material to this manuscript.

Under the assumption that only the fish with valid tracks survived after tagging, the survivorship rate was 5.8%. Because some fish were tagged prior to the start of the study, track duration, defined as the time between each individual's first and last detection on the array, was used to compare and standardize results between individuals. This is in contrast to time at liberty which would encompass the period from an individual's tagging until it's last detection but

Table 3.1. Status of Tagged Fish

The number of tracks sorted by classification status as determined by the classification algorithm and after researcher reclassification.

Status	n Tracks (Algorthmically Determined)	n Tracks (After Reclassification)
Valid	30	10
Uncertain	24	36
Dead	74	82
Excluded from Analysis	40	40
Undetected	11	11
Total	**179**	**179**

would be inappropriate for standardizing analysis results as it would also count days before the analysis period began. Valid tracks ranged in duration between 35 and 538 days (Median = 393 days, IQR: 280 74 days) (Table 3.2).

Testing for Size-selective Survivorship Bias

The mean fork length of P. filamentosus with valid tracks (42.6 cm) fell within the 95% confidence interval from simulation data sampled without replacement (42.1 - 54.5 cm). However, the standard deviation (2.8 cm) did not fall within the 95% confidence interval from simulation data sampled without replacement (4.9 - 14.4 cm). This result indicates that the mean size of surviving fish was not significantly different than expected for a random subset of the total population, and the smallest and largest fish tagged were underrepresented in the data (Figure 3.3).

Analysis Periods

Receivers were recovered and downloaded twice, once mid-study and once at the end of the study, separating the analysis into two periods. All 10 fish with valid tracks were detected on the receiver array during the first of these periods with 8 fish appearing on the array during the

Table 3.2. Descriptive Metrics of Tagged Fish.

Descriptive metrics of valid tracks from tagged opakapaka for analysis period 1 (P1) and period 2 (P2).

Tag ID	Status	Fork Length (cm)	Tagging Date	Time at Liberty (days)	Track Duration (days)	Transmissions Detected	Unique Days Detected	P1: Home Range (km)	P2: Home Range (km)	Boundary Movements Detected	P1: % Time In	P2: % Time In
2133	Alive	43	1/9/18	190	35	457	28	7.19	1.706	6	99%	100%
2136	Alive	42	1/9/18	452	335	21062	301	6.018	2.354	0	100%	100%
28179	Alive	45	1/11/18	454	339	60130	339	5.484	3.778	69	98%	98%
30695	Alive	36.5	8/28/17	716	453	3605	297	9.375	2.354	2	100%	100%
30705	Alive	40.5	8/29/17	724	474	17055	462	8.12	8.12	86	99%	97%
30721	Alive	45	6/24/17	856	538	64477	538	3.242	6.018	0	100%	100%
51582	Alive	41	3/18/17	380	280	8109	222	3.778	0	0	100%	0%
51586	Alive	46	3/18/17	961	447	39084	447	3.242	3.664	0	100%	100%
51588	Alive	44	3/18/17	286	186	16105	186	9.374	0	6	80%	0%
51596	Alive	42.5	8/28/17	726	475	44371	475	3.242	6.018	0	100%	100%

second. During the first analysis period (26 June 2017 – 15 April 2018), two receiver stations from the fence sub-arrays were lost, station 323 (ranged depth: 325 m) and station 340 (ranged depth: 324 m) (Figure 3.1). Losing Station 323 truncated the northern fence so that the 25% minimum detection threshold extended to an estimated depth of 370 m rather than 400 m as planned. Losing Station 340 left a gap in the southern boundary fence inside the BRFA. The possibility that *P. filamentosus* could move into the BRFA through this gap undetected cannot be ruled out. During the second analysis period (6 May 2018 – 6 January 2019) three stations from the fence sub-arrays were lost (Figure 3.1). Stations 314 (ranged depth: 78 m) and 317 (ranged depth: 150 m) were part of the southern fence outside the BRFA. Station 340 (ranged depth: 331 m), part of the southern fence inside the BRFA, once again broke free of its mooring and was recovered. The receiver's logs indicated that it broke free of its mooring within three weeks of deployment. The gaps caused by these losses during the second period mean that during this time, it was possible for tagged individuals to move into and out of the BRFA undetected.

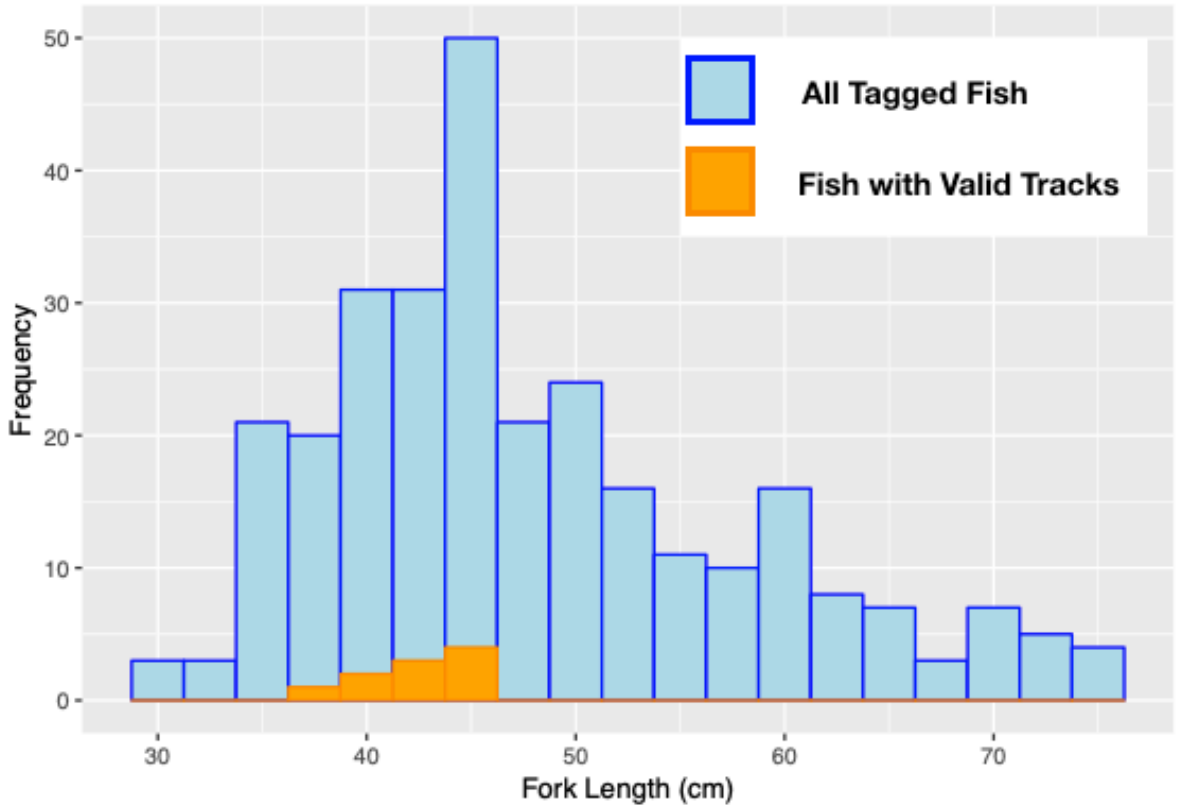

Figure 3.3. Fork Lengths for Tagged Fish.

Orange bars show the distribution of fork lengths for tagged P. filamentosus with valid tracks and blue bars indicate all P. filamentosus tagged during the duration of the project. Simulation results show that the observed distribution mean of fork lengths for fish with tracks classified valid was within the range expected from the total population data, however the observed standard deviation of the distribution was smaller than would be expected if survivorship was random.

Calculating Individual Home Range

Estimates of linear home range distance for the first analysis period varied between 3.2 km and 9.4 km. The median observed home range distance was 5.8 km (IQR: 3.2 - 8.1 km). Home ranges observed during the second analysis period were between 1.7 km and 8.12 km with a median length of 3.7 km (IQR: 2.4 - 6.0 km). Regardless of period, the median home range

calculated for any fish during the study was 6.0 km (IQR: 5.5 - 8.1 km). Across the study, no fish was detected moving more than 9.4 km and the result of a t-test comparing the home ranges calculated for period one and two was not significant ($P < 0.05$) indicating that observations of home range size were consistent between both periods.

Comparing Home Range Distance to BRFA Size

The median linear habitat dimension of the BRFA network was 11.40 km (IQR: 8.32 - 16.02 km) (Figure 3.4). With the exception of BRFA-B, home ranges observed for *P. filamentosus* were less than the linear habitat dimension of the BRFAs (Figure 3.5).

Quantifying Movement Frequency and Site Fidelity

Tracked fish generally stayed within the protection of reserve boundaries. During the first analysis period, 5 of the 10 fish with valid tracks were detected crossing BRFA boundaries a combined 39 times. Site fidelity was high; on average, fish detected in this period spent 97.7% of their time within the BRFA (SD = 6.2%). For the fish that moved between protected and unprotected areas, the median number of total movements across BRFA boundaries was 6 crossings/fish (IQR: 6 - 12 crossings/fish) over a track duration of 280 days (IQR: 230 - 293 days). Standardized by track duration, the median number of movements into or out of the BRFA for the 5 fish was 0.043 crossings•day^{-1}•fish^{-1} (IQR: 0.021 - 0.057 crossings•day^{-1}•fish^{-1}) equivalent to one crossing every 23.3 days. However individual rates were as high as 0.064 crossings/day, equivalent to crossing once every 15.7 days.

Two of eight live fish detected during the second analysis period crossed the BRFA's boundary a combined total of 130 times (74 times and 56 times) each over a track duration of 245 days. On average, the 8 fish spent the majority of their time, 99.3% (SD = 6.2%), within the BRFA. Standardized by their track lengths, these two fish crossed into or out of the BRFA 0.229

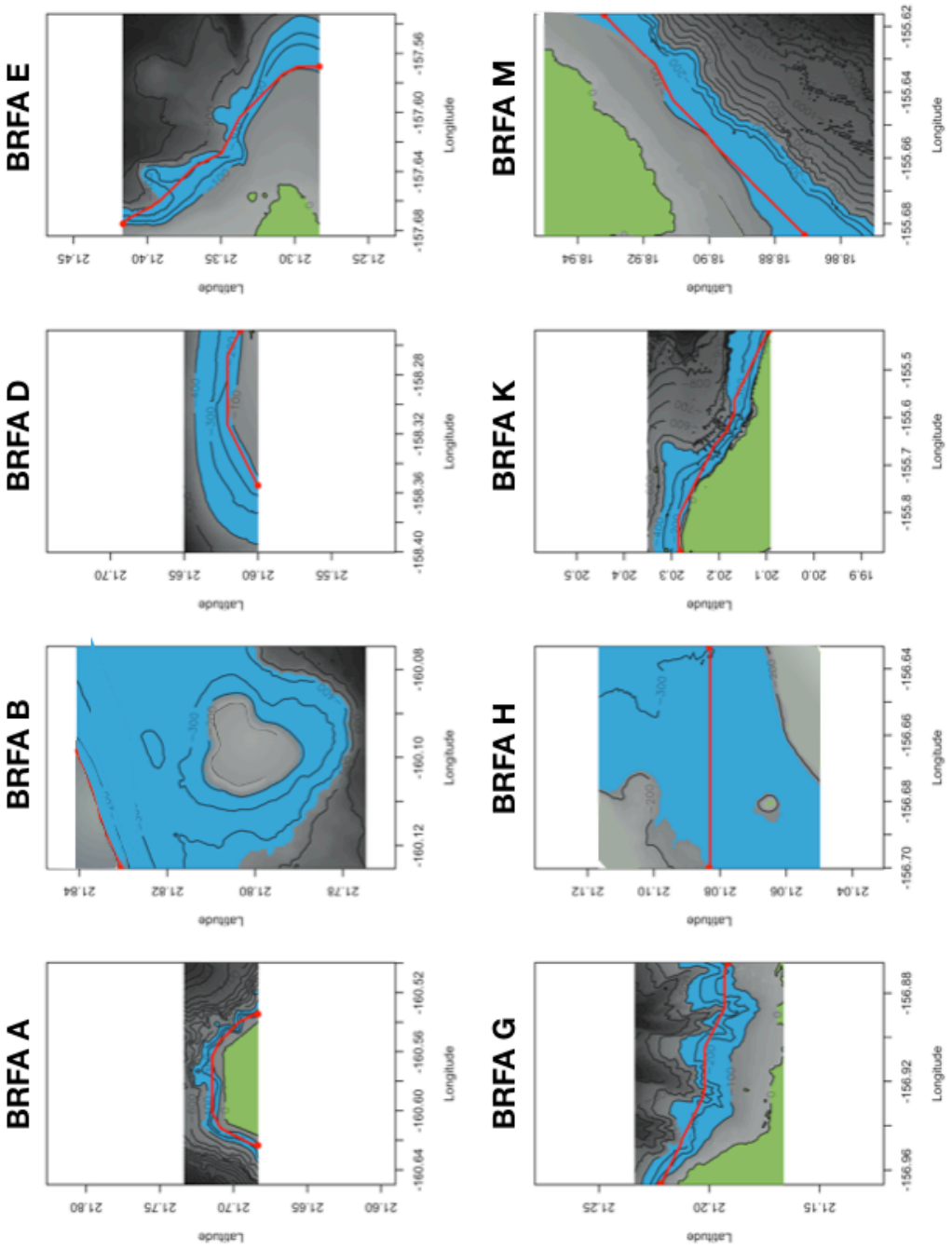

Figure 3.4. Maps of the 8 BRFAs Used to Calculate Their Linear Habitat Dimension. *BRFA Boundaries correspond to the boundaries of each plot. The least cost path approach calculated the distance across the BRFA starting and ending at the 120 m contour. The blue highlighted area indicates the 100 – 400 m depth range used to constrain each path. The red line shows the shortest (least-cost) path through the BRFA.*

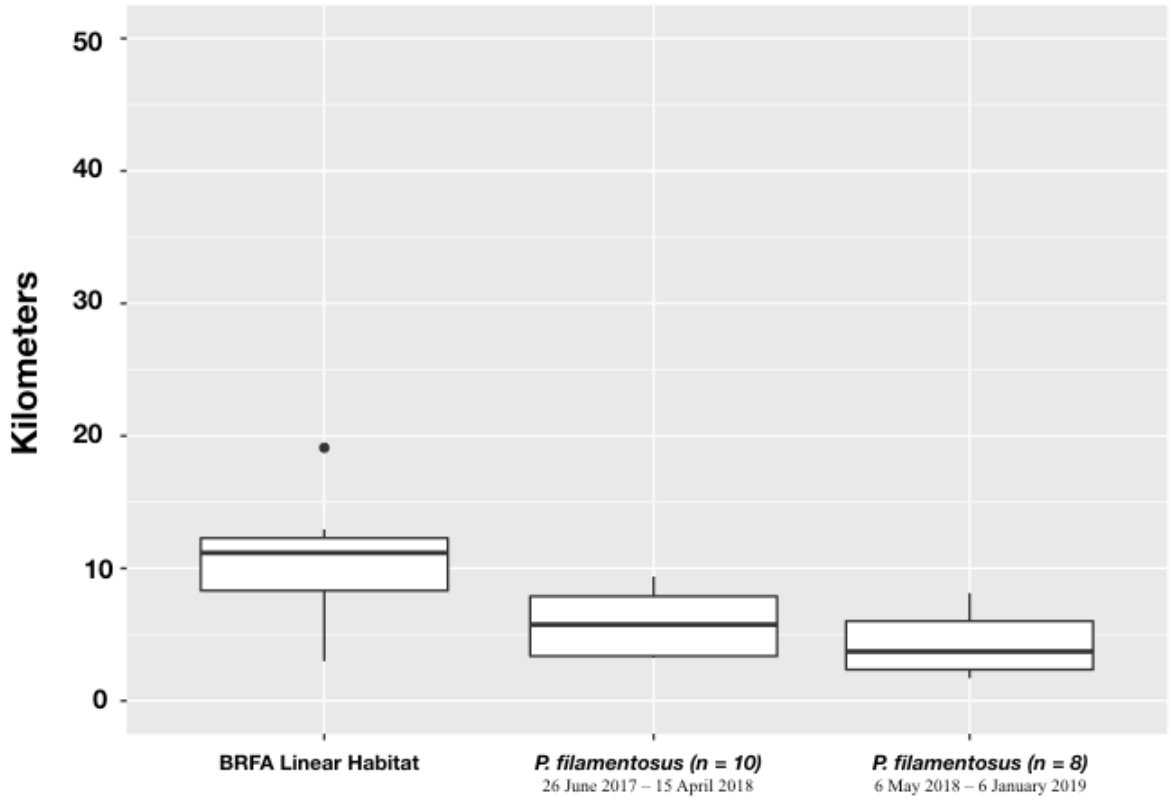

Figure 3.5. Comparing Observed Ranges to BRFA Size.

Comparison of the linear home range distances calculated for P. filamentosus (Valid tracks only) to the linear habitat dimensions of the 8 BRFAs.

and 0.302 times per day respectively, corresponding to a crossing occurring every 4.4 and 3.3 days.

Regardless of analysis period, the 10 fish were detected within the BRFA on 97.6% (SD = 6.2%) of days they were tracked. In total, 226 movements were detected between protected and non-protected areas made by 5 fish over a median track duration of 339 days (IQR: 186 - 453 days). These fish moved across boundaries at a rate of 0.17 crossings•day^{-1}•fish^{-1} (IQR: 0.03 - 0.18 crossings•day^{-1}•fish^{-1}) or one crossing every 5.8 days.

Discussion

In this study, *P. filamentosus* were monitored using acoustic telemetry to compare individual fish home range to the scale of Hawaii's BRFAs. The observed linear home ranges of fish with valid tracks were similar to each other in magnitude and smaller than the linear habitat dimension of BRFA-E, where the fish were tracked. We were unable to detect any long-range movements of *P. filamentosus* because it is not possible to detect acoustic tags beyond the range of the detection array. However, our findings are supported by conventional tagging experiments for the species where the majority of fish (> 85%) were recaptured within 10 km of their tagging location (O'Malley, 2015; Uehara et al., 2019).

When broadening our comparison to include the 7 additional BRFAs, we found that the average home range for tagged *P. filamentosus* was smaller than the minimum linear habitat dimension for all but one BRFA. It should be noted that the small linear habitat estimated for BRFA-B, located off Niihau, is not representative of the total habitat within the area. Since the method used to quantify linear habitat uses the shortest path across the BRFA, it does not account for the large offshore pinnacle within this reserve (Figure 3.4). When a similar least-cost path is applied around the pinnacle, the linear habitat of this reserve increases to 9.17 km.

Our results are consistent with baited underwater camera studies suggesting that the BRFAs do provide protection for bottomfish (Sackett, Kelley, and Drazen, 2017). Our results are also in agreement with the aforementioned conventional tagging work that has been done in the region where the majority of fish were recaptured in close proximity to their tagging location (Kobayashi, 2008; O'Malley, 2015).

Movements of *P. filamentosus* with tracks deemed valid in this study are within the range of those reported for other snappers of family Lutjanidae, characterized by high rates of site fidelity and limited home ranges with rare movements over long distances. Tinhan et. al (2014)

reported *Lutjanus argentiventris* were detected within a 0.61 km^2 fishery reserve in Baja California, Mexico on 49% ± 30% of days after they were tagged. In the Gulf of Mexico, *Lutjanis campechanus* were associated within 26.3 ± 35.4 m of artificial reefs (Piraino and Szedlmayer, 2014). In Hawaii, over 83.5% of tagged *Lutjanus kasmira* showed no discernable movement while 95% were recaptured within 150 m of their initial release location (Friedlander, Parrish, and DeFelice, 2002). Individuals of the Deep-7 species *E. carbunculus* and *E. coruscans* tracked relative to BRFA-B off the island of Niihau spent almost all of their time within the reserve and were detected moving at scales up to 8.9 km (Weng, 2013). Even larger ranges have been described for *Aprion virescens,* a bottomfish not included in the Deep-7 management unit, where individual movements up to 18 km have been reported (Meyer, Papastamatiou, and Holland, 2007). Movements of *P. filamentosus* deemed "alive" in this study fall between these reported ranges. Ranging experiments informed the 2.2 km movement criteria used to categorize fish status. Therefore, any tracks from surviving individuals with movement at smaller scales would have been classified "uncertain" and are included in a less conservative analysis described in the supplemental material. Note that movement for any such individual would still fall within the scale of protection offered by the BRFAs.

While genetic panmixia has been reported for *P. filamentosus* across the Hawaiian archipelago, there is growing evidence to support spatially structured approaches to management (Gaither et al., 2011). Panmixia can occur even through a limited exchange of larvae and adult individuals, but large-scale exchanges are required to support spatially distinct populations (S. Wright, 1931; Botsford, Micheli, and Hastings, 2003). Large-scale movements greater than 300 km have been reported for tagged *P. filamentosus* but the conventional mark-recapture studies and the high degree of site fidelity observed here indicate that these movements are rare[6]

(Kobayashi, 2008). Furthermore, simulation models of larval dispersal across the archipelago indicate larvae is primarily retained in four self-sustained zones with only limited advection (Vaz, 2012).

Post-release survivorship estimates in this study were low, between 5.6 and 25.7% depending on the inclusion of tracks with uncertain status. The low survivorship rates in this study mirror those of conventional mark-recapture work where observed recapture rates for the species were 2.5%[6], 12% (Kobayashi, 2008), and 8.7% (Uehara et al., 2019). Survivorship rates as high as 66.7% were reported for *P. filamentosus* tagged with acoustic transmitters in the Kahoolawe Island Reserve[6], however survival was based on detection of the tag on at least one receiver and no further steps to ascertain survivorship were performed. In this study we applied a rigorous approach to determining the status of our fish. Using our classification algorithm approach, only 30.8% of *P. filamentosus* tagged in the Kahoolawe study had tracks exceeding 14 days. When discussing these results with a co-author of this study, they indicated that tagged fish were evaluated at the surface upon release and those in poor condition were recaptured and their tag removed[2].

Mortality following tagging is a major challenge to study the movement of deep-water fishes (Edwards et al., 2019). The two major drivers of mortality in this study are thought to be barotrauma and predation. Deep-7 species are physoclystic, that is, the gas bladder is not open to the gastrointestinal tract, making them particularly susceptible to barotrauma injuries from expansion of the swim bladder during rapid ascent following hooking (DeMartini, Parrish, and

[2] Kelley, C. 2019, Personal Communications. Department of Oceanography, University of Hawaii, 1000 Pope Rd, Honolulu, HI, USA 96822

Ellis, 1996; Edwards et al., 2019). Severe injury may result in organ damage and death (Rogers, Lowe, and Fernández-Juricic, 2011). Methodological studies to mitigate barotrauma in deep-water rock fish (genus: *Sebastes*) indicate that slow ascent rates, limited on-deck handling times, and rapid recompression improve survivorship outcomes (Parker et al., 2006; Jarvis and Lowe, 2008; Rogers, Lowe, and Fernández-Juricic, 2011; Samuel J. Hochhalter and Reed, 2011; Pribyl et al., 2012). External symptoms of barotrauma observed during this project included esophageal eversion and exophthalmia due to swim bladder expansion. Rapid release of air and deflation of the body cavity while making the peritoneal incision was not uncommon and likely caused by rupturing of the swim bladder. Barotrauma can also lead to physical and behavioral impairment that can lead to subsequent predation (Rankin et al., 2017).

Predation by sharks, jacks, and marine mammals was also a significant source of mortality. While fishing, a number of *P. filamentosus* were consumed partially or totally by predators during ascent. Detection records from 65 tagged fish show a series of rapid movements between receivers immediately after tagging followed by no further detections or persistent detection at a single receiver. This behavior is consistent with the tagged fish being inside the stomach of a predator with movement cessation occurring with expulsion of the tag. We suspect that palu, an attractant used to aggregate bottomfish, also attracted predators, and exacerbated the issue. Future studies would be wise to first consider how variation in tagging methods may offset mortality associated with tagging these and other deep living fishes. With such high rates of post-release mortality, protocols that reliably improve survivorship for this species should be explored.

Acoustic telemetry has an established history for evaluating fishery reserve efficacy but application at greater depths in this study is relatively novel and presents a number of unique

challenges compared to studies in shallow water environments (Arnold and Dewar, 2001; Heupel, Semmens, and Hobday, 2006; Grothues, 2009; Farmer et al., 2013; Pedersen, Burgess, and Weng, 2014; Edwards et al., 2019). A considerable amount of array hardware associated with each receiver station was deployed over the duration of this study to operational depths exceeding those accessible by SCUBA. These additional requirements necessitated servicing of receiver stations from a suitably sized vessel and introduced additional points of uncertainty and failure for receiver stations.

Close proximity detection interference (CPDI) is a factor that must be accounted for when deploying acoustic tracking arrays at depths exceeding 200 m (Scherrer et al 2018). Using a conservative model for predicting CPDI and a detection range of 847 m, we estimated that at 20 m above the seafloor, CPDI effects could extend between 70 m and 451 m from the receiver depending on the receiver's depth. This model assumed no energy was lost at the seafloor and sea surface interfaces and should be considered a "worst case scenario". Given the nominal transmission rate of the tags used and assuming an average swimming speed of 1 body length per second, we do not believe CPDI affected our ability to detect the passage of tagged fish transiting through receiver fence sub-arrays. However, if tagged individuals spent extensive time near receivers, CPDI may have led to an underestimation of residency rates.

The loss of several stations reduced the capacity of the array to monitor fish within and transiting into or out of the BRFA. Under the assumption of random walk behavior, theoretical detection rates were calculated using the Acoustic Web App corresponding to the recovered arrays from both periods. We estimate that receiver losses reduced the proportion of monitored habitat (100 – 400 m) within BRFA-E from the planned 27.0% to 23.2% during the first analysis period. During the first period, the loss of receiver stations 330 and 340 from fence sub-arrays

within the BRFA introduced the potential for undetected passage for individuals that transited into the BRFA, which would result in an underestimation of site fidelity within the BRFA. As observed site fidelity within the BRFA was quite high, it is unlikely that potentially undetected movements significantly alter the conclusions of this analysis. During the second analysis period, loss of stations 317 and 314 from the outer southern fence sub-array and station 340 from the interior southern fence sub-array create a path where fish could theoretically swim undetected between protected and non-protected waters. The loss of these stations means that detected movements between protected and non-protected regions may underestimate true movement frequency and site fidelity within the reserve during this period.

Conclusion

179 *P. filamentosus* were tagged and at least 10 were tracked moving around the bottomfish reserve area located off of Makapuu, Hawaii with track durations that averaged 418 days. High mortality was likely driven by a combination of barotrauma and predation. Eteline snappers are increasingly fished throughout the Indo-Pacific, such that more efforts are needed to monitor their movements. Therefore, a comprehensive study to determine methods for improving survivorship across all size classes should be explored prior to undertaking future tagging of deep-water demersal fishes.

Observed home ranges ranged between 1.7 and 9.4 km and were smaller than the shortest distance required to traverse all but one of the 8 BRFAs. During both analysis periods, tracked fish spent 80% or more of their time within the protected waters of the BRFA, and moved between protected and non-protected waters on average once every 23.3 days (5 of 10 tracked fish or once every 3.9 days (2 of 8 fish) depending on the tracking period. These results indicate that spatial protections at the spatial scale of Hawaii's BRFAs are an appropriate conservation

tool for *P. filamentosus* conferring protection to *the individuals* residing within these protected waters.

CHAPTER 4: MULTIPLE INTERVENTION BEFORE AFTER CONTROL IMPACT PAIRS: A FRAMEWORK FOR QUANTIFYING THE REDISTRIBUTION OF CATCH AND EFFORT COINCIDING WITH FISHERY RESERVES IN HAWAII'S DEEP 7 BOTTOMFISH FISHERY INFERED FROM CATCH DATA

Abstract

Fishery reserves are a management tool that restrict fishing for particular species to provide refugia for fish conservation or assist with rebuilding overfished stocks. In 1998, a network of fishery reserves was implemented for the Hawaiian bottomfish fishery in response to an assessment that the stock was overfished. With an improved understanding of bottomfish habitat, these reserves were modified in size and number prior to the 2008 fishing year. At present, the stock has recovered; the stock is no longer overfished and no overfishing occurring but the contribution of the reserve network to the fishery's recovery is poorly understood. Our goal was to quantify changes in effort, fisher participation, and catch that occurred within the fishery under various management periods and examine if these changes differed between areas with and without protected habitat. We also evaluated each reserve by quantifying changes in metrics of effort and harvest for each area before and after protection. Both catch and effort declined after reserves were implemented and revised and have since remained at similar levels. Effort and catch were disproportionately lower in reporting areas that contained protected habitat relative to adjacent unprotected areas, but the magnitude of their response differed depending on the total amount of habitat within a reporting area, the percentage that was protected, as well as the management period. While the mean individual's median annual catch per trip rose with revision of the reserves, disproportionately fewer fish were harvested per trip by fishers from reporting areas containing protected habitat.

Introduction

Fishery reserves are a popular tool for fishery managers to protect, rebuild, and enhance fish stocks. Mortality from fishing can act as a strong selector on a stock by truncating size and age structures. For heavily fished or overfished populations, lowering the fishing mortality rate by reducing effort can result in enhanced abundance and a greater number of larger older fish (Russell, 1931, 1942; Bellail et al., 2003; Rochet and Trenkel, 2003). Fishery reserves may benefit fishers directly when larger fish accumulate and spillover to adjacent fished areas or indirectly when the higher fecundity associated with older, larger female fish results in greater recruitment (Kikkawa, 1984; M.A. Hixon, Johnson, and Sogard, 2014). Fishery reserves can also protect a portion of a region's fish stock, acting as insurance for managers against overfishing (Sale et al., 2005; Planes, Jones, and Thorrold, 2009).

Successful fishery reserves balance biological, political, and socioeconomic factors to reach their desired outcomes (Lundquist and Granek, 2005). However, the design of fishery reserves can be ad-hoc, the result of political or social processes and, despite their popularity as a management option, biological considerations of the protected species may be neglected (Halpern, 2003). Also important but frequently overlooked is the impact of restricted access on the fishers that depend on these areas for profit or subsistence (Christie, 2004; Slijkerman and Tamis, 2015; Oyafuso, Leung, and Franklin, 2019). Reserves of insufficient size or placement may fail to adequately protect vulnerable fish populations while protection at scales too large may negatively impact fishers relying on these resources (Kramer and Chapman, 1999; Botsford, Micheli, and Hastings, 2003; O'Dor et al., 2004; Sale et al., 2005). Therefore, it is important that the effects of reserve areas on both the fish and fishery are evaluated.

A deepsea species complex of bottomfish made up of snappers, jacks, and one endemic grouper is the target of Hawaii's second largest commercial fishery (CH Moore et al., 2013). The

fishery is managed in reference to seven species, referred to as the deep 7, using annual catch limits and a network of fishery reserves known as the bottomfish restricted fishing areas (BRFAs). Nineteen BRFAs were established to assist with rebuilding the overfished components of the bottomfish complex through localized reductions in fishing effort and associated mortality prior to the 1999 federal fishing year (FY) (Ikehara, 2006; Amendment 14 to the fishery management plan for bottomfish and seamount groundfish fisheries of the Western Pacific region, 2007). In 2006, the Pacific Islands Fishery Science Center determined that Main Hawaiian Islands bottomfish stock remained overfished (Moffitt, Kobayashi, and Dinardo, 2006). In response, the fishery was temporarily closed and the BRFAs redesigned prior to the start of the 2008 FY using an improved definition of bottomfish habitat. This revised system reduced the total number of closed areas from 19 to 12 while protecting a greater amount of adult habitat which is strongly predicted by depth, slope, bottom hardness and rugosity (Table 4.1) (Parke, 2007; Oyafuso et al., 2017). Since 2010, stock assessments have indicated the fishery is no longer in an overfished state nor is overfishing occurring and thus has recovered (Brodziak et al., 2011; Brodziak, Yau, O'Malley, Andrews, Humphreys, DeMartini, et al., 2014a; Langseth et al., 2018). Answering fundamental questions regarding the long-term effects of the BRFA system on the bottomfish stock and fishing community is critical to evaluating the utility of these areas and informing the future management of the fishery.

Ecological effects of the BRFAs have been studied through baited camera and tagging experiments. Baited camera studies have indicated that the size and abundance of some bottomfish species increased in the BRFAs after they were revised (Sackett et al 2014) and that spillover might have occurred as suggested by a decrease in fish size and abundance with

Table 4.1: BRFA Area and Habitat.

The total area and amount of bottomfish habitat (km^2) estimated for each BRFA during the implementation and revision management regimes.

BRFAs - Implementation

BRFA ID	Total Area (km^2)	Habitat Area (km^2)	Nearest Island
1	50.3	32.1	Niihau
2	23.2	12.2	Kauai
3	22.7	14.8	Kauai
4	16.2	5.0	Oahu
5	14.1	10.0	Oahu
6	10.2	9.7	Oahu
7	5.4	5.1	Oahu
8	12.8	10.8	Oahu
9	51.8	26.5	Molokai
10	54.7	31.4	Molokai
11	94.5	40.8	Molokai
12	70.4	38.6	Molokai
13	91.2	65.7	Maui
14	18.2	3.3	Maui
16	44.5	25.3	Hawaii (Big Island)
17	47.6	19.5	Hawaii (Big Island)
18	74.3	8.2	Hawaii (Big Island)
19	37.9	8.2	Hawaii (Big Island)
20	98.1	10.5	Hawaii (Big Island)
Total	838.0	377.9	-

BRFAs - Revision

BRFA	Total Area (km^2)	Habitat Area (km^2)	Nearest Island
A	85.9	18.2	Kaula Rock
B	40.8	32.1	Niihau
C	50.8	23.8	Kauai
D	84.9	55.8	Oahu
E	189.2	56.6	Oahu
F	268.6	155.8	Molokai
G	60.5	26.0	Molokai
H	51.2	48.8	Molokai/Maui
J	161.0	40.8	Maui
K	907.3	325.6	Hawaii (Big Island)
L	118.2	22.7	Hawaii (Big Island)
M	53.6	15.0	Hawaii (Big Island)
Total	2072.0	821.3	-

increasing distance from two of the BRFAs that strengthened over time (Sackett, Kelley, and Drazen, 2017). Additionally, tracking studies of key species components of the complex indicated that the current reserves are likely appropriate in scale to provide benefits to the fish (Weng, 2013, Scherrer & Weng, In Prep).

However, the BRFAs remain controversial amongst fishery participants. Many fishers view the reserves as ineffective and unnecessary in consideration of separate restrictions on the annual harvest (Hospital and Beavers, 2011). Fishers have also raised concerns that these areas have had the unintended consequences of reducing the number of participants in the fishery, limiting access to traditional fishing grounds, and cite safety concerns and economic hardships associated with traveling farther to fish unrestricted areas (Minutes of the 158th meeting of the Western Pacific Regional Fishery Management council, 2013).

Beyond before-after-control-impact-pairs (Beyond BACIP) approaches are a powerful study design for assessing response to a disturbance or intervention (Osenberg et al., 1994; S R Palumbi, 2001; Russ, 2002; Gell and Roberts, 2003; Sale et al., 2005; Smith, Zhang, and Coleman, 2006; Miller and Russ, 2014). Beyond BACIP or Beyond BACIP-derived approaches test hypotheses regarding the effects of fishery reserves by examining proportional differences between pairs of affected (impacted) and unaffected (control) sites before and after changes in management strategy (Miller and Russ, 2014). These approaches accounts for explicit spatial relationships and are robust to temporal autocorrelation (Underwood, 1992). Beyond BACIP designs are frequently used to assess the policy effects of reserve areas on the size and abundance of fishes (Meyer, 2003; Lincoln-Smith et al., 2006; Francini-Filho and Moura, 2008; Mateos-Molina et al., 2014) and distribution of fishing effort (Smith, Zhang, and Coleman, 2006) associated with implementation and removal of reserve areas (Kulbicki et al., 2007).

However, the Beyond BACIP approach is insufficient for testing the effect of multiple interventions. We propose a modified design of the Beyond BACIP approach to quantify changes resulting from multiple interventions. This Multiple Intervention Before-After-Control-Impact-Pairs design (MIBACIP) accommodates additional events while retaining the spatial and temporal benefits of the Beyond BACIP approach. The flexibility of this method also makes it possible to account changes with time and intrinsic differences between areas, such as habitat quantity, which have been previously identified as concerns with the standard framework (Pelletier et al., 2008; Thiault, Osenberg, and Claudet, 2017). We've applied this method to assess changes in the bottomfish fishery associated with the BRFAs, and to understand the relative contribution of these areas to patterns in overall effort distribution, fisher participation, individual effort allocation, total harvested biomass, and average landings per trip. Finally, we've

used this method to evaluate the relationship between redistributed effort and harvest for each individual reserve in the BRFA networks.

Methods

Commercial Fishing Data

The State of Hawaii requires commercial fishermen to submit information on their catch in the form of individual trip reports to the Division of Aquatic Resources (DAR)(Hawaii Administrative Rules §13-74-20 - Commercial marine license, 1998). These records date back to the mid 1940s. The database contains an entry for each species landed on each trip along with pertinent information including the species landed, quantity of pieces and pounds caught, gear type used, the date fishing occurred, port of landing, the fisher's commercial marine license number, and more. These reports are linked to the location where fishing occurred through the state's statistical reporting grids (Figure 4.1). Access to this database was granted to researchers through a memorandum of understanding between DAR and the Hawaii Institute of Marine Biology with the stipulation that trip reports from reporting areas with 3 or fewer reported fishers in a given year were removed prior to analysis to maintain confidentiality. Trips where no catch was reported were also removed from the dataset because reporting these trips is not mandatory, and it is therefore unlikely that the zero-catch trips reported accurately reflect the frequency that these trips occur.

Identifying Overall Changes in the Deep 7 Fishery

Linear models were used to evaluate the total number of trips, total number of fishers, total number of pounds harvested, and the average pounds landed per trip reported for the commercial fishery over a 27-year period. For each hypothesis, the variable being tested (e.g.: number of fishers, pounds landed, etc.) was aggregated by fishing year (FY; September 1-August 31) and

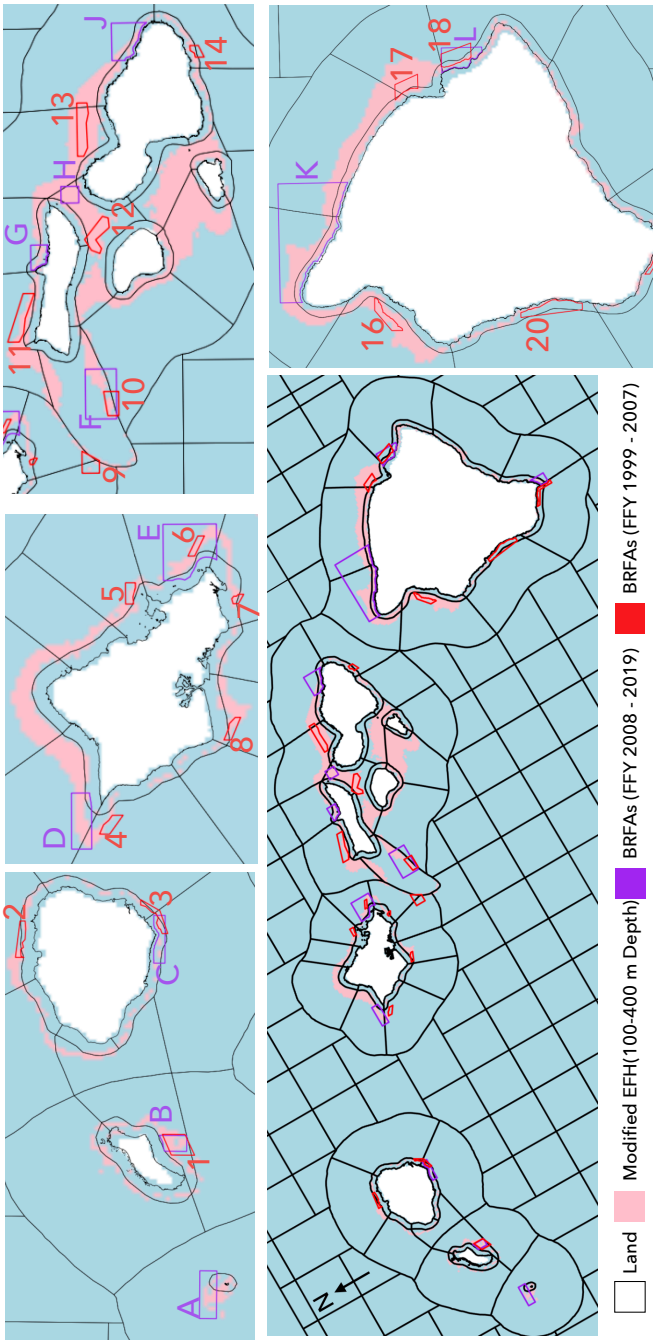

Figure 4.1. Map Indicating the Boundaries of Hawaii's Statistical Reporting Areas and Bottomfish Restricted Fishing Areas (BRFAs).

Map of the Main Hawaiian Islands overlain with the state's statistical reporting grids. The locations of the original 19 BRFAs (1999-2007 FY) are indicated by red polygons while the revised BRFAs (2008-Present) are bounded and labeled in purple.

associated with a management regime. Management regime was specified as a factor with three levels, each corresponding to one of the three periods each consisting of 9 years of data. The "before" period referred to data from FY 1990-1998, prior to introduction of the BRFAs. The regime referred to as "implementation" covered the introduction of the initial 19 BRFAs in FY 1999 through FY 2007. Finally, data from FY 2008 through FY 2016 coinciding with the restructure of the BRFAs into the 12-area configuration and was referred to as "revision". Changes associated with each regime period were tested by comparing values from the before and revision regime periods to the implementation period.

This process was relatively straightforward for effort, participation, and total harvest hypotheses and more complicated for hypotheses of individual effort allocation and average landings per trip. When comparing the total annual trips, total annual fishers, and total pounds harvested annually the corresponding values in the data were summed by year, assigned to a regime, and modeled. When quantifying trends in individual effort, the number of trips each fisher reported was summed annually and then an annual mean was used to compare across all fishers. To quantify average catch per trip, the median pounds of bottomfish landed on each trip annually was determined for each fisher. The median value was used because it provided a robust indication of overall change in an individual's catch over many trips, while the mean value, susceptible to outliers, could be skewed by just one or two trips where an individual's catch was exceptionally high. To generalize across the fishery, the mean of the median annual landings for each fisher was then used to assess changes in landings per-trip. Henceforth, when we refer to average landings per trip we are referring to the mean of the median pounds landed per trip for each individual fisher annually.

Identifying Trends Between Protected and Unprotected Areas

To investigate how spatial management policies may have contributed to overall changes in the fishery, we applied the MIBACIP analysis framework using the same commercial marine landings data to comparing reporting areas containing protected habitat to adjacent unprotected areas following implementation and revision of the BRFA system. To understand how this approach differed, it is helpful to first understand the Beyond BACIP framework.

Traditionally the Beyond BACIP framework identifies pairs of impacted and control areas. The data series is divided into a series of time steps and a delta value is calculated for each control-impact pair at each timestep. Delta values are defined as the difference in value of a metric of interest between an impacted area and its paired control areas. A statistical model is constructed to compare delta values before and after intervention. Absent any intervention, impacted and control areas change in similar ways in response to natural drivers of variability such as cohort recruitment, regional productivity, et cetera. If the relative trajectory of impacted and control areas differs following the intervention, this is manifest as a significant difference between the deltas of pre- and post-intervention periods (Underwood, 1992). The Progressive Changes BACIPs, proposed by Thiault et. al. (2017), expand on this framework to allow for an intervention to produce a delayed temporal response.

Several issues arise when applying these methods towards understanding changes to the bottomfish fishery. The largest is that not one, but two interventions have occurred (implementation and subsequent revision of the BRFA network). Second, there is mismatch between the boundaries of the BRFAs and the statistical grids used to report commercial landings. To resolve these issues, we've modified the linear progressive change BACIP approach to allow us to compare paired areas through time. The conventional approach to modeling the relative trajectory between areas pairs by calculating delta values across fixed time steps is

retained, but unlike the traditional framework, where the areas of each pair are assigned a fixed status of control or impact, individual reporting areas can change status depending on intervention period. Rather than comparing deltas after an intervention to those preceding it, we model the difference between deltas of each status and compare their trajectory relative to deltas calculated from area pairs without protected habitat.

The first step of applying the modified framework was to define the pairs of areas used to calculate each delta value. Area pairs consisted of a primary and comparison area selected from DAR's statistical reporting grids and were analogous to impacted and control areas under the traditional BACIP approach. The primary area of each pair was an area that contained some amount of protected habitat under either management regime. An area pair was defined for each combination of primary area and each of its comparison areas, selected by identifying adjacent reporting areas from the same island group.

Delta values were calculated as the relative difference between primary and comparison areas compared to the average of these areas before reserves were implemented. This was accomplished through the following method:

$$\Delta_{i_j t} = \frac{P_{i,t}(9n) - \sum_{i=1,t=1990}^{i=n,t=1998} P_{i,t}}{\sum_{i=1,t=1990}^{i=n,t=1998} P_{i,t}} - \frac{C_{i_j t}\,(9m) - \sum_{j=1,t=1990}^{j=m,t=1998} C_{j,t}}{\sum_{j=1,t=1990}^{j=m,t=1998} C_{j,t}}$$

Where $\Delta_{i_j,t}$ represents is the delta calculated between the i^{th} of n primary areas (P) at timestep t and j^{th} of m comparison areas defined for the i^{th} primary area at the same timestep. Numeric coefficient 9 is the number of years in the data before reserves were implemented. Each delta was assigned a status based on the corresponding status of the primary and comparison area. Each individual area could have 1 of 3 statuses in a given year: 1. Control areas were those

reporting areas that did not contain and had not previously contained protected bottomfish habitat. 2. Impacted areas were areas that contained protected bottomfish habitat during the year for which the delta was calculated. These were further categorized as "implementation" and "revision" depending on the management regime. 3. Reopened areas were areas that were impacted during the implementation regime but no longer contained protected habitat after the BRFAs were revised. Deltas calculated for pairs where neither area contained protected habitat (control:control), where the primary area contained protected habitat but the comparison area did not (implementation:control, revision:control), and pairs where the primary area had contained protected habitat under the implementation regime but was reopened during the revision period and the comparison area never contained protected habitat (reopened:control) formed the basis for statistical modeling.

Inclusion of missing or zero data was dictated by each hypothesis. For total effort, fisher participation, and total harvest hypotheses analyzed at the fishery level, when one or more area of a delta pair was missing data, zero was substituted for the missing value. This corresponded to areas where no trips were taken, no harvest occurred etc. (in other words, these zeros reflected a real value). Deltas calculated from pairs where one or both areas lacked a value were omitted when comparing individual effort allocation and average landings per trip. For the former case, each fisher does not fish in every reporting area and therefore including zero data would substantially bias the mean trips to each area towards zero such that models would be uninformative. The later would imply a trip reporting zero catch when in fact no such trip had occurred.

Delta values were modeled using the following structure:

$$delta \sim status + time\_protected\_implementation + time\_protected\_revision + (1 \mid primary) + (1 \mid comparison)$$

When fit to a single intervention, this model structure is functionally the same as a Progressive-Change BACIP with a linear temporal component and retains the spatial and temporal benefits of the approach. As with this approach, we assumed that prior to intervention, all areas behave similarly, with the factor level control:control serving as the model's intercept. The remaining factor levels of the status predictor were used to indicate if the relative trajectory of implementation:control, revision:control, and reopened:control deltas differed significantly under these conditions. The terms time_protected_implementation and time_protected_revision corresponded to the years a primary area was protected under implementation and revision periods, respectively and indicated if the trajectory of the associated deltas changed with time. When one or more of the time predictors was not significant, it was removed, and the model was refit. All modeling was performed in R using the function lmer from the package lmerTest (R Core Team, 2014; Kuznetsova, Brockhoff, and Christensen, 2017).

Assessing Individual Reserves

Finally, the performance of individual BRFAs within the network was assessed. This was accomplished by iteratively applying the MIBACIP method to only the area pairs associated with each individual reserve. While the pervious analysis sought to generalize the impacts of multiple interventions across the fishery, this approach charted the progression of individual areas. Each reserve was evaluated by the displacement of total effort (number of trips) and harvest (harvested pounds) using deltas from control:control pairs and the corresponding impact:control pairs (implementation:control for the BRFA configuration during the implementation period and revision:control for the revision configuration). For a given BRFA, a positive shift in deltas

associated with an intervention indicated an increase in effort or catch across area pairs relative to the same pairs prior to protection, while negative values represented decreases in these metrics. Because these areas were evaluated individually, it was important to compare changes as both the percent deviation from the mean of the areas prior to protection, as was done previously, and by subtracting the raw value of each comparison area from the primary area. This distinction is important because, for example, a 50% reduction in fishers for an area that is seldom fished could be as little as two fewer fishers, but for a more popular area with 20 fishers, an equivalent reduction would require to a fivefold reduction in the number of fishers.

Results

In total, 155 area pairs were identified from 51 primary areas. Forty-five primary areas had three comparison areas, three primary areas had four comparison areas, and the remaining three primary areas had one, two, and five comparison areas. This produced a set of 2,547 deltas for the 27 years analyzed. Control:control area pairs accounted for 64.0% of all deltas, while 19.1% were from implementation:control pairs, 9.9% from revision:control pairs, and 7.1% of deltas were from reopened:control area pairs.

Effort

The management periods associated with the BRFA network corresponded to significant decreases in effort across the fishery. In the period following reserve implementation, the number of trips declined by 1,181.67 (Standard Error = ± 211.78) annually ($p < 0.05$). The multiple intervention BACIP model indicated significant differences in effort between reporting areas containing protected habitat and those that did not, with effort in areas containing protected habitat decreasing an additional 33.52% (± 8.05%) relative to pre-BRFA levels ($p < 0.05$). The time an area was protected during this regime period was also significant, as the difference

between protected areas and adjacent control areas narrowed, on an average, 3.11% (± 1.31%) each subsequent year.

After the BRFA system was revised, total effort was not significantly different from the preceding regime period ($p < 0.10$). Similar to the implementation period, the multiple intervention model indicated trips to areas containing protected habitat declined an additional 33.50% (± 10.59%) relative to adjacent areas that remained open to fishing ($p < 0.05$). Time was again a significant factor, with the gap between these areas narrowing by approximately 4.21% (± 1.77%) annually ($p < 0.05$). Deltas calculated between areas that contained protected habitat during under the implementation management regime that were subsequently reopened to fishing and those that were never protected did not differ significantly from those calculated for areas where both were unrestricted ($p < 0.05$). The linear model describing general fishery trends had an R^2 of 0.609 while the MIBACIP model had a marginal R^2 of 0.003 and a conditional R^2 of 0.830 (Table 4.2, Figures 4.2A & 4.3A).

Fisher Participation

Fisher participation also decreased following implementation of the BRFA network. On average, 109.88 (± 21.54) fewer fishers reported catching bottomfish following the introduction of the reserve network ($p < 0.05$). Comparing deltas calculated from reporting areas affected during this regime period and adjacent control areas to deltas calculated for area pairs where neither area was protected indicated the number of fishers in protected areas decreased an additional 28.32% (± 5.85%) relative to the period before the BRFAs were implemented ($p < 0.05$) but the time an area was protected during the implementation regime was a significant predictor, indicating that values from areas containing protected habitat and their unprotected neighbors grew more similar by 2.35% (± 0.87%) annually.

There was some evidence that fisher participation increased following revision of the BRFA network. On average 40 (± 21.54) additional fishers reported catch annually during this time ($p < 0.10$). The number of fishers reporting catch in areas containing protected habitat relative to adjacent control areas was 23.52% (± 4.20%) less than areas pairs where neither area was protected ($p < 0.05$). During this regime, the trajectory of delta pairs calculated for these area pairs did not differ significantly with time ($p > 0.10$). Similarly, there were no significant differences between deltas for areas where the primary area was reopened and those from control:control pairs ($p > 0.10$). The linear model describing the fisher participation across the fishery had an adjusted R^2 of 0.487 and the MIBACIP model had marginal and conditional R^2 values of 0.005 and 0.863 respectively. (Table 4.2, Figures 4.2B & 4.3B)

Allocation of Individual Effort

There was a decrease in the mean number of trips each fisher reported in the period following the implementation of the BRFA network. During this period the mean trips per fisher annually decreased by 0.663 (± 0.299) trips. There was no evidence to suggest a disproportionate decline of trips per fisher for reporting areas containing protected habitat relative to those without on the basis of a delta pair's status, however with each subsequent year these areas were protected, the mean number of trips per fisher increased significantly by 3.32% (± 1.64%).

The mean number of annual trips per fisher further decreased after the BRFAs were revised. Following revision, fishers reported, on average, 0.799 (± 0.299) fewer annual trips. The number of trips per fisher to areas containing protected habitat relative to unprotected areas during this time did not immediately differ from the relative number of trips fishers reported to unprotected area pairs ($p > 0.10$), however the number of trips to protected areas relative to unprotected areas increased annually by 5.60% (± 2.26%) during this regime period indicating

progressively more trips to areas with protected habitat relative to control areas ($p < 0.05$). The adjusted R^2 of the model describing the mean number of trips per fisher across the whole fishery was 0.459, while the MIBACIP model had a marginal R^2 of 0.012 and a conditional R^2 of 0.231 (Table 4.2, Figures 4.2C & 4.3C).

Harvested Biomass

The annual biomass of deep 7 fishes harvested by the commercial fishery decreased after the BRFAs were implemented. On average, the annual number of pounds fishers reported landing fell by 91,065 pounds (± 22,196 pounds) during this period ($p < 0.05$). Deltas from pairs where the primary area contained protected habitat were significantly lower than pairs where neither area was protected. The difference between deltas calculated between implementation:control pairs and control:control pairs was -21.56% (± 6.43%) indicating catch was redistributed away from areas with protected habitat ($p < 0.05$). There was not a significant relationship between the time these areas were protected and their delta values ($p > 0.10$).

The overall biomass harvested annually did not differ significantly after the BRFAs were revised compared to the implementation period ($p > 0.10$). However, once the areas were revised, the relative distribution in harvest further shifted from areas with protected habitat to those without, such that unprotected areas accounted for roughly twice of the catch of revision:control pairs (Est = -46.25% ± 7.91%, $p < 0.05$). Like the implementation period before, there was no significant relationship between deltas calculated for these pairs and the time the primary area was protected ($p > 0.10$). Catch in reporting areas that were reopened following the implementation period was also down 29.05% annually relative to their comparison areas compared to their control:control counterparts ($p < 0.05$). The adjusted R^2 of the linear model

describing widespread changes in harvested biomass was 0.390. The marginal R^2 of the MIBACIP model was 0.020 and the conditional R^2 was 0.255 (Table 4.2, Figures 4.2D & 4.3D).

Average Landings per Trip

The average pounds landed per trip remained fairly consistent between management regimes. The mean of the median annual catch per fisher was unchanged between implementation and revision periods ($p > 0.10$). The relative trajectory of reporting areas containing protected habitat decreased an additional 15.12% (± 6.28%) relative to areas which did not contain protected habitat ($p < 0.05$).

There was marginal support suggesting that average landings per trip increased by 6.33 pounds following revision of the BRFA network ($p < 0.10$). During this time, the average landings per trip differed significantly between areas containing protected habitat and unprotected areas. Deltas calculated for these areas indicated a relative decrease of 23.70% (± 7.41%) in pounds landed per trip in the affected area compared to deltas with control:control status ($p < 0.05$). Furthermore, the discrepancy between areas that contained protected habitat that was reopened to fishing during the revision period was even greater, decreasing in these areas by 27.01% (± 9.60%) compared to adjacent areas that were never protected. Like the prior period, there was no significant relationship between the time areas that were protected, and the corresponding delta values calculated for those area pairs ($p > 0.10$). The Adjusted R^2 of the linear model comparing the average landings per trip by management regime for the entire fishery was 0.194, while the marginal and conditional R^2 of the MIBACIP model was 0.013 and 0.241 respectively (Table 4.2, Figures 4.2E & 4.3E). Model summaries and diagnostic plots are presented in full for general trend models in Appendix 4.1 and for MIBACIP models in Appendix 4.2.

Table 4.2. MBACIP Model Results.

Parameter estimates and associated confidence intervals from delta (linear mixed effects regression) models used to quantify trends within the fishery based on protection status.

Predictor	H1: Total Trips	H2: Total Fishers	H3: Mean Trips per Fisher
Control:Control (Intercept)	25.31 (-27.41 - 78.07)	21.16 (-22.29 - 64.63)	-1.62 (-16.02 - 12.89)
Implementation:Control	-33.52 (-49.28 - -17.76)**	-28.32 (-39.77 - -16.86)**	-15.52 (-34.12 - 3.04)
Revision:Control	-33.5 (-54.23 - -12.77)**	-23.52 (-31.75 - -15.28)**	-15.93 (-42.37 - 10.49)
Reopened:Control	0.06 (-14.41 - 14.53)	-1.6 (-12.13 - 8.91)	12.35 (-4.94 - 29.78)
Time Protected - Implementation	3.11 (0.55 - 5.68)**	2.35 (0.49 - 4.22)**	3.32 (0.12 - 6.53)**
Time Protected - Revision	4.21 (0.74 - 7.68)**	-	5.6 (1.18 - 10.03)**
Observations	1629	1629	1081
R^2 *Marginal / Conditional*	0 / 0.83	0 / 0.86	0.01 / 0.23

Predictor	H4: Lbs Harvested	H5: Mean Lbs Per Trip
Control:Control (Intercept)	8.1 (-12.24 - 28.34)	-1.85 (-17.95 - 13.99)
Implementation:Control	-21.56 (-34.18 - -8.98)**	-15.12 (-27.46 - -2.84)**
Revision:Control	-46.25 (-61.72 - -30.66)**	-23.7 (-38.18 - -9.04)**
Reopened:Control	-29.05 (-48.74 - -9.42)**	-27.09 (-46 - -8.28)**
Time Protected - Implementation	-	-
Time Protected - Revision	-	-
Observations	1629	1081
R^2 *Marginal / Conditional*	0.02 / 0.26	0.01 / 0.24

* p < 0.10 ** p < 0.05

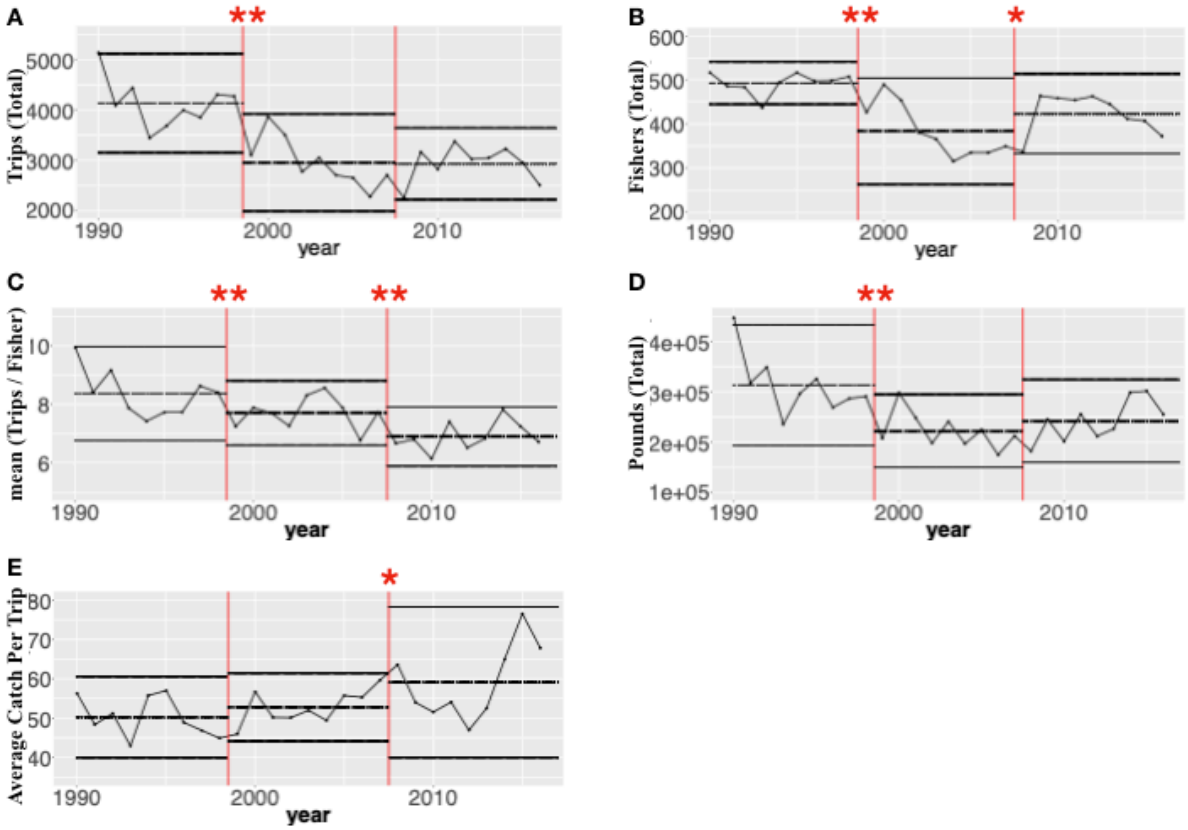

Figure 4.2. Comparing Fishery Wide Trends for Each Hypothesis Across the Three Management Periods.

Each plot shows the value of the response variable for each year between 1990 and 2016. The two red vertical dashed lines denote changes in management regime, before spatial management to initial implementation, and initial implementation to the revised network. Double asterixis above these lines indicate a significant difference between the two regimes ($p < 0.05$) while single asterixis indicate marginally significant differences ($p < 0.10$). Horizontal lines between each period denote the mean as well as two standard deviations above and below.

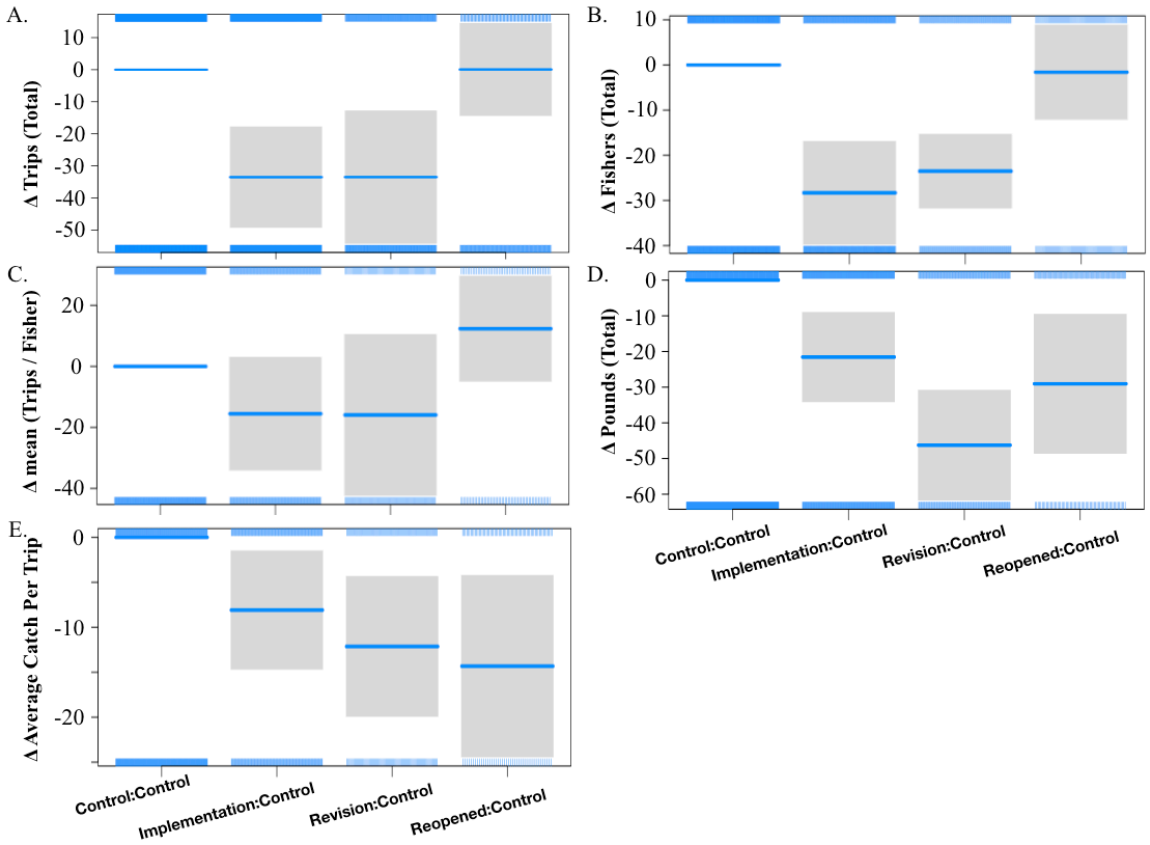

Figure 4.3. Contrast Plots Created from Predictions of MIBACIP Models.

Plots depict the difference in delta values between area pairs of different status. Control:Control areas are centered at zero such that area pairs that are lower indicate a decrease in the corresponding metric for the primary (impacted/affected) areas relative to adjacent control areas.

Assessing Individual Reserves

Comparing the raw values of the data, after the initial implementation of the BRFAs, 2 BRFAs had a persistent and significant change ($p < 0.05$) in effort relative to adjacent unprotected areas. These BRFAs were 17 and 18. Effort in area 20 increased after the reserves were implemented, initially there were fewer fishers in protected areas relative to adjacent reserves, but at the end of the regime period, the opposite was true. All of these areas were located around the island of Hawaii. Harvest in areas 17 and 20 did not significantly change when the reserves were

implemented, nor did harvest change with time. Harvest initially decreased in area 18 when the reserves were implemented but increased with time so that by the end of the implementation period there was no discernable difference from pre-implementation values. In areas containing BRFAs 1, 2, 4, 8, 9, 10, 11, 13, 16, and 19 total effort was persistently lower after implementation ($p < 0.05$) relative to the period before. Effort decreased significantly with time for areas 5 and 6. Of areas with significant negative effort displacement, there was an immediate, persistent, and significant decrease in harvested biomass from areas making up BRFAs 2 and 10 ($p < 0.05$). Relative harvest increased with time for areas making up BRFAs 1 and 16, decreased significantly ($p < 0.05$) for areas 4, 8, and 11, and decreased marginally ($p < 0.10$) for area 9. There was a significant increase ($p < 0.05$) in the number of pieces harvested for BRFA 12 and a marginally significant ($p < 0.10$) increase in the number of pieces harvested with time for BRFA 7, but no change in effort was detected ($p > 0.10$). No significant changes in harvest or effort were detected for area 14 ($p > 0.10$). Results were largely consistent between those obtained modeling raw values and those from a percent change-based method. Harvested biomass was no longer significantly different from the period before implementation for BRFA 10 ($p > 0.10$). While the quadrat relationship between the relative displacement of biomass and effort remained the same between periods, the position within each quadrat differed using this metric (Figure 4.4A & 4.4C)

Under the revised BRFA scheme, comparing models fit using raw values, effort only changed in areas making up BRFA L following reserve establishment, and this change was persistent ($p < 0.05$) while effort decreased significantly and was persistent in areas containing BRFAs A, B, D, F, and K ($p < 0.05$). Effort increased significantly with time for areas making

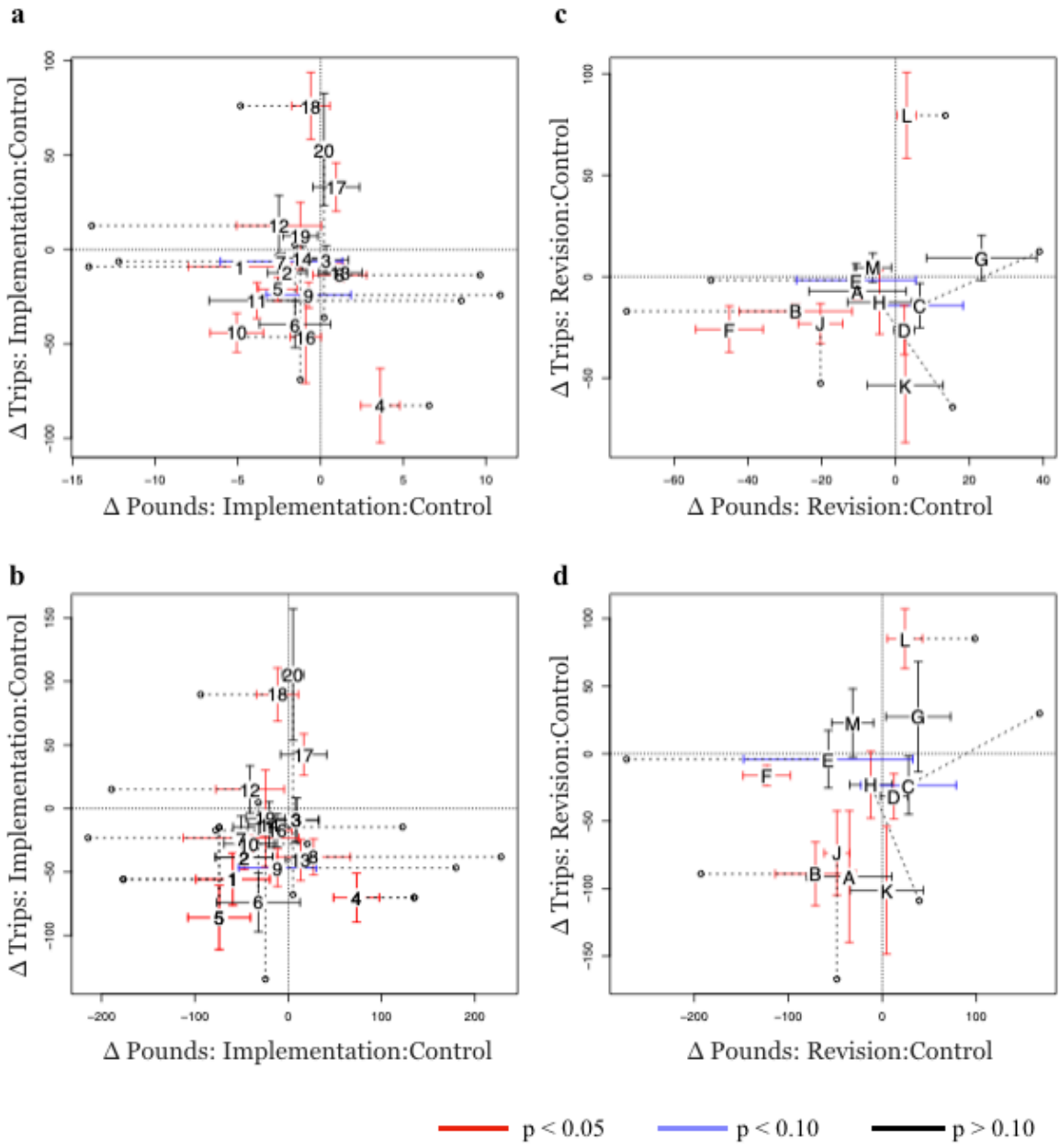

Figure 4.4. Relative Displacement of Individual BRFAs Under Each Management Period.

Comparing relative displacement, measured by delta, of the total number of trips (y-axis) and total number of pounds harvested (x-axis) for the BRFAs during both periods of spatial management relative to estimates before each area was protected. Each BRFA's number or letter corresponds to the location of the associated parameter estimates while bars provide the standard error associated with each. Negative values indicate areas where effort and/or harvest decreased in reporting areas containing protected habitat relative to adjacent

unprotected areas following establishment of the corresponding BRFA. When time was a significant predictor, the trajectory of parameter estimates is indicated by the dashed line which connects the position of parameter estimates at the beginning of the regime period (as indicated by a circle) and the position at end of the regime period (indicated by the area's ID and associated parameter error bars). The left column compares individual reserves during the implementation regime and the right column compares reserves during revision. The top row compares deltas using the percent change in an area relative to the areas before reserves were implemented while the bottom row compares delta values using raw, unstandardized, values.

up BRFAs H, and J relative to adjacent unprotected areas and decreased in areas making up BRFA C ($p < 0.05$). There was a significant and persistent decrease in areas making up F and J while catch in areas making up BRFAs B and E increased significantly with time ($p < 0.05$) and decreased significantly for areas making up BRFA C ($p < 0.05$). When the percent relative to before the BRFAs were implemented approach was used, areas again rearranged. Notably, the magnitude of displacement for BRFA F shifted, such that while a large number of trips were displaced, they accounted for only a small fraction of the percentage of overall trips in that area. Conversely, BRFA A experienced the opposite effect. Most of the relative relationships between BRFA areas were preserved when comparing displaced harvest, though BRFA E shifted places with J, indicating a greater displacement biomass in that area as calculated by a relative percent change (Figure 4.4B, 4.4D).

Discussion

The use of fishery reserves as a tool for managing fisheries, and efforts to study and quantify the effects of these areas, have only grown in the decades since Hawaii introduced the BRFAs. The most robust method for analyzing the effect of these areas on the dynamics of fisheries and ecosystems are methods derived from the Beyond BACIP design (Miller and Russ, 2014).

However, these methods have been limited to detecting the effect of a single intervention. Here we've proposed the MIBACIP design capable of accommodating such an analysis. Like Progressive Change BACIPs, MIBACIP also incorporates the effect of time and can control for heterogeneity through the incorporation of random effects. Both of these features are important considerations when comparing biological responses in spatially distinct areas (Pelletier et al., 2008; Miller and Russ, 2014; Thiault, Osenberg, and Claudet, 2017).

Applying this framework to commercial fishing data from Hawaii's deep 7 bottomfish fishery, we were able to assess changes in effort, fisher participation, mean trips per fisher, total harvest, and average landings per trip coinciding with two configurations of a fishery reserve network. Our results indicated disproportionate decreases in total effort, participation, and harvest between areas of the fishery containing protected habitat and those that did not while the average number of pounds landed per trip and number of trips per fisher were more variable. Beyond BACIP methods are often used to assess the ecological effects of fishery reserves on fish stocks, however application of these tools to quantify changes in fishery effort and fleet dynamics has received considerably less attention (Horta e Costa, Gonçalves, and Gonçalves, 2013; Rife et al., 2013; Stevenson, Portland, and Tissot, 2013; Abbot and Haynie, 2015; Batista et al., 2015). This study joins a growing body of work applying these methods to quantify the degree to which fishery reserves displace fishing activities.

Following the introduction of the BRFAs as a management strategy, overall effort (number of trips) declined significantly because there were significantly fewer fishers participating in the fishery, and significantly fewer trips made by each fisher, on average (Figure 4.2A-C). There were disproportionate decreases in effort and fisher participation in areas containing protected habitat, but evidence that the proportion of trips by the mean individual

changed was less compelling. This suggests that rather than adapting their fishing patterns, affected fishers left the fishery when their preferred fishing grounds were closed and this decrease in these fishers contributed to the changes observed in total effort. Discrepancies in the number pounds harvested per trip between areas containing protected habitat and those that did not persisted even when reserves were removed, perhaps suggesting the cultural knowledge of the most productive fishing grounds within the closed areas was lost when fishers left the fishery.

While the revision period saw a slight uptick in the number of total fishers, these results are potentially confounded by management decisions coinciding with BRFA revision. In 2008 the regional management council introduced a 5 piece recreational bag limit among other changes to incentivize recreational fishers to obtain commercial licenses (Fisheries in the Western Pacific; bottomfish and seamount groundfish fisheries; management measures in the Main Hawaiian Islands, 2008). At the time, recreational fishers are believed to have outnumbered commercial fishers approximately 2.1 to 1 but the number of recreational fishers that transitioned to the commercial fishery as a result of these changes is unknown because there were no licensing or reporting requirements for recreational fishers (Zeller et al., 2008).

Changes in individual fisher catch were not standardized with time in this analysis. This metric is analogous to catch-per-unit-effort (CPUE), used for stock assessment purposes in this fishery, however caution should be exercised when fishery dependent CPUE data is used to analyze policy effects on stock abundance without first accounting for increased catchability (Smith, Zhang, and Coleman, 2006). The widespread availability and adoption of GPS plotters, fish finders, and other technologies over the last three decades have dramatically increased the ability of fishers to seek out productive fishing grounds and precisely target aggregations of fish (Moffitt et al., 2011). CPUE standardization is accounted for in stock assessment models for this

fishery and these assessments are therefore a better indicator of abundance while the models here reflect the actual harvest by fishers during the period analyzed, decoupled from abundance (Brodziak, Moffitt, and DiNardo, 2009). This distinction may reflect why we did not find increases in individual fisher catch for reporting areas containing protected areas and support claims that relocated fishers were less productive. This could also explain why our fishery results differ from Sackett et al (2017) who showed positive ecological relationships between BRFA proximity and size and abundance of fish using fishery independent survey data.

In general, patterns of effort and harvest were positively correlated. After revision of the BRFA system, the total number of pounds harvested did not differ significantly from the implementation period but there was a marginally significant increase in the number of pieces harvested. This decoupling between pieces and pounds harvested likely reflects changes in size structure, shifts in the composition of the harvest, or both. The catch of all seven species declined following implementation of the BRFAs (Figure 4.5A), however during revision, there was a relative decrease in *Etelis coruscans* caught compared to *Pristipomoides filamentosus* (Figure 4.5B). *P. filamentosus* and *E. coruscans* account for roughly 2/3 of bottomfish harvested by the commercial fleet. Using the reported weight and number of pieces reported each trip as a proxy for average individual size, *E. coruscans* were 1.2 pounds heavier than *P. filamentosus* (5.4 vs. 4.2 pounds respectively). This difference likely explains some of the discrepancy between the number of pounds and pieces caught per trip.

Individual assessment of the revised BRFAs is critical at a time where the role of the BRFAs are in question. Four of the 12 revised BRFAs will open preceding the 2020 FY, including BRFAs C, F, J, and L (https://dlnr.hawaii.gov/wp-content/uploads/2019/01/F-1.pdf).

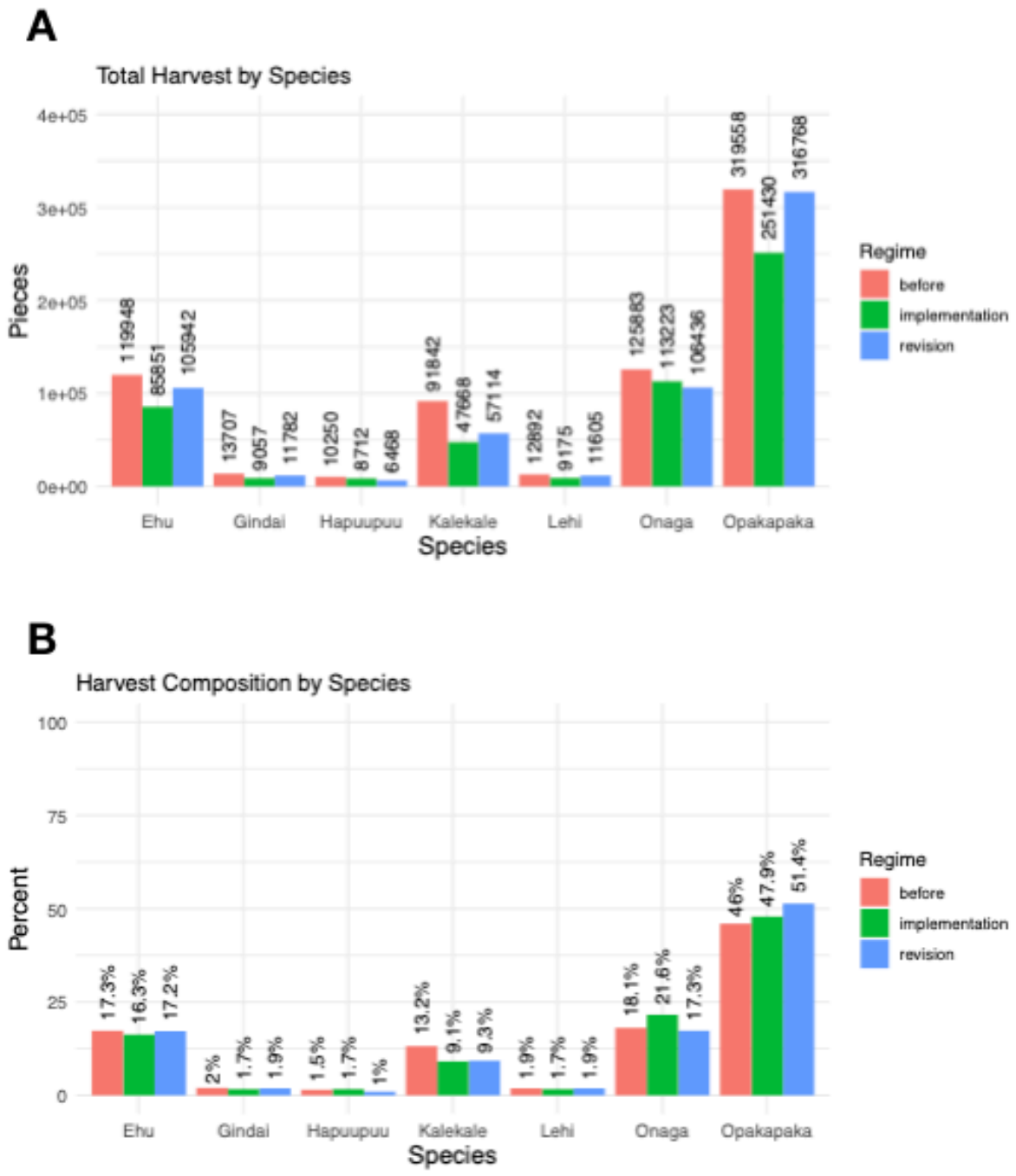

Figure 4.5. Catch Composition by Management Regime

Deep 7 catch as reflected in (A) the total number of pieces harvested by management period and (B) the relative contribution of each species to the total harvest.

Of these areas, catch was observed declining in BRFAs F and J and effort declined in F, J and C. Continued assessment of these areas to understand how effort and catch redistribute once reserves are removed should be a key consideration in determining the future of spatial management for the fishery.

Despite our efforts to understand the effect of these areas, our interpretations are limited by the source, resolution, and quality of the available data. Ecological outcomes of fishery reserves include enhanced larval output and increased spillover and are expected to accrue with time following a change in fishing mortality (Halpern, 2003; Smith, Zhang, and Coleman, 2006). Testing for these ecological outcomes requires observations of larval and adult fish, respectively. Inferences into these processes from fishery dependent catch data like that used here may not reflect biological realities (Smith, Zhang, and Coleman, 2006; Erisman et al., 2011). So, while we can understand how the dynamics of the commercial fishery has changed, we are unable to directly assess changes in the stock. Furthermore, while we used random effects in our models to account heterogeneity between reporting areas, the spatial mismatch of reserves and reporting areas and the potential misreporting of reporting areas where fishing took place increases the uncertainty associated with these results. Finally, a survey of fishers indicated that some fishers may underreport catch and misreport reporting area (Hospital and Beavers, 2011). We have assumed that these issues are negligible. Ultimately, however, the relationship between the models presented here, and the in-situ dynamics of the fishery can only be as accurate as the data that links the two, and ecological and fishery perspectives are required to fully assess the impacts of these areas.

Conclusion

In this study, we proposed a method for expanding the utility of Beyond BACIP studies to quantify multiple interventions. This was applied to commercial landings data reported to the State of Hawaii to model trends in effort and catch across and within the deep 7 bottomfish fishery associated with changes in management policy. There was a significant decrease in fishing effort driven by fewer fishers and fewer overall trips following the implementation of reserve areas with the greater decreases in effort occurring in areas where protections were enacted. Harvested biomass also decreased following the implementation of reserve areas. While there was an increase in the average landings per trip following revision of the BRFAs, fishers reporting catch in areas containing protected habitat were negatively affected suggesting they were displaced to less productive grounds. However, processes associated with fishery productivity, poor spatial resolution, and other factors make it difficult to be conclusive about the effect these areas have had. If fishery reserves will continue to be used as a management tool in this fishery, it is essential for managers to consider ways to improve the spatial resolution of data reported by the fishers.

CHAPTER 5: COMPARING AGE AND GROWTH ESTIMATES FROM BAYESIAN AND INTEGRATIVE DATA APPROACHES FOR THE DEEP-WATER SNAPPER *PRISTIPOMOIDES FILAMENTOSUS* IN THE HAWAIIAN ISLANDS

Submitted as Scherrer SR., Kobayashi DK., Weng KC., Okamoto HY., Oishi FG., Franklin EF. Comparing age and growth estimates from Bayesian and integrative data approaches for the deep-water snapper *Pristipomoides filamentosus* in the Hawaiian Islands. *Canadian Journal of Fisheries and Aquatic Sciences.* November 2019.

Abstract

Pristipomoides filamentosus is an economically and culturally important species of deep-water snapper in the Hawaiian archipelago. From 1989 to 1993, the State of Hawaii initiated a fisher participation mark-recapture study to quantify growth and other life history parameters for the species. Over a span of approximately 10 years, 10.5% of 4,179 tagged fish were recaptured. We compared Bayesian and maximum likelihood approaches to estimate von Bertalanffy growth parameters from the tagging data. In addition, direct aging and length frequency data previously used in other published regional growth studies were incorporated to produce integrated estimates of growth. Results from our preferred integrated model reconcile 30+ years of effort from various methods to estimate growth parameters (L_∞ = 67.6 cm FL and K = 0.22) and demonstrate the importance of individual variability in *P. filamentosus* due primarily to the asymptotic length parameter L_∞. These results have management implications as growth is often an input for age-based stock assessment models and used as a proxy for other life history traits.

Introduction

Pristipomoides filamentosus (Valenciennes, 1830) is a species of long-lived deep-water snapper distributed throughout the tropical Pacific and Indian Oceans (Allen, 1985; Andrews et al., 2012). Known as opakapaka in Hawaii, the species constitutes a significant fraction of the Hawaiian commercial bottomfish fishery, a complex of 6 snapper and 1 grouper species (Ralston and Polovina 1982, Langseth et al. 2018). While the current stock assessment for this fishery used a surplus production model for the entire complex, there is interest in the potential use of species-specific, age-structured assessments that require improved life history studies of age and growth of bottomfish (Langseth et al., 2018).

Growth parameters have been estimated for *P. filamentosus* using a variety of methods in Hawaii and elsewhere (Table 5.1). Parameter estimates were determined using direct aging approaches from length-at-age data using otolith growth increments (Ralston & Miyamoto, 1983; Uchiyama & Tagami, 1984; Radtke, 1987; DeMartini, Landgraf & Ralston, 1994, Ralston & Williams, 1988). However, age estimates relying on the integration of daily otolith bands may be biased due to episodic growth and/or poor increment resolution in early (< 5 years) life stages (Andrews et al., 2012; Wakefield et al., 2017). Growth was also estimated using modal progression approach during a length frequency study targeting juvenile fish (< 2 years) but did not consider individual variability when extrapolating growth to larger size classes (Moffitt and Parrish, 1996b). Preliminary results of an ongoing tagging study have been limited by the size distribution of recaptured individuals and use model parameterizations incompatible with other methods for determining growth (O'Malley, 2015). While these studies produced individual estimates of growth parameters, none of them holistically integrated across the three classes of data (direct aging, modal progression, growth increment) to explicitly evaluate the parameter values and sources of uncertainty.

Analytical and statistical advances to methods for estimating growth have been developed to account for sources of variability and permit parameter comparisons across length-at-age, length frequency, and tagging based approaches (Francis, 1988; Wang, Thomas, and Somers, 1995; Eveson, Laslett, and Polacheck, 2004). Structural modifications to Fabens (1965) parameterization of the von Bertalanffy growth model address issues of compatibility between growth parameters estimated from tagging studies and other methods, and can reduce bias through the accommodation of modest measurement errors (Maller and Deboer 1988, James 1991, Palmer et al. 1991, Laslett et al. 2002, Eveson et al. 2004, 2007, Zhang et al. 2009). Maximum likelihood and Bayesian model fitting procedures accommodate individual growth variability by describing population parameters using probability distributions (Francis, 1988; Kimura, Shimada, and Lowe, 1993; Wang, Thomas, and Somers, 1995; Zhang, Lessard, and Campbell, 2009). The flexibility of Bayesian approaches allows K and L_∞ to be sampled in this manner and can account for prior information when estimating parameters. Maximum likelihood approaches typically treat K as a fixed effect but flexibility in their implementation has allowed for the development of model structures that can estimate a single set of growth parameters from direct aging, length frequency, and growth increment data simultaneously (Wang, Thomas, and Somers, 1995; Laslett, Eveson, and Polacheck, 2002; Eveson, Laslett, and Polacheck, 2004; Zhang, Lessard, and Campbell, 2009).

Here previously unreported tagging data collected in the main Hawaiian Islands (MHI) are used to estimate growth parameters for *P. filamentosus* using Bayesian and maximum likelihood procedures. A series of models integrating previous length-at-age and length frequency data collected from the MHI and Northwestern Hawaiian Islands (NWHI) with the tagging data are developed to describe growth across most of the species' life history. Models are

Table 5.1. Estimates of von Bertalanffy Parameters.

Estimated parameters include average asymptotic length (L_∞) the Brody growth coefficient (k), and theoretical age at length zero t0 for P. filamentosus estimated in the Main Hawaiian Islands (MHI), Northwestern Hawaiian Islands (NWHI) and pooled across the Hawaii Archipelago. When available in the literature, 95% confidence intervals for parameter estimates are presented in brackets under to parameter point estimates.

	Method	Region	Otolith Growth Bands	Otoliths (Bomb-Carbon)	Pooled Otoliths (Lead-Radium)	Monthly Length Frequency	Recaptured Fish	Linf (95% CI)	K (95% CI)	t_0 (95% CI)	Source
Direct Aging	Daily Increments	NWHI	17	-	-	-	-	-	-	-	Moffitt (1980)
	Daily Increments	NWHI	N.R.	-	-	-	-	80.5	0.16	-	Ralston (1980)
	Daily Growth Integration	NWHI	64	-	-	-	-	78	0.146	-1.67	Ralston & Miyamoto (1983) - Constrained Linf
	Daily Growth Integration	NWHI	64	-	-	-	-	66.4	0.235	-0.81	Ralston & Miyamoto (1983) - Unconstrained Linf
	Daily Increments & Integration	NWHI	N.R.	-	-	-	-	69.8	0.534	0.18	Radtke (1987)
	Daily Increments & Integration	MHI & NWHI	92	-	-	-	-	70.4 (63.9 - 76.9)	0.25 (0.20, 0.31)	-0.22 (-0.39, -0.06)	DeMartini et al. (1994)
	Annual Increments	NWHI	N.R.	-	-	-	-	97.1	0.31	0.02	Uchiyama & Tagami (1984)
	Daily Increments, Integration, & Radioisotopes	MHI & NWHI	100	33	3	-	-	67.5 (65.7, 69.3)	0.242 (0.185, 0.299)	-0.29 (-0.38, -0.20)	Andrews et. al (2012)
Growth Increment	Modal Progression	MHI	-	-	-	13		78	0.21	0	Moffit & Parrish (1996) - Constrained Linf
	Mark Recapture	MHI	-	-	-	96		71.55	0.15	-	O'Malley (2015) - Gulland and Holt
	Mark Recapture	MHI	-	-	-	96		57.80 (55.97, 58.67)	0.28 (0.25, 0.31)	-	O'Malley (2015) - Francis
	Mark Recapture	MHI	-	-	-	387		65.92 (60.9 - 71.6)	0.24 (0.19 - 0.30)	-	Present Study Francis
	Mark Recapture	MHI	-	-	-	387		59.7 (56.9 - 63.0)	0.32 (0.27 - 0.38)	-	Present Study Bayesian Model 1
	Mark Recapture	MHI	-	-	-	387		60.2 (57.3 - 61.2)	0.35 (0.07 - 0.39)	-	Present Study Bayesian Model 2
	Mark Recapture	MHI	-	-	-	387		76.8 (13.7 - 162.7)	0.17 (0.14 - 0.20)	-	Present Study Bayesian Model 3
	Mark Recapture	MHI	-	-	-	387		77.3 (12.36 - 162.7)	0.24 (0.04 - 0.76)	-	Present Study Bayesian Model 4
	Mark Recapture	MHI	-	-	-	387		61.0 (56.1, 66.7)	0.30 (0.23, 0.39)	-	Present Study Maximum Likelihood Model 5
	Integrative	MHI & NWHI	113	33	3	13	378	67.6 (65.4, 69.6)	0.22 (0.12, 0.25)	-0.37 (-0.47, -0.28)	Present Study - Integrative Model 11

tested to determine a preferred model structure. New growth parameters are estimated and compared to those previously reported for the Hawaiian Archipelago.

Methods

Opakapaka Tagging Program

Tagging data used for this analysis were obtained by biologists from Hawaii's Division of Aquatic Resources (DAR) within the state's Department of Land and Natural Resources (DLNR). Between 1989 and 1993 the Opakapaka Tagging Program (OTP), led by staff biologist Henry Okamoto and operating from fishing vessels contracted out of Honolulu Harbor, targeted and tagged *P. filamentosus*.

All tagging effort occurred in the main Hawaiian Islands (MHI) and was concentrated primarily around the island of Oahu and the Maui Nui complex consisting of the islands of Maui, Molokai, Lanai and Kahoolawe. Since 1990, these areas have accounted for approximately 67.7% of Hawaii's commercial bottomfish harvest. Coarse location data were provided in the form of the commercial statistical reporting grid areas in which individuals were tagged and recaptured (Table 5.2, Figure 5.1). Less than 1% of fish in this study were tagged off the islands of Niihau or Hawaii (Big Island). Adult bottomfish occupy depths between 100 and 400 m along undersea shelves and banks (Parke 2007, Oyafuso et al. 2017). In total, the OTP tagged 4,179 juvenile and adult *P. filamentosus*.

Fish were caught with hook-and-line gear and brought to the surface at a rate of 2 - 5 feet per second. Prior to tagging, each fish was placed in a holding container with aerated seawater to ascertain survival likelihood. If the stomach was inverted and full of gas, it was punctured using a small sharp instrument (e.g., scalpel, hypodermic needle, fishhook). A few scales were carefully removed and a small (~1 cm) incision was made near the fish's anal opening to assist in

Table 5.2. Summary of OTP Tagging and Recapture Data for Fish with Valid Locations. *Release and recapture location numbers correspond to the State of Hawaii's statistical reporting grids (Figure 5.1). Adapted from Kobayashi, Okamoto & Oishi (2008).*

TAGGING LOCATION \ RELEASE LOCATION	127	304	306	307	308	309	311	312	313	320	321	327	331	332	351	401	402	403	404	405	407	408	409	421	423	424	428	429	452	505	528	Total
127							1																									1
304				1						2																						3
306			1							1																						2
307				5								1																				6
308			1		2						5																					8
309											2																					2
311							25	1					4																			30
312							1	1																								2
313				1				1					3																			5
320			1	3						24		1																				29
321											31																					31
327				3						2		2																				7
331							46	2					128			4																180
332													1																			1
351													1																			1
401																131																131
402																1																1
403																1																1
404																						1										1
405							1															1										2
407													1									12										13
408													1																			1
409																4								1								5
421																14						1										15
423											1					14						1										16
424					1								4			3						3										11
428							2	1					2																			5
429							2				1		1			1																5
452											1		1																			2
505										1																						1
528							2																									2
No Recovery	1	3	44	278	35	2	582	168	5	333	429	84	875	1	1	937	7	1	1	2	2	293	4	20	16	9	8	5	2	1	2	4151
Total	1	3	47	291	38	2	662	174	5	363	470	88	1022	1	1	1110	7	1	1	2	2	312	4	21	16	9	8	5	2	1	2	4671

expelling gas from the body cavity. Fish appearing lively and upright were deemed likely to survive and thus suitable candidates for tagging. These fish were surgically implanted with unique identifiable internal anchor tags with a monofilament streamer protruding from the incision in the peritoneal cavity. The fork length of each fish measured to the nearest ¼ inch was recorded before the fish was returned headfirst to sea with enough downward momentum to assist in counteracting buoyancy caused by any residual gas.

There were 487 recaptures recorded for 439 unique individuals for a recapture rate of 10.5% of tagged fish. Recaptures of marked *P. filamentosus* were reported up to a decade after tagging with the most recent fish reported in October of 2003 (Okamoto, 1993; Kobayashi, Okamoto, and Oishi, 2008). Individuals recaptured by OTP personnel were outfitted with an

additional tag following procedures similar to their initial capture. For each individual, the location of capture (DAR statistical reporting grid), length at tagging, and date of capture were recorded. Local commercial and recreational fishers were made aware of the program through fliers distributed at the local fish markets, to fish dealers, at fishing supply outlets, and posted at small boat harbors. Fishers were incentivized to report the location, depth, fork length, and date that tagged fish were landed with a $10 reward.

Tagging Data Management

The data collected by OTP were entered into an Excel spreadsheet with subsequent analyses performed in R (R Core Team, 2014), the Bayesian statistical software JAGS (Plummer, 2003), and the R package R2Jags (Su and Yajima, 2012). Fish were removed from the dataset if they were not the correct species of interest, if no recapture was reported, or if there was no record of the tag identification number. Fork lengths for the remaining fish recorded at tagging and recapture were linearly transformed from inches to centimeters prior to model fitting. Observed growth (Δl) and time at liberty (Δt) were calculated for each fish. If an individual was recaptured on more than one occasion, Δl and Δt were only calculated between the first marking event and the last recapture so as to not violate assumptions of independence. Fish with Δt less than 60 days were excluded from the dataset.

Parameter Estimation from Tagging Data: Bayesian Approach

Growth parameters were estimated for the *P. filamentosus* tagging data following the Bayesian methodology of Zhang et al. (2009). This approach uses a Fabens version of the von Bertalanffy

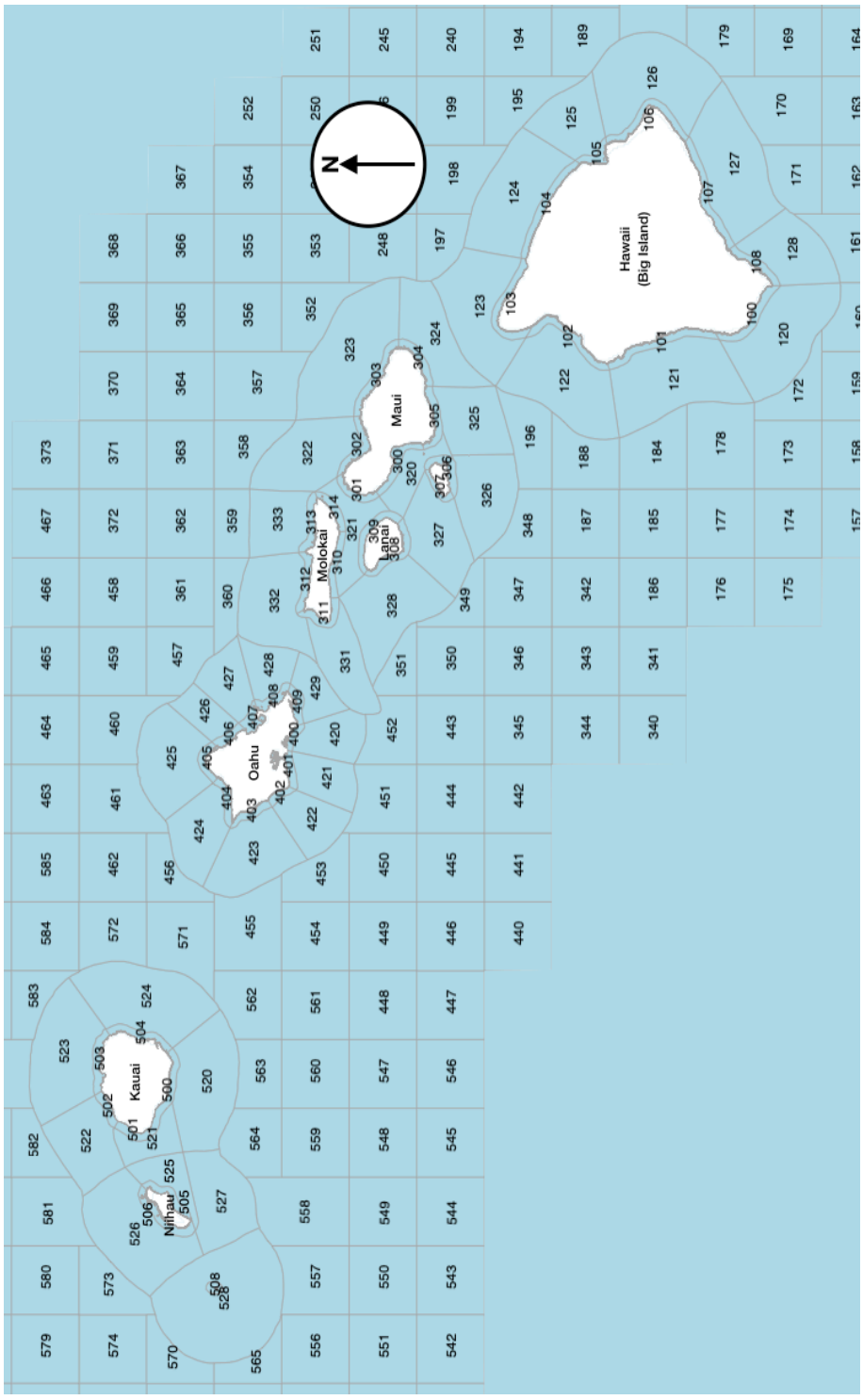

Figure 5.1. Reporting Grid Map.

Map showing the location and number of the State of Hawaii's statistical reporting grids corresponding to the reported location of tagging and recaptured for fish summarized in Table 5.2.

growth curve but allows the parameters to vary among individuals. Hence the length upon recapture is expressed as:

$$(E1)\ L_{i,j} = L_{\infty,i}(1 - e^{-K_i(A_i + t_{i,j})})$$

This is parameterized such that $L_{i,j}$ is the length of individual *i* for the *jth* recapture, $t_{i,j}$ is the time-at-liberty for individual *i* for the *jth* recapture, A_i is the relative age of individual *i* at tagging (age minus T_0), and K_i and $L_{\infty,i}$ are the von Bertalanffy growth parameters for the *ith* individual. These individual parameters were drawn from Gaussian distributions defining the population mean values for K and L_∞. Uninformative priors were used for all input parameters, using Gaussian, gamma, beta, and uniform distributions following the approach of Zhang et al. (2009). The JAGS code for specifying these parameters and performing this analysis is provided in Appendix 5.1.

The model which allowed both the K parameter and L_∞ parameter to vary across individuals as described above is henceforth referred to as Model 1. Three additional models were run in modified versions of the JAGS code. Model 2 used a fixed K parameter while allowing the L_∞ parameter to vary across individuals. Model 3 used a fixed L_∞ parameter while allowing the K parameter to vary across individuals. Lastly, Model 4 used both a fixed K parameter and a fixed L_∞ parameter. The term "fixed" in this context does not imply a user-specified constant value, but instead refers to the value that is estimated by the Bayesian modeling approach from a single distribution used to represent the mean growth process across all individuals. Model 4 would *a priori* be most similar to the Fabens approach, with both fixed K and L_∞, but with the added feature of estimating ages at initial tagging, A_i, within the Bayesian framework. Inclusion of the A_i term represents a significant improvement over prior methods by modeling growth as a function of age, rather than observed length, allowing growth

parameters to be compared between models using tagging data and length-at-age methods (Wang, Thomas, and Somers, 1995). Model 1 is the presumptive best estimate for *P. filamentosus* von Bertalanffy growth curve parameters since it would allow the most flexible incorporation of individual variability in the parameter estimation process.

For each Bayesian hierarchical model run, the first 150,000 samples from the posterior distribution were treated as burn-in and discarded from the Monte Carlo simulation. Every 50th sample from the following 1,400,000 samples (number kept = 28,000) was tabulated into the posterior distributions to reduce potential autocorrelation between sequential values or strings of values. The mean K and L_∞ values from the 28,000 kept samples were used as metrics of population mean values. Median values deviated from mean values by less than one half of 1 percent (Table 5.3), indicative of symmetrical distributions easily characterized by any descriptor of value tendency (i.e., mean, median, or mode). The results from the Fabens (1965) approach fit using non-linear least squares provided estimates of K and L_∞ (Table 5.1) were used as initial starting points in the Bayesian hierarchical approach. Two additional chains were run starting with initial values 50% lower and 100% higher than the initial estimates which resulted in nearly identical solutions as shown in Table 5.3. Convergence was also ascertained by examination of the Gelman-Rubin statistic (Gelman and Rubin, 1992).

The fit of each model was assessed by calculating its Bayesian p-value from the posterior predictive distribution and the models were compared using the DIC criterion. Bayesian p-values were derived from data simulated by model parameters and test whether simulated data are more extreme than the observed data. Bayesian P-values approaching 0.5 indicate the model is a good fit to the data, while extreme Bayesian p-values near 0 or 1 indicate that a given model does not adequately represent the data (Meng, 1994). Comparisons among models 1-4 were accomplished

by comparing parameter estimates to model 1 where both K and L_∞ varied for individuals. If the parameter was relatively stable when allowed to be variable across individuals or fixed for the population, it might be inferred that treating this parameter on an individual basis is not warranted. However, if the parameter increased when the parameter distribution was fixed for the entire population, then it might be inferred that treating this parameter on an individual basis is necessary. Additional model comparisons were made using DIC.

Parameter Estimation from Tagging Data: Maximum Likelihood Approach

Model 5 was fit using the maximum likelihood approach of Laslett, Everson, and Polacheck (2002) using Equation 2.

$$(E2) \quad l_{ij} = \mu_\infty\left(1 - e^{-K(a_i + \Delta t_i)}\right) + \varepsilon_{ij}$$

This method derived growth parameters from the joint distribution of an individual's length at tagging and recapture to estimate growth parameters. This approach was most similar to model 2 of the Bayesian approach in that asymptotic length, L_∞, was treated as a normal random effect $N(\mu_\infty, \sigma_\infty^2)$ while K was treated as a fixed unknown parameter. The distribution of L_∞ was treated as normal with a mean μ_∞ and standard deviation σ_∞^2, accounting for individual deviation from the population mean. Rather than using length increments to fit observed growth, a bivariate normal joint distribution of lengths recorded at marking and recapture was used to estimate each individual's age at tagging a_i. The distribution of individual a_is is A and is treated as a random effect with a lognormal distribution $L(\mu_{logA}, \sigma_{logA}^2)$. Measurement error was also treated as a random normal distribution $N(0, \sigma^2)$. An unconditional joint density was then derived for each individual by integrating their individual joint distribution with respect to a. A detailed description of this process is described by Laslett et. al. (2002).

Growth function parameters were estimated through minimizing of the negative log-likelihood function obtained by summing the unconditional joint density $\mathrm{h}(l_1, l_2)$ of each individual (E3).

$$(E3)\ -\ln(\lambda_1) = -\sum_i \ln\ \mathrm{h}\left(l_{m,i}, l_{r,i}\right)$$

This approach was used to estimate values of the parameters μ_∞, σ_∞^2, K, $\mu_{\log A}$, σ_{logA}^2, and σ^2. Two-sided 95% confidence intervals (2.5%, Median, 97.5%) were then estimated from the distribution of each parameter following 10,000 successful bootstrap iterations to obtain population parameters. For each bootstrap iteration, the model was refit on data randomly resampled from the original tagging data with replacement.

Estimation of Integrative Growth Parameters using sources of growth data

Datasets previously used to estimate regional growth for *P. filamentosus* in the MHI and NWHI and our tagging data exclusively from the MHI were used to produce a single set of parameter estimates using a modified form of the integrated method proposed by Eveson, Laslett, and Polachek (2004). Additional datasets that were included represent both direct aging and length frequency approaches.

Parameter Estimation: Length Frequency Data

Length frequency data consisted of the size distributions of juvenile *P. filamentosus* sampled over 13 months between October 1989 and February 1991 reported by Moffitt and Parrish (1996). The reported fork length of captured fish was binned by 1 cm increments and presented in 13 histograms corresponding to each month of sampling. The number of fish of a given fork length captured during each month of sampling was determined by overlaying a series of evenly spaced horizontal lines across the Y-axis of each histogram corresponding to the addition of a single fish. Using this method to reconstruct monthly length frequency data resulted

Table 5.3. Bayesian Hierarchical Growth Model Specifications.

Monte Carlo simulation was burned in for n=10,000 runs with every 50th of the following 500,000 runs retained for tabulation into the posterior distributions. Variable names are kept consistent with the Appendix 5.1 JAGS code and are not consistent with text references to von Bertalanffy growth parameters but remain intuitively similar (e.g., Brody Growth Coefficient = K = k_mu, Asymptotic Length = L∞ = Linf_mu).

	Parameter	Mean	SD	2.50%	Median	97.50%	Rhat	n eff
Model 1	Linf_mu	59.89	1.58	57.10	59.80	63.24	1.00	2000.00
	Linf_std	5.47	0.34	4.80	5.46	6.15	1.00	36000.00
	Linf_tau	0.03	0.00	0.03	0.03	0.04	1.00	36000.00
	Shape	26.85	4.40	19.63	26.36	36.86	1.00	2500.00
	deviance	3351.95	120.29	3106.84	3355.69	3575.02	1.00	3700.00
	k_mu	0.32	0.03	0.27	0.32	0.37	1.00	1800.00
	k_std	0.01	0.00	0.01	0.01	0.02	1.00	38000.00
	k_tau	10741.60	7970.11	2241.98	8492.59	32025.77	1.00	38000.00
	rate	10.52	1.59	7.88	10.35	14.10	1.00	2800.00
	tau	0.27	0.04	0.20	0.26	0.36	1.00	5700.00
	variance	3.85	0.60	2.77	3.82	5.11	1.00	5700.00
Model 2	Linf_mu	60.12	1.62	57.21	60.04	63.52	1.00	30000.00
	Linf_std	5.50	0.34	4.85	5.50	6.17	1.00	84000.00
	Linf_tau	0.03	0.00	0.03	0.03	0.04	1.00	84000.00
	Shape	26.64	4.21	19.63	26.24	36.04	1.00	7900.00
	deviance	3356.96	119.45	3110.59	3361.29	3578.22	1.00	28000.00
	k_mu	0.35	0.16	0.07	0.32	0.79	1.00	63000.00
	k_std	1.14	85.41	0.01	0.10	3.24	1.00	84000.00
	k_tau	1294.41	3430.44	0.10	105.30	10874.77	1.00	84000.00
	rate	10.36	1.49	7.85	10.22	13.67	1.00	5200.00
	tau	0.26	0.04	0.19	0.26	0.36	1.00	21000.00
	variance	3.88	0.60	2.77	3.85	5.14	1.00	21000.00
Model 3	Linf_mu	76.89	31.95	17.19	74.42	160.86	1.00	84000.00
	Linf_std	88.68	4772.30	0.01	1.32	364.22	1.00	84000.00
	Linf_tau	570.00	2323.38	0.00	0.57	6238.55	1.00	84000.00
	Shape	62.32	13.32	41.03	60.49	92.62	1.00	1400.00
	deviance	3937.75	46.81	3847.12	3937.23	4030.55	1.00	41000.00
	k_mu	0.17	0.01	0.14	0.17	0.20	1.00	3200.00
	k_std	0.02	0.00	0.01	0.02	0.03	1.00	8000.00
	k_tau	2543.07	807.09	1398.95	2400.92	4491.85	1.00	8000.00
	rate	17.93	3.84	11.85	17.41	26.63	1.00	1600.00
	tau	0.13	0.01	0.11	0.13	0.15	1.00	84000.00
	variance	7.92	0.61	6.80	7.89	9.20	1.00	84000.00
Model 4	Linf_mu	77.32	33.39	13.20	74.63	166.14	1.00	25000.00
	Linf_std	132.25	9204.30	0.01	1.65	429.54	1.00	84000.00
	Linf_tau	529.45	2244.18	0.00	0.37	5947.71	1.00	84000.00
	Shape	32.76	3.60	26.33	32.55	40.48	1.00	13000.00
	deviance	4090.50	39.61	4016.26	4089.51	4171.26	1.00	34000.00
	k_mu	0.24	0.18	0.04	0.18	0.77	1.00	84000.00
	k_std	5.93	1357.98	0.01	0.09	3.67	1.00	84000.00
	k_tau	1293.51	3336.91	0.07	115.99	10767.12	1.00	84000.00
	rate	9.24	0.95	7.53	9.18	11.25	1.00	21000.00
	tau	0.11	0.01	0.09	0.10	0.12	1.00	45000.00
	variance	9.57	0.67	8.34	9.54	10.98	1.00	45000.00

in a total count of 1,048, individuals while in the original study reported 1,047 (Moffitt and Parrish, 1996b).

The reconstructed length frequency data were incorporated into integrative models using the two-step method described in Laslett et al 2004. During the first step, a Gaussian mixture model was fit using maximum likelihood and used to decompose the distribution of fork lengths from individuals sampled during discrete time periods for each cohort present in the data. This was accomplished using the normalmixEM function from the mixtools package in R (Benaglia et al., 2009) by constraining the mean of each distribution to the observed mode. A bimodal Gaussian mixture model was fit for the months of October - February, as the original study reported that two cohorts were present during this period, while a single cohort was present the remainder of the year. The estimated mean fork length, $\hat{\mu}_{ijk}$, and standard error, s_{ijk}, of each cohort during each sampling period was used to estimate growth parameters (E4).

$$(E4) \quad \hat{\mu}_{ijk} = \mu_{\infty}\left(1 - e^{-K(a_{ijk} - a_0)}\right) + e_{ijk} + \varepsilon_{ijk}$$

With this model, $i, j,$ and k reflect the fishing year, month, and age cohort, respectively. The estimated age of each cohort during a sampling period is denoted by a_{ijk}. July is the month of peak spawning for *P. filamentosus* (Luers, DeMartini, and Humphreys, 2017) which resulted in age estimates between 3 and 19 months. Sampling and residual model errors were described using random normal distributions $e_{ijk} \sim N(0, s_{ijk}^2)$ and $\varepsilon_{ijk} \sim N(0, \sigma_{\varepsilon}^2)$ respectively. In contrast to tagging and direct aging components, there is a dearth of information available to estimate the variance component of asymptotic length, L_{∞}, using length frequency methods, so this term was modeled as fixed effect, μ_{∞}. From this, the expected mode fork length of each cohort (E6), and associated variability during each sampling period (E7) were calculated and used to construct the

negative log likelihood function (E8). The rationale for these approximations is discussed to greater depth in Eveson et al. 2004.

$$(E6) \quad E\left(\hat{\mu}_{ijk}\right) = \mu_{\infty}\left(1 - e^{-K\left(a_{ijk} - a_0\right)}\right)$$

$$(E7) \quad V\left(\hat{\mu}_{ijk}\right) = s_{ijk}^2 + \sigma_{\varepsilon}^2$$

$$(E8) \quad -\ln(\lambda_2) = \frac{1}{2}\sum_i \sum_j \sum_k \left[\ln\left(2\pi\, V\left(\hat{\mu}_{ijk}\right)\right) + \frac{\left(\hat{\mu}_{ijk} - E\left(\hat{\mu}_{ijk}\right)\right)^2}{V\left(\hat{\mu}_{ijk}\right)}\right]$$

Parameter Estimation: Direct Aging Data

Sources of direct aging data consisted of four previously reported length-at-age datasets from three studies. Age estimates for length at age data were obtained through analytical integration of otolith bands (Ralston and Miyamoto, 1983; n = 65), counts of otolith micro increments (DeMartini et al., 1994; n = 35), comparison of bomb radiocarbon ($\Delta^{14}C$) derived from otoliths relative to a standard reference obtained from hermatypic coral cores from the Hawaiian Archipelago (Andrews et al., 2012; n = 33), and the lead-radium ratios of individuals pooled by size class (Andrews et al., 2012; n = 3).

Details of the method for estimating growth parameters from direct aging data components are described in Eveson et al. 2004. Briefly, parameters were modeled using the VBGF model described by equation E9.

$$(E9) \quad l_i = l_{\infty i}\left(1 - e^{-K\left(a_i - a_0\right)}\right) + \gamma_i$$

Expected length for each individual and the variance of the measurement error was described by equations E10 and E11.

$$(E10) \quad E(l_i) = \mu_{\infty}(1 - e^{-K(a_i - a_0)})$$

$$(E11) \quad V(l_i) = \sigma_{\infty}^2(1 - e^{-K(a_i - a_0)})^2 + \sigma_{\gamma}^2$$

l_i denoted the length of the i^{th} fish, at age a_i and a_0 was a fixed parameter analogous to t_0 when a fish has a hypothetical length of zero. As with the model for tagging data, $l_{\infty i}$ was the individual asymptotic length of the i^{th} fish drawn from the random normal distribution $L_\infty = N(\mu_\infty, \sigma_\infty)$. γ_i represented the distribution of individual measurement error and was similarly random, drawn from the distribution $\gamma = N(0, \sigma_\gamma)$. Equation 12 describes the log-likelihood function derived from these equations.

$$(E12)\ -ln(\lambda_2) = \frac{1}{2}\sum_i \left[\ln(2\pi V(l_i)) + \frac{(l_i - E(l_i))^2}{V(l_i)}\right]$$

An appropriate overall objective likelihood function (E13) was then defined from the sum of the negative log-likelihood functions for tag-recapture, direct aging, length frequency, and growth increment approaches, each with its own scaling constant, β.

Defining an objective function and estimating integrative growth parameters

A single set of growth parameters best describing the data was obtained by minimizing the objective likelihood function Λ (E13).

$$(\text{E13})\ \ \Lambda = \beta_1 ln(\lambda_1) + \beta_2 ln(\lambda_2) + \beta_3 ln(\lambda_3) \ldots + \beta_n ln(\lambda_n)$$

By manipulating the value of scaling constants, how similar datasets were treated, and which datasets were included, six additional model structures were developed and evaluated (Table 5.4). Two approaches were used to define the scaling constants (β) within each model's objective likelihood function. The first equally weighted each likelihood function so that each data source had equal influence on the resulting parameter estimates. This was achieved by selecting a β for each data source equal to the inverse of the number of observations for the data. The second weighted each data source relative to the number of observations of that particular data set ($\beta_1 = \beta_2 = \beta_3$).

The structure of model 5 fit only tagging data from the OTP study while models 6 - 11 incorporated the additional length-at-age and length frequency data and differed from one another in the treatment of β coefficients, whether direct aging data sources were considered independently and assigned their own log-likelihood function or if these data sources were pooled and contributed to estimation of a single log-likelihood function. Omission of direct aging data where ages were estimated by integrating daily growth increments was also considered as this method is likely to result in underestimations of age (Table 5.4; Wakefield et al 2017).

The six candidate integrative model structures (Models 6 - 11) were evaluated against one another using the following repeated training-testing cross validation procedure (Burman, 1989) to determine the combination of model weighting, data pooling, and data sources parameter estimates that consistently best predicted observed growth from tagging data. Each model structure was trained using two-thirds of the tagging data (n = 258) selected at random while the remaining one-third (n = 129) was reserved for evaluating each model's predictive ability. Model performance was evaluated using the parameters μ_∞ and k estimated from training data, applied to the length at tagging and time at liberty of each individual in the validation set to predict length at recapture using Equation 2. The variance (s^2) between the predicted ($\widehat{L_{r,i}}$) and observed ($L_{r,i}$) length of each fish recapture was used as a metric for comparing the performance of competing model structures (E14).

$$(E14) \quad s^2 = \frac{1}{n}\sum\left(L_{ri} - \widehat{L_{ri}}\right)^2$$

The preferred model structure was the one whose estimated parameters most frequently produced the smallest variance. This procedure was repeated 10,000 times. The preferred model structure

Table 5.4. Integrative Model Structures.

A reference for the candidate model structures used to determine the preferred integrative model structure.

Data Source	Model 5	Model 6	Model 7	Model 8	Model 9	Model 10	Model 11
Growth Increment OTP Mark Recapture	X	X	X	X	X	X	X
Direct Aging Ralston & Miyamoto (1983) Integrated Daily Otolith Counts	-	X	X	X	X	-	-
Direct Aging Demartini et al. (1994) Otolith Microincrements	-	X	X	X	X	X	X
Direct Aging Andrews et al. (2012) Bomb Carbon	-	X	X	X	X	X	X
Direct Aging Andrews et al. (2012) Lead:Radium	-	X	X	X	X	X	X
Length Frequency Moffitt & Parrish (1996) Modal Progression	-	X	X	X	X	X	X
Weighting	NA	Equal	By n	Equal	By n	Equal	By n
Pooled Within Data Types?	NA	Yes	Yes	No	No	No	No

was that which most frequently reported the lowest variance across all of these iterations. To determine if incorporating additional data sources improved predictive performance, cross validation variances for the preferred model structure were compared to those calculated using a model structure identical to Model 5, calculated including only tagging data.

The integrative model structure that best predicted observed growth most frequently was refit using the entire data set. Two-sided 95% confidence intervals were estimated for each parameter from the results of 10,000 bootstrap iterations. As with tagging data, the procedure for resampling direct aging data was straightforward and involved random sampling with replacement from the dataset to construct pseudo data sets with an equal number of observations as the original data. Bootstrapping length frequency data was slightly more complicated with each study period in the pseudo data resampled from the corresponding period of the

reconstructed study data. Each study period in the pseudo dataset contained the same number of observations as in the corresponding time period of the original study data.

Results

Opakapaka Tagging Program

Of the 4,179 *P. filamentosus* tagged 439 individuals were recaptured at least once (10.5%, Table 5.2). Mortality of fish upon release appeared to be generally low, facilitated by the strong tagging selectivity for healthy fish in good condition. Some immediate mortality was observed due to sharks and cetaceans or capture stress (4 individuals). Long-term mortality was thought to be relatively low based upon the high rates of tag return spanning many years. Hydra (small cnidarian polyps) biofouling of the tags was observed for some individuals with large times at liberty, with some lesions apparent around the opening where the tag exited the body cavity. This was not thought to be a serious health issue since the fish appeared to be feeding and swimming normally.

Initial fork length at capture across all individuals ranged in size from 16.5 to 53.3 cm (mean = 31.9 cm, standard deviation (s.d.) = 5.5) and ranged from 19.1 cm and 52.8 cm (mean = 32.8, s.d. = 5.1) for fish that were later recaptured. For those fish that were later recaptured, fork length at recapture ranged between 22.9 cm and 76.2 cm (mean = 41.9, s.d. = 8.7). The minimum time at liberty for any fish between tagging and recapture was a single day while the maximum time at liberty was 10.3 years (3,748 days) (Figure 5.2). The mean time at liberty was 1.82 years or 666 days (s.d. = 625).

One fish was excluded from further analysis as its fork length at capture was not recorded. Seven fish were removed because the recapture date was not properly recorded. Of the remaining 432 fish recaptured, 351 were recaptured a single time, 33 fish were recaptured a total of two times, one fish recaptured 3 times, and two fish were recaptured 4 times. We also

excluded from analysis 45 individuals for whom time at liberty was less than 60 days yielding a data set of 387 unique individuals.

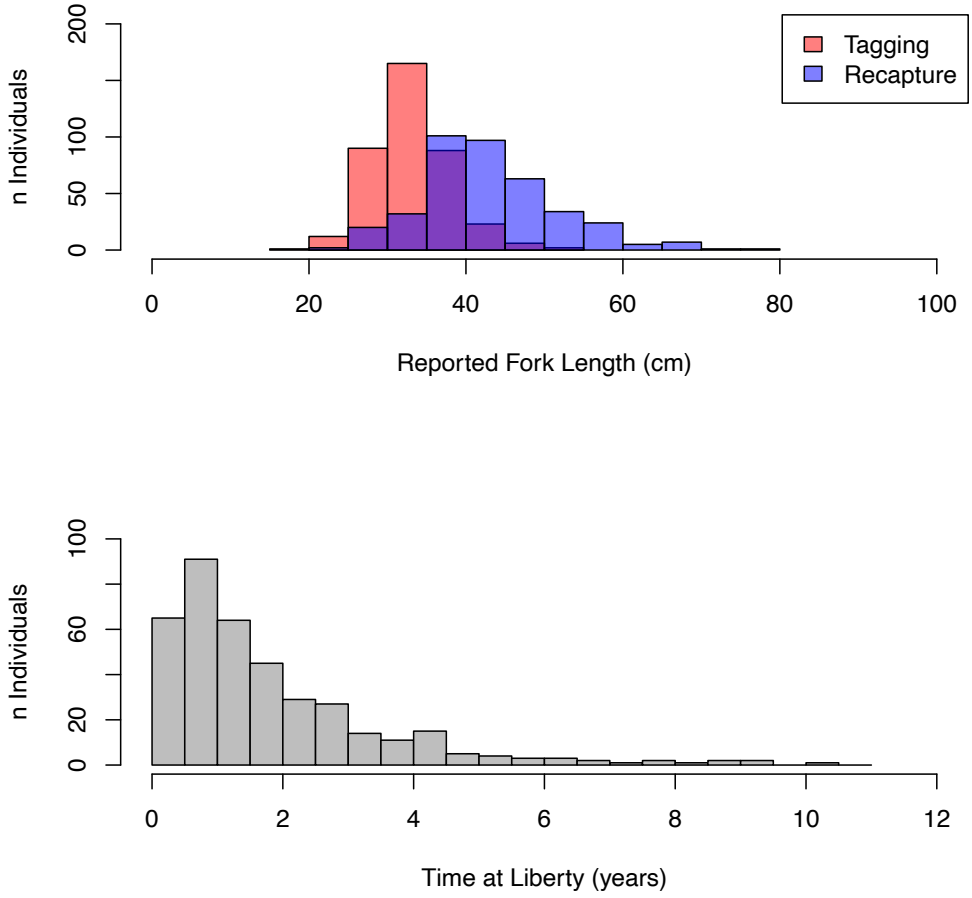

Figure 5.2. Length and Time at Liberty for OTP Data.

The length of P. filamentosus recaptured and included in analysis of OTP tagging data and the distribution of times at liberty. The fork length of fish during tagging is highlighted in red while length at recapture is shown in blue.

Parameter Estimation from Tagging Data: Bayesian Approach

The Bayesian hierarchical approach using the JAGS software yielded mean estimates of L_∞ and K for each of the Models 1–4 examined (Table 5.3). Model 1, which incorporated individual variability in both L_∞ and K yielded mean parameter estimates of L_∞ = 59.9 cm (coefficient of

variation [c.v.] = 2.59) and K = 0.32 (c.v. = 8.57). L_∞ and K parameter estimates for Model 2, where K was fixed, were 60.1 cm (c.v. = 2.74) and 0.35 (c.v. = 45.7) respectively. Under Model 3, where L_∞ was fixed and K was fit freely L_∞ = 76.9 cm (c.v. = 42.2) and K = 0.17 (c.v. = 8.62) and L_∞ = 77.3 cm (c.v. = 43.1) and K = 0.24 (c.v. = 73.1) for Model 4, where both parameters were fixed. Additional parameters for each of the four models are presented in table 5.3. The Gelman-Rubin convergence criteria indicated that the model solutions were credible, with asymptotic convergence clearly occurring after ~4000 iterations, well within the burn-in phase of the Bayesian modeling runs. All 4 models appeared to fit the the data well; the mean Bayesian p-values from all retained posterior samples for all models ranged between 0.500 and 0.501. Model 1 had the largest DIC score (10582.86) followed by model 2 (10490.96), model 3 (5033.42), and model 4 (4874.83). Treating model parameters as fixed under models 2-4 resulted in excessively large coefficients of variation suggesting that individual variability in L_∞ and K is important, with perhaps variability in L_∞ being more important based upon the response of L_∞ standard deviation from the base case of Model 1 to the constrained individual variability in Model 3 and Model 4 (Figure 5.3).

Parameter Estimation from Tagging Data: Maximum Likelihood Approach

The maximum likelihood approach used for Model 5 successfully converged to produce estimates of μ_∞, σ_∞^2, K, $\mu_{\log A}$, σ_{logA}^2, and σ^2 (Table 5.5). Bootstrap confidence intervals of

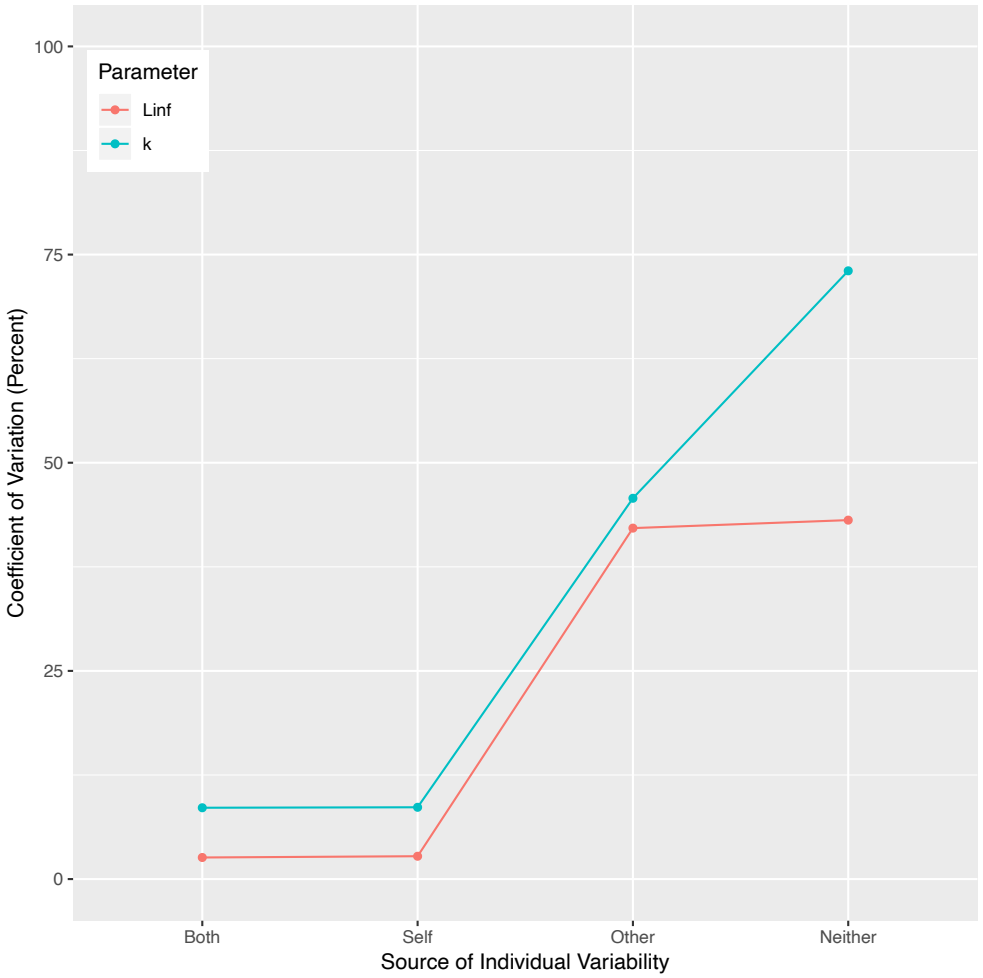

Figure 5.3. Coefficient of Variation for von Bertalanffy Growth Function Parameters. *Coefficient of variation for 2 von Bertalanffy growth function parameters (Brody growth coefficient, K) and (Mean asymptotic length L∞) for P. filamentosus. Individual variability was examined incorporating individual variability in both parameters, in either one of the parameters in series, or in neither parameter.*

parameters μ_∞ and K overlapped L_∞ and K parameters from Bayesian models 1 and 2 (Table 5.1). From these results, it was concluded that estimates produced by maximum likelihood were satisfactorily similar to estimates from the Bayesian approach. Model residuals were distributed around zero fairly consistently for all but the largest fish. For fish with recapture lengths exceeding 60 cm, growth models underestimated observed recapture lengths (Figure 5.4).

Table 5.5. Sample and Population Parameter Estimates from Maximum Likelihood Growth Models.

Model 5 was fit to only the tagging data and Model 11 is the preferred model. For both models, parameter estimates fit to the full data set are reported in the Sample Estimate columns while bootstrapped parameter estimates (Median, 2.5%, 97.5%) are reported under the Population CI column.

Parameter Estiamtes for Integrated Growth Models

	Model 5		Model 6		Model 7		Model 8	
Parameter	Sample	Population	Sample	Population	Sample	Population	Sample	Population
Linf_mu	60.92	60.98 (56.17,66.67)	77.96	66.79 (70.27, 78.69)	64.74	64.80 (61.91, 67.17)	66.87	66.89 (63.90, 70.10)
Linf_std	5.32	5.3 (4.53,6.07)	6.02	5.256 (4.00, 6.83)	5.62	5.57 (4.72, 6.36)	5.53	5.31 (2.61, 6.25)
K	0.300	0.299 (0.229,0.393)	0.122	0.189 (0.121, 0.235)	0.262	0.260 (0.231, 0.302)	0.253	0.25 (0.21, 0.29)
A_mu	0.95	0.95 (0.8,1.09)	1.5	1.21 (1.06, 1.50)	1	1.00 (0.92, 1.08)	0.99	0.98 (0.89, 1.10)
A_sig	0.19	0.19 (0.15,0.24)	0.13	0.16 (0.12, 0.19)	0.18	0.18 (0.14, 0.22)	0.18	0.18 (0.15, 0.21)
Sig	2.1	2.08 (1.50,2.55)	2.97	2.51 (2.05, 3.11)	2.2	2.20 (1.74, 2.62)	2.32	2.36 (1.94, 2.93)
t0	-	-	-0.86	-0.50 (-0.90, -0.34)	-0.31	-0.32 (-0.44, -0.20)	-0.27	-0.27 (-0.43, -0.17)
oto_sig	-	-	6.79	3.93 (1.31, 7.09)	1.82	1.76 (0.68, 3.03)	1.33	1.30 (0.47, 3.14)
lf_sig	-	-	1.33	3.06 (1.31, 4.06)	4.07	4.39 (3.86, 4.98)	3.93	4.32 (3.53, 5.03)

	Model 9		Model 10		Model 11	
Parameter	Sample	Population	Sample	Population	Sample	Population
Linf_mu	64.74	64.80 (62.22, 67.03)	69.34	68.72 (65.23, 71.68)	68.52	67.55 (65.42,69.55)
Linf_std	5.62	5.58 (4.74, 6.37)	4.26	4.08 (3.00, 5.11)	4.22	5.00 (4.26,5.68)
K	0.261	0.26 (0.23, 0.30)	0.146	0.17 (0.13, 0.21)	0.173	0.219 (0.198,0.245)
A_mu	1	1.00 (0.925, 1.08)	1.5	1.37 (1.19, 1.60)	1.34	1.11 (1.03,1.19)
A_sig	0.18	0.18 (0.15, 0.22)	0.14	0.155 (0.119, 0.184)	0.16	0.17 (0.14,0.2)
Sig	2.2	2.20 (1.75, 2.61)	3.29	2.99 (2.45, 3.62)	2.9	2.39 (2,2.77)
t0	-0.31	-0.32 (-0.43, -0.21)	-0.8	-0.65 (-0.96, -0.43)	-0.63	-0.37 (-0.47,-0.28)
oto_sig	1.82	1.74 (0.66, 2.94)	1.61	1.42 (0.97, 1.84)	1.4	0.96 (0.49,1.31)
lf_sig	4.07	4.38 (3.88, 4.94)	1.43	2.41 (1.43, 3.29)	3.09	4.63 (4.15,5.15)

Comparing model performance

Across all 10,000 cross validation iterations to determine model structure, the mean predictive variance metric ranged between 7.29 and 24.96 (mean = 14.20, s.d. = 2.20) where a lower predictive variance indicates a better model fit. From all candidate likelihood models, the structure of Model 11 best predicted cross validation data in 3,486 of 10,000 iterations. The predictive variance for Model 11 ranged between 7.29 and 20.10 (mean = 13.64, s.d. = 1.91). The structure of Model 5, fit exclusively using tagging data, ranged in predictive variance

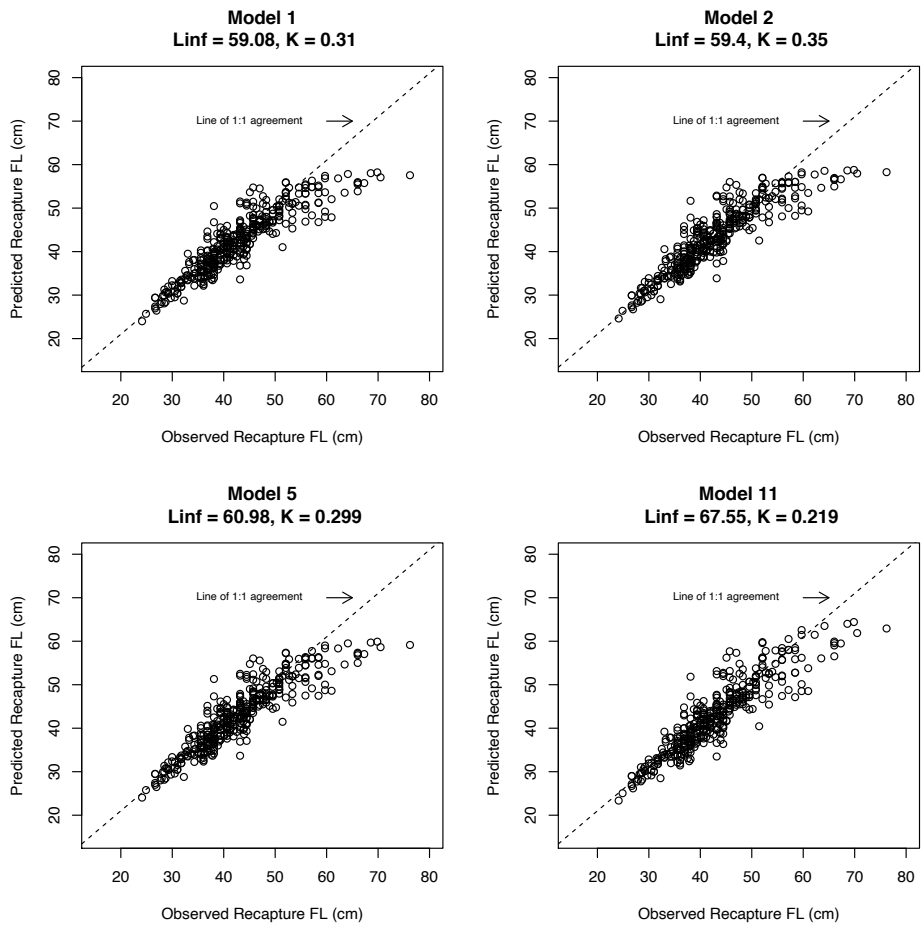

Figure 5.4. Plots Comparing Predicted and Observed Length at Recapture.

Predicted lengths at recapture fit using parameter point estimates from Bayesian Models 1 and 2 and population parameter estimates from Maximum likelihood Models 5 and 11 compared to observed length at recapture. Length at recapture was predicted as a function of length at marking and time at liberty. The 1:1 line indicates where points would fall if model parameters perfectly predicted length at recapture.

between 7.17 and 26.09 (mean = 14.35, s.d. = 2.44). The structure of Model 11 performed better than the structure of Model 5 in 6,351 of 10,000 cross validation iterations. Differences in predictive variance between these two competing structures ranged between -1.60 and 10.80 (mean = 0.72, s.d. = 1.37) and indicated that the inclusion of additional growth data did improve the predictive capability of growth models compared to tagging data alone. Bootstrapped

parameter estimates refit using the prefered model structure and Model 5's tagging only data are summarized in table 5.1 and all parameters for models 5 - 11 are reported in full in table 5.5. When fit to the entire tagging data set, the residual pattern of Model 11 also underestimated lengths at recapture length for the largest individuals.

Discussion

Our integrative model results reconcile 30+ years of efforts to determine growth for *P. filamentosus* in the Hawaiian Archipelago and provide robust support for some observed life history parameters. Growth parameters derived using integrative models that incorporated additional length frequency and length-at-age data were better able to predict observed growth in recaptured fish. These parameters were in agreement with those derived from; 1) the fit of only integrated daily growth increments from otoliths collected in the NWHI without constraining L_∞ (S. Ralston and Miyamoto, 1983), 2) integrated daily growth increments and microincrement counts (DeMartini et al. 1994), and 3) the radioisotopic composition of otolith material and counts of otolith increments from the MHI and NWHI (Andrews et al. 2012) and support the implicit assumption that tagging individuals did not disrupt their growth trajectory. Integrative parameters differed from estimates from an ongoing mark recapture study in the MHI which reported faster growth and smaller asymptotic lengths (O'Malley, 2015). These differences could arise from real changes in growth between the periods fish were collected, methodological differences, as well as that thus far, none of the fish recaptured during the ongoing study have been of the largest size classes (maximum size reported = 47.6 cm FL).

Compared to their broader distribution, *P. filamentosus* from the Hawaiian archipelago were slower growing but obtained larger asymptotic lengths than those from the Mariana Archipelago (Stephen V. Ralston and Williams, 1988) and Papua New Guinea (Fry et al. 2006,

Andrews et al. 2012), and were faster growing but ultimately smaller in their asymptotic length when compared to estimates from the Seychelles (Mees, 1993; Hardman-Mountford, Polunin, and Boulle, 1997; Mees and Rousseau, 1997; Pilling, 2000).

Comparing growth parameter estimates fit exclusively with OTP data indicate that Bayesian and maximum likelihood fitting methods performed similarly. The treatement of individual variability in parameters estimated in Model 2 were identical to those used to fit Model 5 (OTP data only). Parameters estimated by Models 1 and 2 were contained within the 95% confidence intervals of Model 5. Integrative Models 6 - 11 were evaluated under the same assumptions of parameter variability as models 2 and 5.

Of the Bayesian models, Model 1 was the presumed optimal because it incorporated individual variability in both L_∞ and K parameters. The additional Models 2 - 4 suggest that individual variability in both K and L_∞ is important, with perhaps variability in L_∞ being more important based upon the response of L_∞ standard deviation from the base case of Model 1 to the constrained individual variability in Model 3 and Model 4 (Figure 5.3). While Models 3 and 4 had lower DIC values, based upon parameter estimates and patterns of standard deviation, it is likely that these models were not credible. Similar parameter estimates obtained from Models 1 and 2 suggested that the primary source of individual variability was due to variability in the L_∞ parameter. This is consistent with other studies where the best models accounted for individual variability in both terms but accounting for individual variation in the L_∞ term alone was sufficient to describe growth while significantly reducing computational complexity (Eveson et al. 2007, Zhang et al. 2009).

Across all models, the parameters from Model 11 best predicted length at recapture across validation iterations and therefore represents the best estimated parameter set. Information

from older/larger fish was very important for grounding the upper end of integrative growth curves resulting in parameters that better predicted length at recapture. Omission of the largest individuals from Models 1-5 resulted in lower estimates of L_∞, causing growth curves to asymptote prematurely. When included, additional data sources resulted in growth parameters that were better able to predict the length of fish recaptured from the MHI in the OTP study.

Additional data sources included in integrative models represent collections spanning several decades and were collected across both the MHI and NWHI. When incorporating these additional data sources, it must be assumed that growth within the population did not differ significantly with time or region. Genetic homogeneity between NWHI and MHI stocks (Gaither et al. 2010, Gaither et al. 2011) justified incorporating data from both regions and with the exception of Ralston and Miyamoto (1983), all subsequent studies of growth for *P. filamentosus* in the Hawaiian archipelago have included data or parameter estimates from one or more previous studies in their calculations regardless of time and place of collection (DeMartini et al. 1994, Moffitt and Parrish 1996, Andrews et al. 2012). However, these spatial and temporal assumptions may not reflect phenotypic realities and further work is required to resolve whether differences in growth exist between the two regions.

Parameters obtained from our models and those published elsewhere underestimate the size at recapture for the largest fish in the OTP dataset (approximate fork length > 50 cm) (Figure 5.4). Sexual size dimorphism may explain this poor predictive ability. If one sex attains a greater asymptotic length than the other, that sex is likely to be overrepresented in the largest size classes relative to the total population. At sizes where the sex ratio of individuals is similar to the sex ratio of the total sampled population, averaging of model parameters between sexes results in excess model deviation. However, for the largest sizes where sex ratios are not

representative of the population as a whole, estimated growth parameters represent an average of both sexes and will underestimate recapture lengths for largest individuals from one sex while overestimating the recapture length of the largest individuals of the other. While not pronounced, dimorphic size differences have been observed in a number of lutjanid species (Grimes, 1987; Mees, 1993; Stephen J. Newman, Cappo, and Williams, 2000; S. J. Newman and Dunk, 2002; A. J. Williams et al., 2017; Taylor et al., 2018; Nichols, 2019). Estimations of growth parameters for *P. filamentosus* in the Central Pacific are sex agnostic and the method for non-invasive sexing of this species was unknown until recently (Luers et al. 2017). However, elsewhere in their distribution, larger asymptotic lengths have been reported for male *P. filamentosus* in the Seychelles while during research fishing in the Northwestern Hawaiian Islands, the number of females outnumbered males almost 2:1 in the largest size classes, and in Guam no differences between sexes were observed (Harry T. Kami, 1973; Kikkawa, 1984; Mees, 1993).

Accurate estimates of von Bertalanffy growth parameters are very important for management. Growth parameters are often used directly or indirectly in stock assessment and fisheries management (J J Polovina, Ralston, and Ralston, 1987; Haight, Kobayashi, and Kawamoto, 1993). These efforts are sensitive to both growth parameters and the model used to estimate those parameters. For example, the rate of instantaneous natural mortality M is a value of interest often inferred using empirical relationships between M and K (S. V. D. Ralston, 1987; Jensen, 1996; Thorson et al., 2017). Underestimating K will underestimate M, characterizing a stock as less productive than it actually is while overestimating K will overestimate M. If the management regime is linked to such a flawed estimate of stock productivity, then the stock is likely to be mismanaged and under or over harvested, respectively, relative to its true biological

potential. Future work to refine growth estimates for *P. filamentosus* should consider that growth trajectories may differ between males and females.

Chapter 6: Summary and Future Directions

Synthesis

The primary contribution of this dissertation is an improved understanding of deep-water fishes in relation to their population assessment and fisheries management. Complexes of deep demersal fishes are an important resource across much of the globe. In the last 60 years deep-water stocks have increasingly become a target of the global fishing industry (Haedrich, Merrett, and Dea, 2001; Morato et al., 2006). Those tasked with ensuring the sustainable future of these resources require information about the behavior and life history of these species to reduce uncertainty and implement appropriate management strategies. An important component of this process is the evaluation of implemented strategies to ensure their outcome is consistent with management objectives.

Management of deep-water fishes is complicated by the inherent difficulty to directly observe the stock and their life histories. Unlike shallow-water species, observing fish residing in deeper water requires specialized equipment. This means it is often costly and resource intensive to verify management outcomes (Haedrich, Merrett, and Dea, 2001; Murphy and Jenkins, 2010). Deeper living fish also often possess life history traits such as long-life spans and late maturity (Haight, Kobayashi, and Kawamoto, 1993; Morato et al., 2006; Drazen and Haedrich, 2012). The difficulty in observing these fish, and their associated life history traits, make these stocks particularly vulnerable to over-exploitation. Reducing the uncertainty in the tools available to assess and manage these resources is therefore of paramount importance.

Deep-water fishery reserves have emerged as a tool for rebuilding and maintaining deep-water stocks (A. Williams et al., 2009; Huvenne et al., 2016; Uehara, Ebisawa, and Ohta, 2018). Key to understanding the benefits of these reserves is quantifying their ability to retain and protect fish during critical life stages to confer positive, beneficial effects (Roberts et al., 2014). However, biological considerations are often unknown or neglected when reserve areas are

designed, which can lead to uncertain outcomes (Halpern, 2003). Understanding the spatial ecology and movement dynamics of these fishes relative to proposed or implemented areas is therefore critical to both the planning and evaluation processes (Stephen R. Palumbi, 2004).

Passive tracking using acoustic telemetry has become a popular and versatile tool for quantifying fish movements in relative to fishery reserves (Crossin et al., 2017). These systems facilitate long-term observations of movement for tagged individuals as they move within and beyond the boundaries of protected areas. However, to date there have been far more studies using this technology in shallow-water settings compared to deeper environments (Edwards et al., 2019). As a consequence, the performance of these systems in deeper environments is poorly understood.

Through extensive testing in deep, shallow, and controlled tank environments, my collaborators and I were able to show that additional considerations must be accounted for when this technology is applied in a deep-water setting (Chapter 2). Close proximity detection interference (CPDI) is a phenomenon where transmissions from acoustic tags are heard but undetected by receiver units when they are co-located or near in space. We showed that CPDI is caused by the arrival of a transmission's multipath acoustic energy interfering with the arrival of the same transmission's direct path resulting in the receiver's failure to decipher and record the transmission's encoded data.

We were able to demonstrate that the market leading acoustic telemetry system is affected by CPDI, particularly in environments where the depth exceeds approximately 200 meters. Initially, two ranging experiments were performed in relatively deep (approximately 300 m) and shallow (approximately 25 m) settings. CPDI was present in the results of the deep-water experiment and absent from the shallow water test. By coupling information from our

experiments with a tank experiment and background research to understand how these systems encode data, we were able to construct a simulation model to predict when CPDI would occur. The results of two additional range tests validated CPDI occurrence as predicted by the simulation model.

This work ultimately culminated in an improved understanding of the CPDI phenomena and the identification of depth as a key factor. We were able to extend our model to suggest optimal vertical placement to minimize the effect of CPDI on receivers given operating and environmental parameters These models were then packaged as software tools and distributed to the broader community so this phenomenon can be accounted for when designing the configuration of receiver arrays for future tracking studies.

Hawaii introduced the bottomfish restricted fishing areas (BRFAs) in 1998 to curb the overfishing of the demersal fish complex by the commercial fishery (Ikehara, 2006). There BRFAs originally numbered 19 but were reduced in number and revised in size prior to the 2008 fishing year after work to better understand preferred bottomfish habitat (Parke, 2007) and on 1 September 2019, the start of the 2020 Federal Fishing Year, the State of Hawaii reopened 4 of the 12 remaining reserve areas. However, the utility and role of the BRFAs remains a contentious issue among fishery stakeholders (Hospital and Beavers, 2011).

We tracked *Pristipomoides filamentosus,* the species most represented in the catch of the commercial bottomfish fishery, using acoustic telemetry relative to one of the BRFAs to understand how individual fish moved out of, into, and within this protected space (Chapter 3). Our work also revealed a high probability of post-release mortality when individuals were released, a serious implication for other studies investigating this species. However, high rates of residency within the BRFA were observed for surviving fish. Individuals were detected within

reserve boundaries on upwards of 90% of the total days they were tracked. Using a constrained path linear home range estimator to quantify the scale of movement for our fish, I calculated a home range length that was less than 10 km in length. Using the shortest depth-constrained path across each of the BRFAs as a course proxy for the minimum protection they afford, I found the length of this path was longer than the home range of *P. filamentosus* in each of these areas. These results suggest the BRFAs are of an appropriate size for protecting fish residing within their borders.

While the BRFAs may be of an appropriate scale to protect *P. filamentosus,* and other studies show that these fish often increase in size and abundance inside the BRFAs (Sackett et al 2014), the role they have played in recovery of the Deep-7 bottomfish fishery, in terms of catch metrics, has gone largely unquantified. Bottomfish stocks recovered following revision of the BRFA management system but whether this was a consequence of the BRFAs or other management measures introduced at the time was poorly understood (Brodziak et al. 2011, 2014, Langseth et al. 2018). Using a dataset of commercial marine landings maintained by the State of Hawaii, I found that overall fishing pressure, the number of fishers, the number of trips per fisher, and total harvest decreased with the establishment of the reserves. After the reserves were revised, similar levels of effort and total harvest persisted but there was a further decrease in the number of trips per fisher, though the number of fishers increased. There was also some evidence that the number of fish caught on a single trip increased. Following implementation and revision of the reserves, the fishery redistributed with disproportionate decreases in effort, the number of fishers for reporting areas containing protected habitat, though this effect lessened with time. There was also a persistent decrease in harvested biomass between areas containing protected

habitat and those that didn't for both of these time periods. Furthermore, the average catch per trip in these areas also decreased following the revision of the BRFA network.

Another critical job of fisheries management is to accurately forecast future stocks in response to competing management scenarios. This requires precise estimates of key life history parameters for the species. Over the last 40 years, a number of studies have used various methods to obtain growth parameter estimates for *P. filamentosus* (S. Ralston and Miyamoto, 1983; DeMartini, Landgraf, and Ralston, 1994; Moffitt and Parrish, 1996b; Andrews et al., 2012). I was able to combine data from each of these prior studies with data from a previously unpublished tagging experiment using an integrative method to produce a single set of parameters that best described the growth that was observed in the tagging dataset. These parameters were similar to and support those estimated using radio-isotopes and direct aging methods several years ago lending confidence to their accuracy (Andrews et al., 2012). Furthermore, this work revealed that these parameters are insufficient for describing the growth observed in the largest of individuals potentially explained by dimorphic differences in the growth of males and females of this species.

This dissertation has begun to address some of the knowledge gaps surrounding the use of fishery reserves for managing deep-water fishes. However much remains to be done to build upon the work presented here and integrate specific results into future management policy.

Future Directions

Incorporating our findings linking depth to CPDI (Chapter 2), space state models are one area that would benefit from additional work. Space state models have emerged as a method for estimating a tagged individual's position within a study area using the number of detections over a time-interval to estimate position relative to receivers (Pedersen and Weng, 2013; Alós et al.,

2016). Studies relying on space state models require information on dynamic changes to the receiver's detection range throughout the study. This is typically achieved by a transmitter located a fixed distance from the receiver and modeled using a sigmoidal, or similarly shaped, detection function (Pedersen and Weng, 2013; Alós et al., 2016). However, when CPDI is present, the shape of the detection function closest to the receiver is truncated. One possible avenue to pursue would be incorporating results from our predictive model to dynamically account for this truncation, however work would be needed to overcome challenges determining if a fish was close to or far from a receiver when associated with low detections.

CPDI can also introduce holes when acoustic receivers have been spaced with overlapping detection ranges in a fence configuration. Performance of the fence may be compromised if tagged individuals are able to navigate undetected through one of these holes (Kessel et al., 2015b). The CPDI model we developed was used to verify the integrity of the fences used to track *P. filamentosus* in chapter 3. This practice should be a practical consideration of all studies using a fence array format.

Another possible avenue for this work would be to improve the predictive model of CPDI. Multipath arrivals off the air-sea surface are a major concern for CPDI due to negligible energy loss at this interface and have a geometry that was relatively easy to estimate, however the benthic interface may also reflect energy sufficient for detection by the receiver and modeling complex bathymetry at a unique study site is more challenging. Due to the design of our range tests and an inability to validate additional geometries, the benthic interface of our model is treated as a horizontal plane. Future work could improve arrival time estimates by incorporating sloped geometries or moving to a ray tracing model for simulating more complex bathymetry.

Other methodological considerations brought up by this dissertation include ways of mitigating post-release mortality in deep-water teleosts. Admittedly there have been several studies that have looked at this very issue with recommendations ranging from improving handling protocols, to devices for securely delivering fish to the seafloor (Hannah and Matteson, 2007; Jarvis and Lowe, 2008; Roach, Hall, and Broadhurst, 2011; S J Hochhalter and Reed, 2011; Mclennan, Campbell, and Sumpton, 2014). Our work with *P. filamentosus* (Chapter 3) reinforces that there is no one panacea for all species. If the resources are available, it would be wise for future studies of *P. filamentosus* and other deep-water species to conduct a survivorship study as part of the initial tagging effort. Such an undertaking would involve identifying a number of treatments that may affect survivorship and randomly assigning tagged fish to one of these protocols. These treatments could include whether the fish's swim bladder was vented, if the fish is held for a recovery period or immediately released, if the release occurs at midwater, the seafloor, or at the surface, and other factors that could lead to different outcomes. Data should be downloaded from the receiver array after an appropriate time has elapsed and a logistic model fit to assess which treatments resulted in the highest rates of survivorship. While more costly than tags without sensors, tags with pressure sensors supplied depth records that were incredibly helpful for determining whether fish were alive or dead. The detections of one highly resident fish was otherwise indistinguishable from stationary tags except for changes in depth. Similarly, there were records of two fish that met all of our criteria for being "alive", but with diel vertical movements that closely resembled the behavior of predator species. Additionally, high output tags were used on this project to minimize the number of receivers required to instrument the Makapuu study area. Combined with low background noise at the depths our receivers were placed, these tags could be detected by receivers to at a range of approximately

846 m, increasing position uncertainty. Had lower output tags with depth sensors been used, the positions of fish, and their fate could be assessed with greater fidelity.

Specific to management of Hawaii's bottomfish, observed site fidelity and relatively limited home ranges for *P. filamentosus* and other bottomfish species reported elsewhere (Weng, 2013), as well as low rates of regional larval flow (Vaz, 2012), indicate that a spatially structured approach to management may be appropriate for these fishes. The current method for bottomfish assessment pools data across all island areas but evidence from our study and conventional tagging work indicate that inter-island movements of adult fish are rare, implying discrete adult subpopulations (Kobayashi, 2008; O'Malley, 2015; Langseth et al., 2018). Furthermore, habitat distribution modeling has shown different bottomfish species differ in habitat preference and the distribution of preferred habitat is not uniform across the archipelago (Oyafuso et al., 2017). Assessment of these resources in Hawaii and elsewhere throughout the Indo-Pacific could be improved by incorporating this information into the stock assessment process.

The BRFAs were originally established to curb the overfishing of key bottomfish species. Since 2010, stock assessments have indicated that overfishing of these resources is no longer occurring, nor are they overfished (Brodziak et al. 2011, 2014, 2014, Langseth et al. 2018). With this goal achieved, it is not clear what the present role of the BRFAs is. Fishery reserves can serve a number of roles beyond rebuilding overfished populations, including enhanced larval output and export to non-protected areas as well as acting as insurance against uncertainty (Lockwood, Hastings, and Botsford, 2002; Sale et al., 2005; Planes, Jones, and Thorrold, 2009) but failure to adequately set objectives and assess the performance of these areas can result in the loss of stakeholder support (Lundquist and Granek, 2005). It is therefore important that Hawaii's

bottomfish fishery make clear the intent of these areas moving forward and convey this information to the greater fishing community.

To this end, the reopening of four of the 12 restricted fishing areas on 1 September 2019 presents an interesting opportunity to understand how subpopulations differ in these areas relative to the broader fishery. Managers have requested commercial fishers reporting catch in any of the 4 reopened areas do so with a new unique reporting grid identifier. Using methods similar to those in chapter 5 will allow future work to track how metrics of effort, catch, and catch-per-unit-effort change for fishers in these regions relative to the unprotected adjacent areas. While commercial landings data provide a fisheries dependent view of any changes these areas undergo, baited stereo-cameras offer an opportunity to study these changes in-situ. Such systems have been used to collect data on the size and abundance of fish in protected and non-protected areas and are currently being used to perform a fisheries-independent surveys for the purpose of stock assessment (Merritt et al., 2011; CH Moore et al., 2013; Misa et al., 2013; Richards et al., 2016; Sackett, Kelley, and Drazen, 2017; Langseth et al., 2018). These records provide a unique time series that fits well within the traditional BACIP framework, specifically tracking the relative trajectories in size and abundance of bottomfish before and after the removal of these areas relative to adjacent areas that have never been protected. Such an analysis would allow managers to infer how the remaining bottomfish restricted fishing areas, and fishery reserves in general, contribute to maintaining bottomfish stocks.

Despite extensive efforts to quantify growth for *P. filamentosus*, there are a number of considerations that could refine growth models. As previously noted, parameters obtained from integrative models indicate the potential for dimorphic growth between males and females. Dimorphic differences have been observed in the species elsewhere (Mees, 1993) in its

distribution and but dimorphism has not been considered in any study of the Hawaiian population. Until recently, the only way to sex *P. filamentosus* was internally, requiring the animal to be sacrificed, limiting the collection of sex data to direct aging studies. But recent advancements in external sexing mean that sex can be accounted for using growth increment and length frequency methods as well (Luers, DeMartini, and Humphreys, 2017). At this point there is no reason future studies of *P. filamentosus* should not collect this information.

There were also spatio-temporal assumptions made when fitting growth curve parameters that are worth investigating. Namely, that fish collected from the Main Hawaiian Islands were similar to those from the Northwestern Hawaiian Islands and that it was appropriate to fit a single set of parameters from specimens collected over a period of nearly 30 years. Justification for these assumptions was discussed in chapter 4, however in light of sub-regional differences identified in other eteline snappers (Nichols, 2019) these are concerns that any future study to quantify growth for *P. filamentosus* in the region should seek to address.

Recent years have seen an expansion of commercial fisheries targeting deep-water demersal fishes in the Indo-Pacific. However, in many cases management is constrained by limited data and financial resources (A. J. Williams et al., 2012). The studies comprising this dissertation, and others looking at the outcome of the BRFAs on Hawaii's bottomfish indicate these areas are appropriate in scale and have resulted positive benefits to the stock (Weng 2013, Sackett et al. 2017, Chapter 3). Similar reserve systems may be an attractive solution to uncertainties in the management of demersal fishes elsewhere. However, in addition to ecological considerations, well defined goals, regular assessment, community buy-in and engagement, socio-economic characteristics, local governance, and enforcement are all factors determining success of these areas (Grafton and Kompas, 2005; Rossiter and Levine, 2014).

Ultimately, it will be up to the managers of these fisheries to determine if such a system is feasible for meeting their local needs, given their resources.

Deep-water fishery reserves are an important instrument in a manager's toolbox. However, each system of reserves and the fishes they protect is unique in both implementation and objectives. As such, there is no one size fits all method to assess their utility. The work presented here demonstrates how understanding the biology and spatial ecology of the intended beneficiaries of these protections provides a method for evaluating the appropriateness of spatial management for these species and improves our understanding of how these areas can rearrange the complex dynamics of a fishery. As fisheries move into deeper waters, so too must fishery management.

SUPPLEMENTAL MATERIALS AND APPENDICIES

Appendix 3.1. Results Inclusive of Uncertain Tag Results

The following supplemental material presents an alternative scenario where both valid (alive) fish tracks and fish with tracks of uncertain status are analyzed together. The latter group likely

includes both valid tracks of fish that are highly resident and only detected at a single receiver as well as tracks from fish that did not survive following release and who's tags now sit an intermediate distance from a receiver station.

Results

Categorizing Fish Status

Of the 158 tracks from tagged *P. filamentosus* detected on the array between 26 June 2017 and 6 January 2018 10 were classified valid, 36 classified as uncertain and 82 classified as dead. Tracks of 40 individuals with track durations less than 14 were excluded from analysis and 11 tags were not detected on the array during the analysis period (Table 3.1). The classification algorithm initially assigned 30 tracks a valid status, however 20 tracks were reclassified post-facto with 12 tracks reclassified uncertain while 8 appeared dead. The following analyses are for the 46 fish with valid or uncertain tracks. Because the group of uncertain tags likely contained a mixture of tags from fish that are dead and alive, a less conservative analysis that includes these additional tracks is included as supplemental material to this manuscript.

Under the assumption that only the fish with valid tracks survived after tagging, the survivorship rate was 25.7%. Because some fish were tagged prior to the start of the analysis period, track duration, defined as the time between each individual's first and last detection on the array, was used to compare and standardize results between individuals. This is in contrast to time at liberty which would encompass the period from an individual's tagging until it's last detection but would be inappropriate for standardizing analysis results as it would also count days before the analysis period began. Valid and uncertain tracks ranged in duration between 66 and 559-days with a mean of 358-days (s.d. = 145) (Table A3.2).

Table A3.2: Descriptive metrics of valid and Uncertain tracks from tagged opakapaka for analysis period 1 (P1) and period 2 (P2).

Tag ID	Status	Fork Length (cm)	Tagging Date	Time at Liberty (days)	Track Duration (days)	Transmissions Detected	Unique Days Detected	P1: Home Range (km)	P2: Home Range (km)	Boundary Movements Detected (Total)	P1: % Time In	P2: % Time In
2122	Unknown	47	1/9/18	216	95	483	16	5.484	4.707	4	93%	100%
2127	Unknown	49.5	1/9/18	96	95	950	68	5.119	0	14	96%	0%
2133	Alive	43	1/9/18	190	35	457	28	5.484	1.706	6	99%	100%
2136	Alive	42	1/9/18	452	335	21062	301	6.018	2.354	0	100%	100%
2139	Unknown	50	1/9/18	456	338	470	127	3.778	5.119	0	100%	100%
2140	Unknown	39.5	1/9/18	234	49	68	13	3.412	4.707	0	100%	100%
2157	Unknown	52.5	1/10/18	66	66	515	35	5.484	0	18	56%	0%
28171	Unknown	52	1/11/18	446	331	2351	212	2.354	2.354	0	100%	100%
28175	Unknown	48	1/11/18	391	276	920	125	11.767	3.664	0	100%	100%
28177	Unknown	42.5	1/11/18	437	144	679	41	13.192	3.778	4	100%	16%
28178	Unknown	50	1/11/18	352	158	19	11	3.412	5.119	0	100%	100%
28179	Alive	45	1/11/18	454	339	60130	339	5.484	3.778	69	98%	98%
28181	Unknown	53	1/11/18	446	331	9716	170	1.706	0	0	100%	100%
28185	Unknown	34	1/11/18	453	338	549	163	3.243	1.622	0	0%	0%
30683	Unknown	41.5	8/28/17	714	463	18651	397	1.622	0	0	0%	0%
30684	Unknown	43	8/28/17	726	475	77111	475	3.664	2.354	28	0%	0%
30690	Unknown	42	8/28/17	725	474	44580	467	6.018	0	0	100%	100%
30694	Unknown	36	8/28/17	725	474	44364	457	6.132	0	2	100%	100%
30695	Alive	36.5	8/28/17	716	453	3605	297	7.061	2.354	2	100%	100%
30703	Unknown	54	8/28/17	681	429	577	94	2.354	2.354	0	100%	100%
30705	Alive	40.5	8/29/17	724	474	17055	462	6.132	8.12	86	99%	97%
30707	Unknown	53	8/29/17	724	474	33067	456	0	1.706	0	100%	100%
30714	Unknown	47	6/24/17	764	410	12364	152	0	1.706	0	100%	100%
30715	Unknown	38	6/24/17	856	538	57792	535	0	1.706	0	100%	100%
30717	Unknown	36.5	6/24/17	73	71	277	7	0	0	0	100%	0%
30721	Alive	45	6/24/17	856	538	64477	538	3.242	6.018	0	100%	100%
30722	Unknown	45	6/24/17	856	538	99377	522	0	1.706	0	100%	100%
30729	Unknown	49.5	6/25/17	187	186	1175	60	8.371	0	0	100%	0%
30734	Unknown	55.5	6/25/17	772	435	570	75	1.621	2.354	0	100%	100%
30739	Unknown	40	6/26/17	121	121	77	24	1.621	0	0	100%	0%
30742	Unknown	47	6/26/17	505	116	199	25	1.621	2.354	0	100%	100%
30743	Unknown	43	8/28/17	726	475	63462	465	1.621	2.354	0	100%	100%
30747	Unknown	44	8/28/17	176	176	22474	172	3.243	0	0	100%	0%
30749	Unknown	61	1/11/18	201	78	111	42	2.354	2.354	0	100%	100%
30751	Unknown	70	1/11/18	364	249	11103	221	1.621	4.707	0	100%	100%
36810	Unknown	44	6/24/17	637	319	1558	61	0	1.706	0	100%	100%
51581	Unknown	61.5	1/13/17	1012	370	22062	276	0	0	0	100%	100%
51582	Alive	41	3/18/17	380	280	8109	222	3.778	0	0	100%	0%
51584	Unknown	51	3/18/17	813	299	5446	234	1.706	0	0	100%	100%
51585	Unknown	44	3/18/17	820	234	152	50	1.621	1.621	0	100%	100%
51586	Alive	46	3/18/17	961	447	39084	447	3.242	3.664	0	100%	100%
51587	Unknown	48	3/18/17	982	397	629	139	1.621	1.621	0	100%	100%
51588	Alive	44	3/18/17	286	186	16105	186	7.061	0	6	80%	0%
51596	Alive	42.5	8/28/17	726	475	44371	475	3.242	6.018	0	100%	100%
51598	Unknown	44.5	8/29/17	514	256	114	59	1.706	0	0	100%	100%

Size selective survivorship bias

The mean fork length of P. filamentosus classified alive (46.5 cm) fell within the 95% confidence interval from simulation data sampled without replacement (45.3 - 50.6). The standard deviation of fork length for these fish was 7.165-cm and did not fall within the 95% confidence interval obtained from simulation data (8.149 – 11.81-cm). This result indicates that the mean size of surviving fish was not significantly different than expected for a random subset

of the total population, and the smallest and largest fish tagged were underrepresented in the data (Supplemental Figure A3.3).

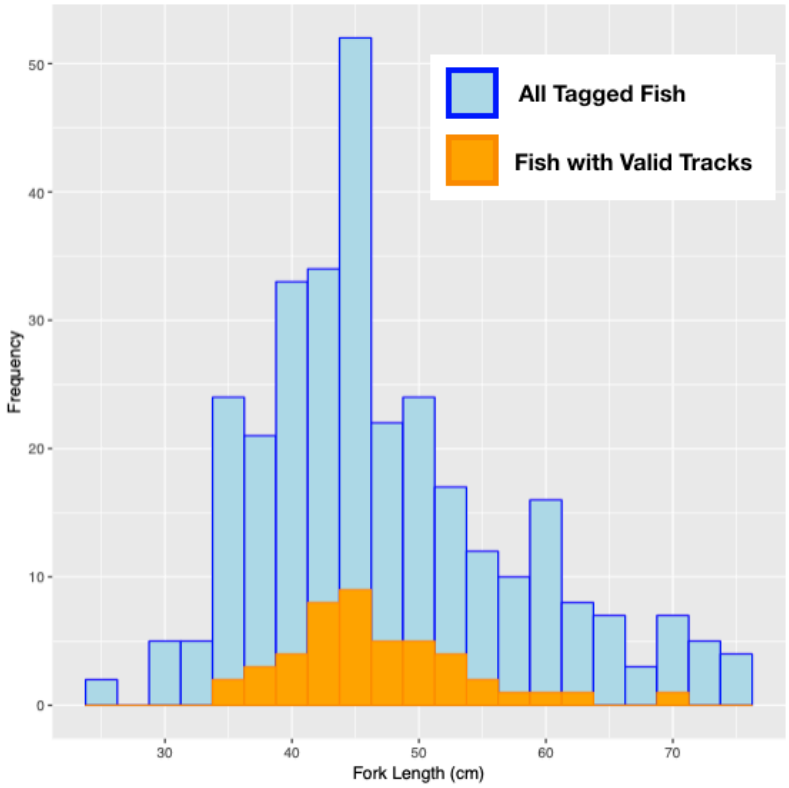

Figure A3.3. Simulated and Observed Fork Lengths for Surviving Fish

Orange bars show the distribution of fork lengths for tagged P. filamentosus with valid and uncertain tracks and blue bars indicate all P. filamentosus tagged during the duration of the project. Simulation results show that the observed distribution mean of fork lengths for fish with tracks classified valid was within the range expected from the total population data, however the observed standard deviation of the distribution was smaller than would be expected if survivorship was random.

Analysis Periods

Receivers were recovered and downloaded twice, once mid-study and once at the end of the study, separating the analysis into two periods. 45 fish of 46 fish with valid or uncertain tracks

were detected on the receiver array during the first of these periods with 38 fish appearing on the array during the second.

Individual Home Range

Estimates of linear home range for the first analysis period varied between 0.0-km and 19.7-km. The median observed home range distance was 3.2-km (IQR: 1.6-6.1-km). Home ranges observed during the second analysis period were between 0.0-km and 8.1-km with a median distance of 2.4-km (1st Quartile = 1.7, 3rd Quartile = 3.7). Regardless of array shape, the median home range calculated was 3.7-km (IQR: 1.7-7.2-km) (Figure A3.5).

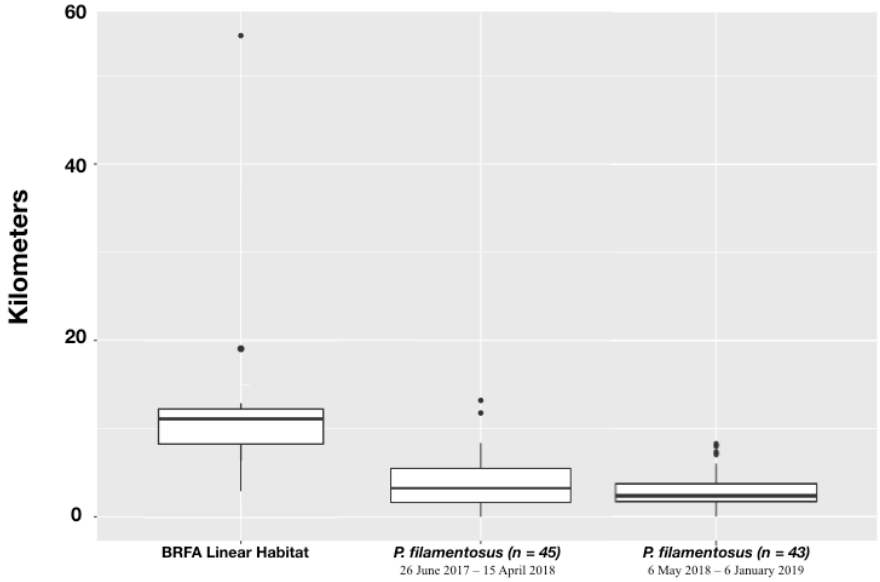

Supplemental Figure A3.5. Comparing Observed Ranges to BRFA Size

Comparison of the maximum movement distances observed for P. filamentosus (Valid and uncertain tracks) to the linear habitat dimensions of the 8 BRFAs.

Quantifying Movement Frequency and Reserve Retention

Tracked fish generally stayed within the protection of reserve boundaries. During the first period, 11 of the 45 fish with valid or uncertain tracks were detected crossing BRFA boundaries a

combined 94 times. Site fidelity was high; on average, fish detected in this period spent 91.6% of their time within the BRFA (s.d. = 25.8%). For the fish that moved between protected and unprotected areas, the median number of total movements across BRFA boundaries was 6-crossing-per-fish (IQR: 3.5-13.5-crossings-per-day-per-fish) over a median track duration of 95-days (IQR: 76.5-224.5-days). Standardized by track duration, the median number of movements into or out of the BRFA for the 11 fish was 0.061-crossings-per-day-per-fish (IQR: 0.028- 0.168-crossings-per-day-per-fish) equivalent to one crossing every 16.4-days. However individual rates were as high as 0.273-crossings-per-day, equivalent to crossing once every 3.6-days.

During the second analysis period, 5 of the 43 tracks were detected crossing the BRFA boundaries a combined total of 146 times. Site fidelity was high; on average, fish detected in this period spent 89.8% of their time within the BRFA (s.d. = 28.9%). The median fish crossed the BRFA's boundaries at an average rate of 0.028-crossing-per-day-per-fish (IQR: 0.003-0.149-crossings-per-day-per-fish) over a mean track duration of 245-days (IQR: 245-245-days). Standardized by track duration, this corresponded to one movement over reserve boundaries every 35.4-days. However individual rates were as high as 0.156 -crossings-per-day, equivalent to crossing once every 6.4-days.

Without respect to analysis period or array shape, 11 of the 45 tracks were detected crossing the BRFA boundaries a combined total of 94 times. Rates of site fidelity within the reserve were high; on average, the median fish spent 100% of their time within the BRFA (IQR: 100-100%). For fish detected moving across boundaries, the median fish crossed BRFA boundaries 6 times (IQR: 3.5-24) over a median track duration of 350-days (IQR: 173.5-495.5-days), resulting in 0.04-crossings-per-day-per-fish (IQR: 0.015-0.21-crossings-per-day-per-fish).

This corresponds to one movement over reserve boundaries every 27, however individual rates were as high as 0.27-crossings-per-day, equivalent to crossing once every 3.7 days.

Appendix 4.1. Full Model Summaries and Diagnostic Plots for Fishery Wide Linear Models

The following appendix includes model summaries and diagnostic plots presented in the section "General Trends in the Deep 7 Fishery"

Hypothesis 1: Effort Distribution

```
Call:
lm(formula = n_trips ~ regime, data = trips_per_year)

Residuals:
    Min      1Q  Median      3Q     Max 
-694.78 -269.44   22.33  202.28 1006.22 

Coefficients:
               Estimate Std. Error t value Pr(>|t|)    
(Intercept)     2951.11     149.75  19.706 2.50e-16 ***
regimebefore    1181.67     211.78   5.580 9.66e-06 ***
regimerevision   -28.44     211.78  -0.134    0.894    
---
Signif. codes:  0 '***' 0.001 '**' 0.01 '*' 0.05 '.' 0.1 ' ' 1

Residual standard error: 449.3 on 24 degrees of freedom
Multiple R-squared:  0.6393, Adjusted R-squared:  0.6092 
F-statistic: 21.27 on 2 and 24 DF,  p-value: 4.855e-06
```

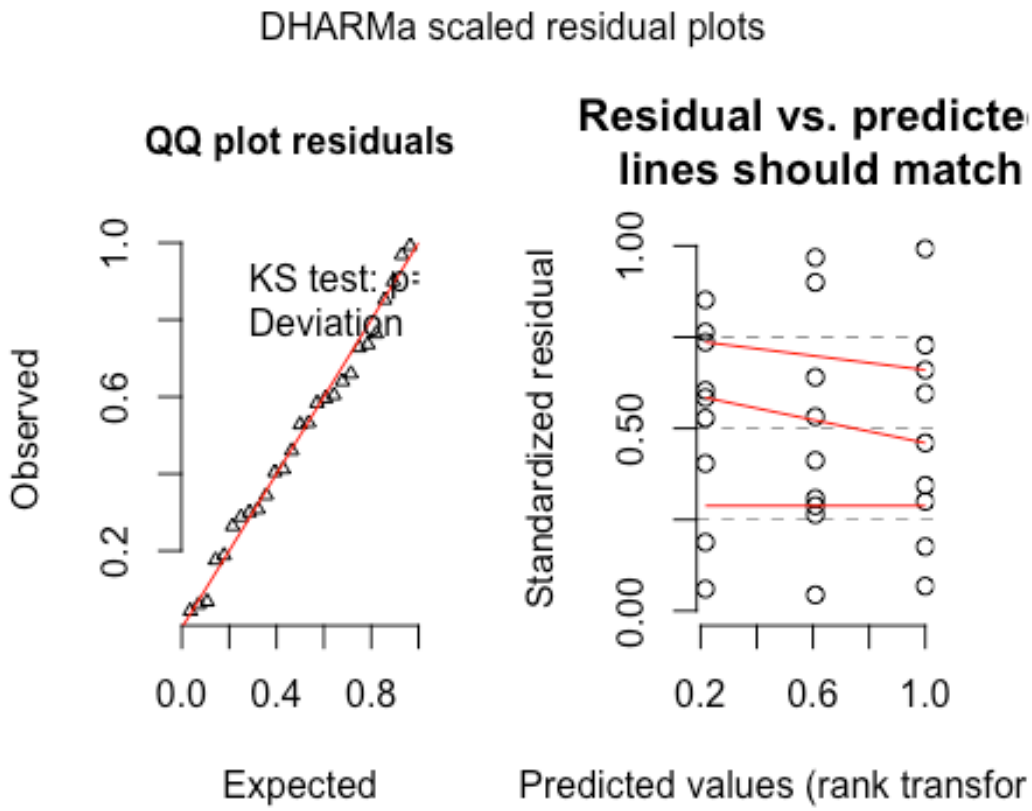

Hypothesis 2: Fisher Participation

```
Call:
lm(formula = n_fishers ~ regime, data = fishers_per_year)

Residuals:
    Min      1Q  Median      3Q     Max
-86.556 -26.056   1.556  27.000 106.444

Coefficients:
               Estimate Std. Error t value Pr(>|t|)
```

```
(Intercept)      383.56      15.23  25.179  < 2e-16 ***
regimebefore     109.89      21.54   5.101 3.22e-05 ***
regimerevision    40.00      21.54   1.857   0.0757 .
---
Signif. codes:  0 '***' 0.001 '**' 0.01 '*' 0.05 '.' 0.1 ' ' 1

Residual standard error: 45.7 on 24 degrees of freedom
Multiple R-squared:  0.5263, Adjusted R-squared:  0.4868
F-statistic: 13.33 on 2 and 24 DF,  p-value: 0.0001278

Model family was recoginzed or set as continous, but duplicate values were de
tected in the simulation - changing to integer residuals (see help for detail
s)
```

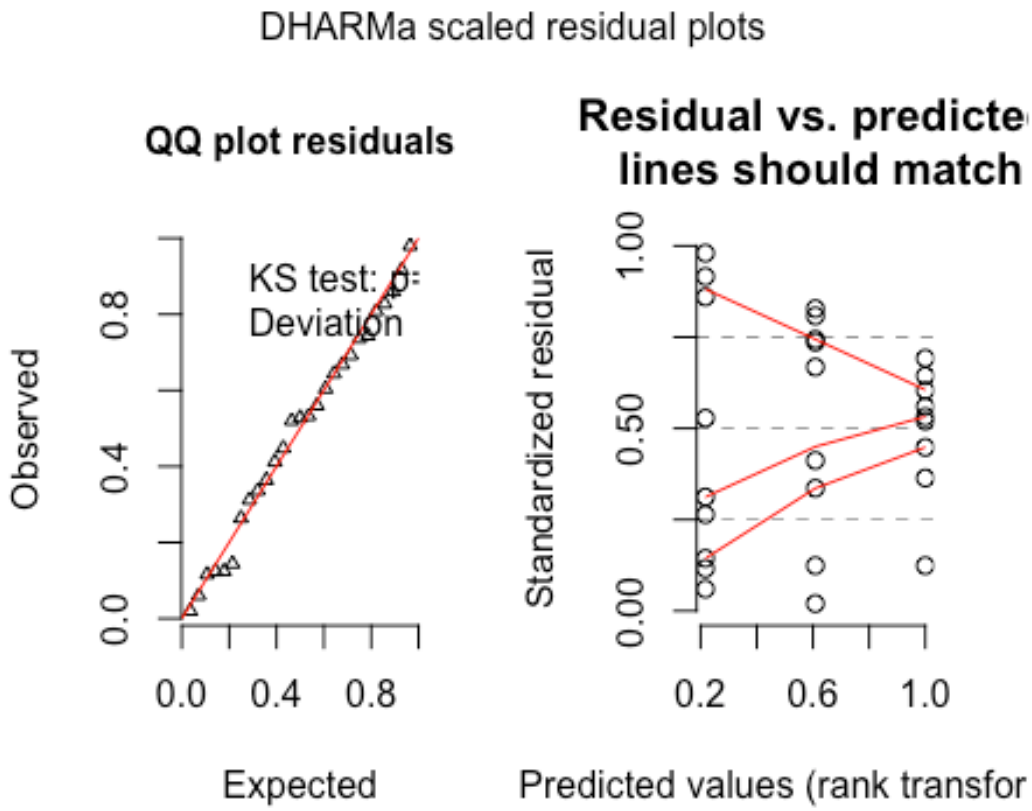

Hypothesis 3: Allocation of Individual Effort

```
Call:
lm(formula = mean ~ regime, data = trips_per_fisher)

Residuals:
     Min       1Q   Median       3Q      Max
-0.94009 -0.44948 -0.00543  0.29495  1.57368

Coefficients:
               Estimate Std. Error t value Pr(>|t|)
```

```
(Intercept)      7.7037     0.2111  36.490   <2e-16 ***
regimebefore     0.6627     0.2986   2.220   0.0361 *
regimerevision  -0.7988     0.2986  -2.675   0.0132 *
---
Signif. codes:  0 '***' 0.001 '**' 0.01 '*' 0.05 '.' 0.1 ' ' 1

Residual standard error: 0.6333 on 24 degrees of freedom
Multiple R-squared:  0.5003, Adjusted R-squared:  0.4587
F-statistic: 12.02 on 2 and 24 DF,  p-value: 0.0002423
```

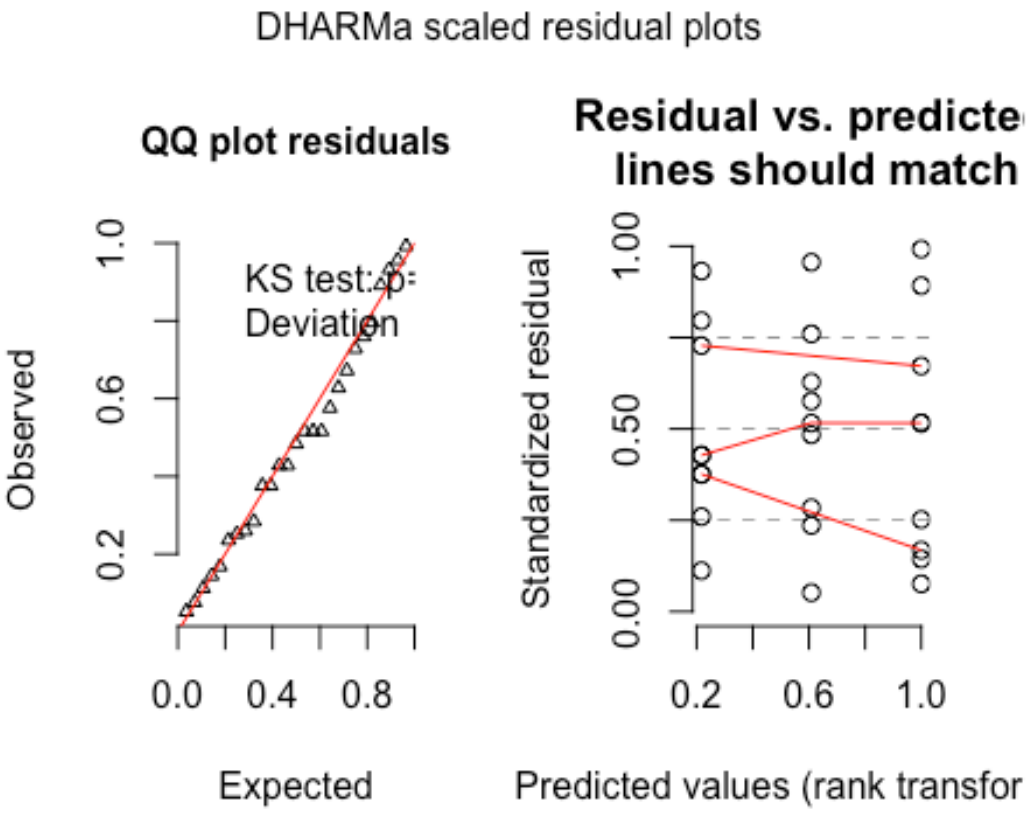

Hypothesis 4: Harvested Biomass

```
Call:
lm(formula = lbs ~ regime, data = lbs_harvested_per_year_wo_spp)

Residuals:
   Min     1Q Median     3Q    Max
-77600 -26037 -10213  15914 134528

Coefficients:
               Estimate Std. Error t value Pr(>|t|)
(Intercept)      221955      15695  14.142 3.89e-13 ***
regimebefore      91065      22196   4.103 0.000406 ***
regimerevision    19816      22196   0.893 0.380844
---
Signif. codes:  0 '***' 0.001 '**' 0.01 '*' 0.05 '.' 0.1 ' ' 1

Residual standard error: 47090 on 24 degrees of freedom
Multiple R-squared:  0.4369, Adjusted R-squared:   0.39
F-statistic: 9.311 on 2 and 24 DF,  p-value: 0.001016
```

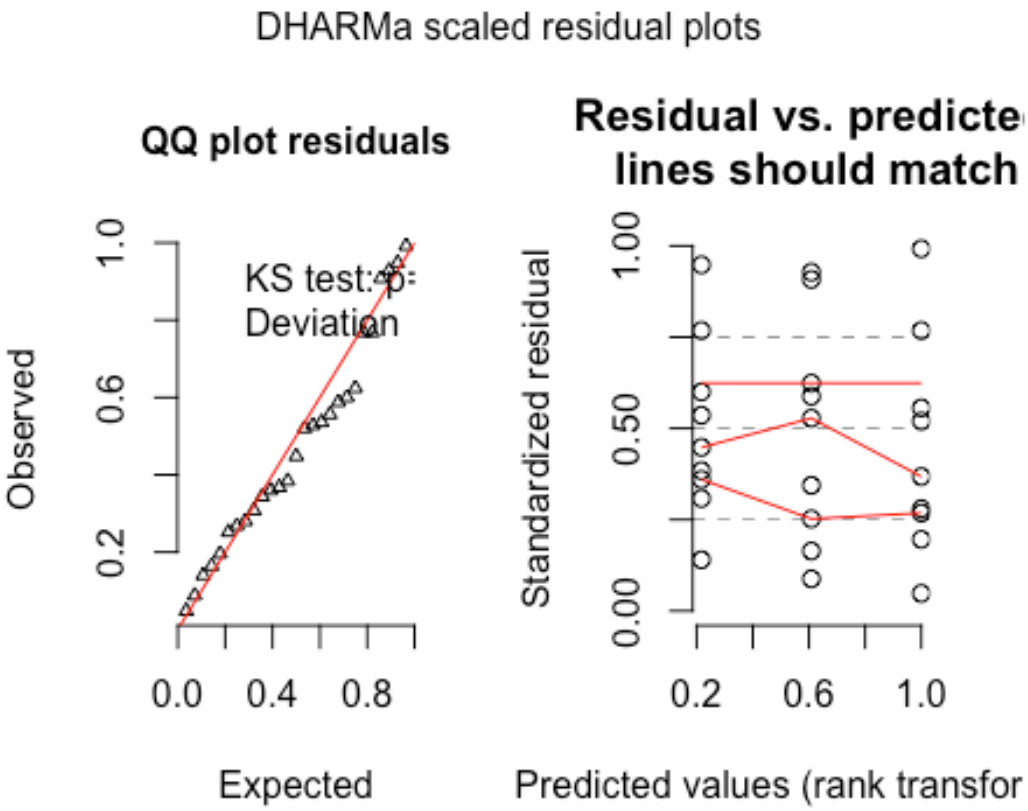

Hypothesis 5: Average Landings Per Trip

```
Call:
lm(formula = mean ~ regime, data = annual_cpue_lbs)

Residuals:
    Min      1Q  Median      3Q     Max
-12.208  -4.994  -1.341   4.981  17.399

Coefficients:
               Estimate Std. Error t value Pr(>|t|)
```

```
(Intercept)      52.812      2.252  23.448   <2e-16 ***
regimebefore     -2.569      3.185  -0.807   0.4279
regimerevision    6.330      3.185   1.987   0.0584 .
---
Signif. codes:  0 '***' 0.001 '**' 0.01 '*' 0.05 '.' 0.1 ' ' 1

Residual standard error: 6.757 on 24 degrees of freedom
Multiple R-squared:  0.2563, Adjusted R-squared:  0.1943
F-statistic: 4.135 on 2 and 24 DF,  p-value: 0.02864
```

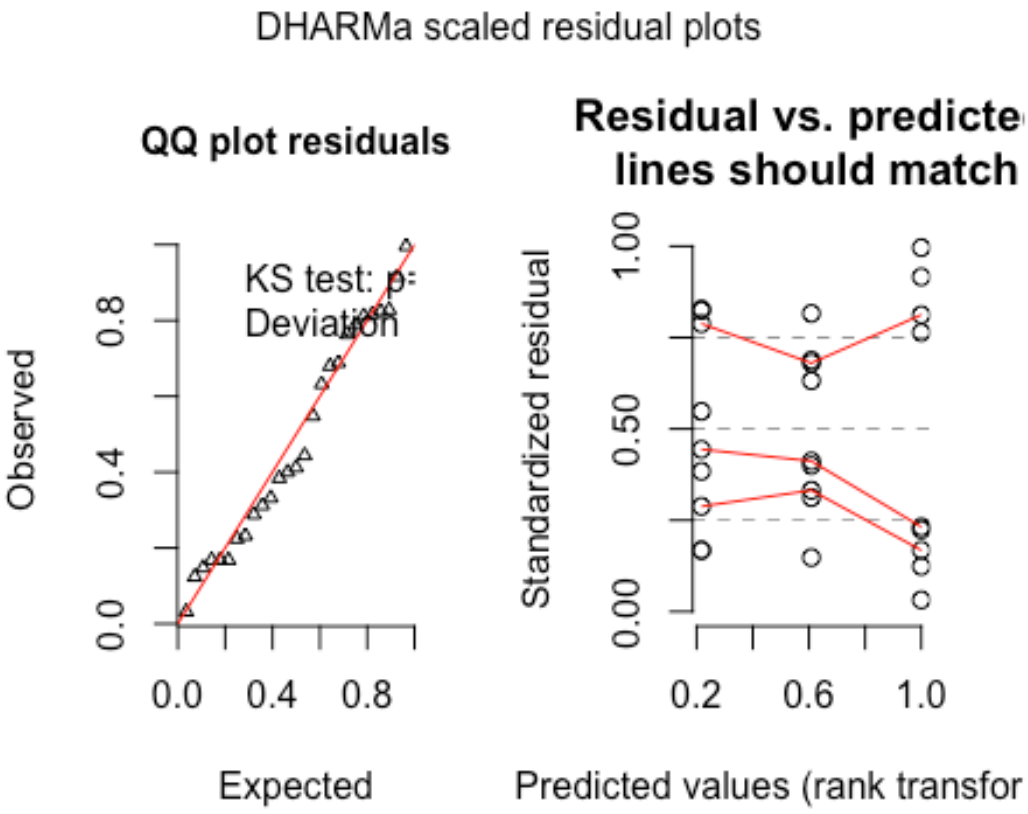

Appendix 4.2. Full Model Summaries and Diagnostic Plots for Delta Models

The following appendix includes model summaries and diagnostic plots presented in the section "Trends Between Protected and Non-protected Areas"

Hypothesis 1: Effort Distribution

```
Linear mixed model fit by REML. t-tests use Satterthwaite's method [
lmerModLmerTest]
Formula:
percent_delta ~ status + time_protected_implementation + time_protected_revis
ion +
    (1 | primary) + (1 | comparison)
   Data: h1_deltas

REML criterion at convergence: 18948.6

Scaled residuals:
    Min      1Q  Median      3Q     Max
-7.0586 -0.3543 -0.0124  0.3375  7.2236

Random effects:
 Groups     Name        Variance Std.Dev.
 comparison (Intercept) 10527    102.60
 primary    (Intercept) 16926    130.10
 Residual                5661     75.24
Number of obs: 1629, groups:  comparison, 41; primary, 39
```

```
Fixed effects:
                               Estimate Std. Error         df t value
(Intercept)                     25.31289   26.70091   58.88062   0.948
statusimplementation:control   -33.52121    8.05032 1560.50468  -4.164
statusrevision:control         -33.49955   10.58725 1561.77771  -3.164
statusreopened:control           0.06079    7.38996 1572.72007   0.008
time_protected_implementation    3.11266    1.30976 1559.36829   2.377
time_protected_revision          4.21164    1.77342 1559.36829   2.375
                              Pr(>|t|)
(Intercept)                    0.34700
statusimplementation:control   3.3e-05 ***
statusrevision:control         0.00159 **
statusreopened:control         0.99344
time_protected_implementation  0.01760 *
time_protected_revision        0.01768 *
---
Signif. codes:  0 '***' 0.001 '**' 0.01 '*' 0.05 '.' 0.1 ' ' 1

Correlation of Fixed Effects:
            (Intr) sttsm: sttsrv: sttsrp: tm_prtctd_m
sttsmplmnt: -0.040
sttsrvsn:cn -0.027  0.082
sttsrpnd:cn -0.044  0.183  0.048
```

```
tm_prtctd_m  0.000 -0.813  0.000   0.000
tm_prtctd_r  0.000  0.000 -0.838   0.000   0.000
```

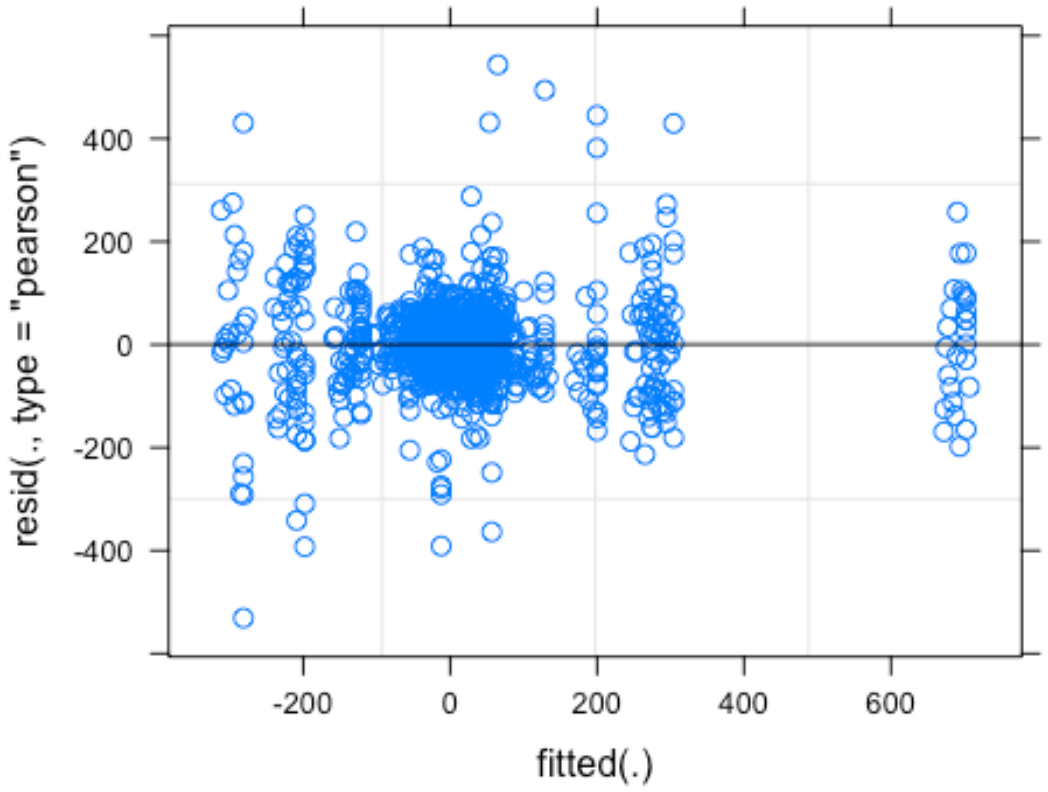

Hypothesis 2: Fisher Participation

```
Linear mixed model fit by REML. t-tests use Satterthwaite's method [
lmerModLmerTest]
Formula: percent_delta ~ status + time_protected_implementation + (1 |
    primary) + (1 | comparison)
   Data: h2_deltas

REML criterion at convergence: 17931.5
```

```
Scaled residuals:
    Min      1Q  Median      3Q     Max
-4.8252 -0.5050 -0.0132  0.5082  4.9711

Random effects:
 Groups     Name        Variance Std.Dev.
 comparison (Intercept)  8114     90.08
 primary    (Intercept) 10625    103.08
 Residual                2987     54.66
Number of obs: 1629, groups:  comparison, 41; primary, 39

Fixed effects:
                              Estimate Std. Error        df t value
(Intercept)                    21.1595    22.0064   60.5866   0.962
statusimplementation:control  -28.3167     5.8484 1561.4882  -4.842
statusrevision:control        -23.5155     4.2037 1566.7013  -5.594
statusreopened:control         -1.6043     5.3711 1571.1777  -0.299
time_protected_implementation   2.3538     0.9515 1560.5579   2.474
                             Pr(>|t|)
(Intercept)                    0.3401
statusimplementation:control  1.41e-06 ***
statusrevision:control        2.62e-08 ***
statusreopened:control          0.7652
time_protected_implementation   0.0135 *
---
```

```
Signif. codes:  0 '***' 0.001 '**' 0.01 '*' 0.05 '.' 0.1 ' ' 1


Correlation of Fixed Effects:

            (Intr) sttsm: sttsrv: sttsrp:

sttsmplmnt: -0.036

sttsrvsn:cn -0.043  0.150

sttsrpnd:cn -0.039  0.183  0.087

tm_prtctd_m  0.000 -0.813  0.000   0.000
```

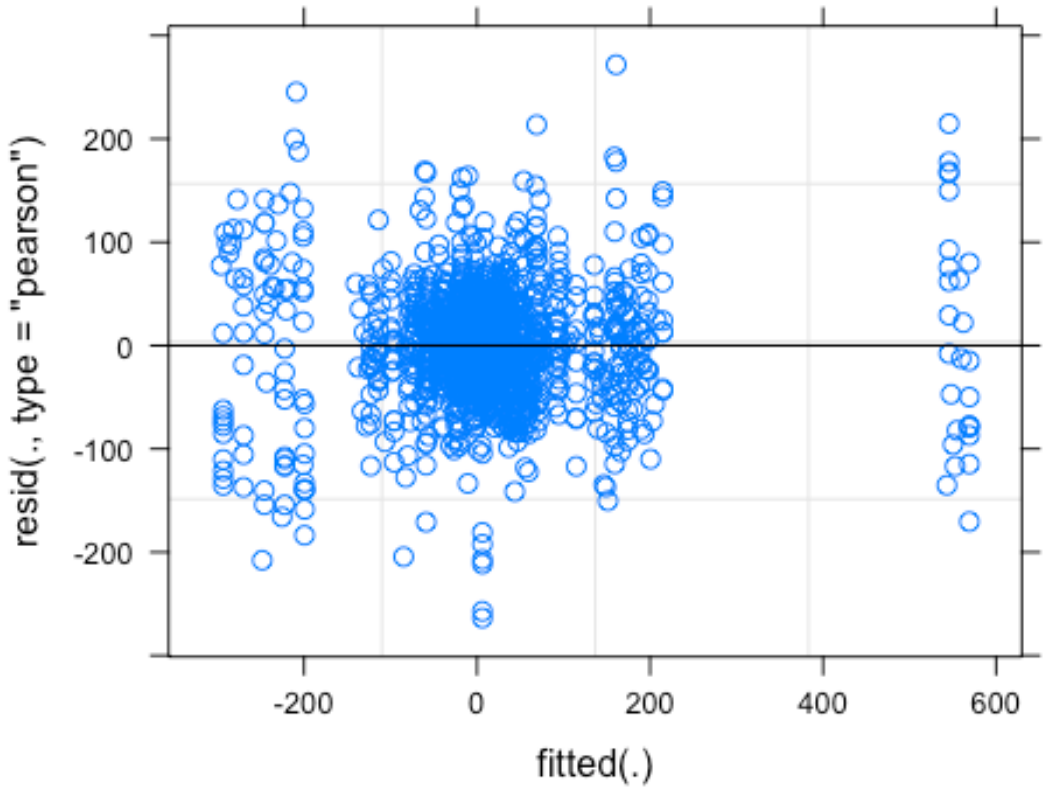

Hypothesis 3: Allocation of Individual Effort

```
Linear mixed model fit by REML. t-tests use Satterthwaite's method [

lmerModLmerTest]
```

```
Formula:
percent_delta ~ status + time_protected_implementation + time_protected_revis
ion +
    (1 | primary) + (1 | comparison)
   Data: h3_deltas_mean

REML criterion at convergence: 12410.6

Scaled residuals:
    Min      1Q  Median      3Q     Max
-4.0153 -0.5129  0.0260  0.5638  4.6961

Random effects:
 Groups     Name        Variance Std.Dev.
 comparison (Intercept)  503     22.43
 primary    (Intercept) 1023     31.98
 Residual               5371     73.29
Number of obs: 1081, groups:  comparison, 41; primary, 39

Fixed effects:
                             Estimate Std. Error       df t value
(Intercept)                    -1.624      7.310   50.639  -0.222
statusimplementation:control   -15.525      9.491 1038.486  -1.636
statusrevision:control         -15.929     13.503 1036.073  -1.180
statusreopened:control          12.351      8.845 1071.693   1.396
```

```
time_protected_implementation    3.324      1.639 1024.211   2.027

time_protected_revision          5.604      2.262 1023.068   2.477

                               Pr(>|t|)

(Intercept)                      0.8251

statusimplementation:control     0.1022

statusrevision:control           0.2384

statusreopened:control           0.1629

time_protected_implementation    0.0429 *

time_protected_revision          0.0134 *

---

Signif. codes:  0 '***' 0.001 '**' 0.01 '*' 0.05 '.' 0.1 ' ' 1


Correlation of Fixed Effects:

            (Intr) sttsm: sttsrv: sttsrp: tm_prtctd_m

sttsmplmnt: -0.165

sttsrvsn:cn -0.096  0.072

sttsrpnd:cn -0.181  0.176  0.052

tm_prtctd_m  0.004 -0.794  0.011  -0.010

tm_prtctd_r -0.004  0.001 -0.863  -0.001  -0.005
```

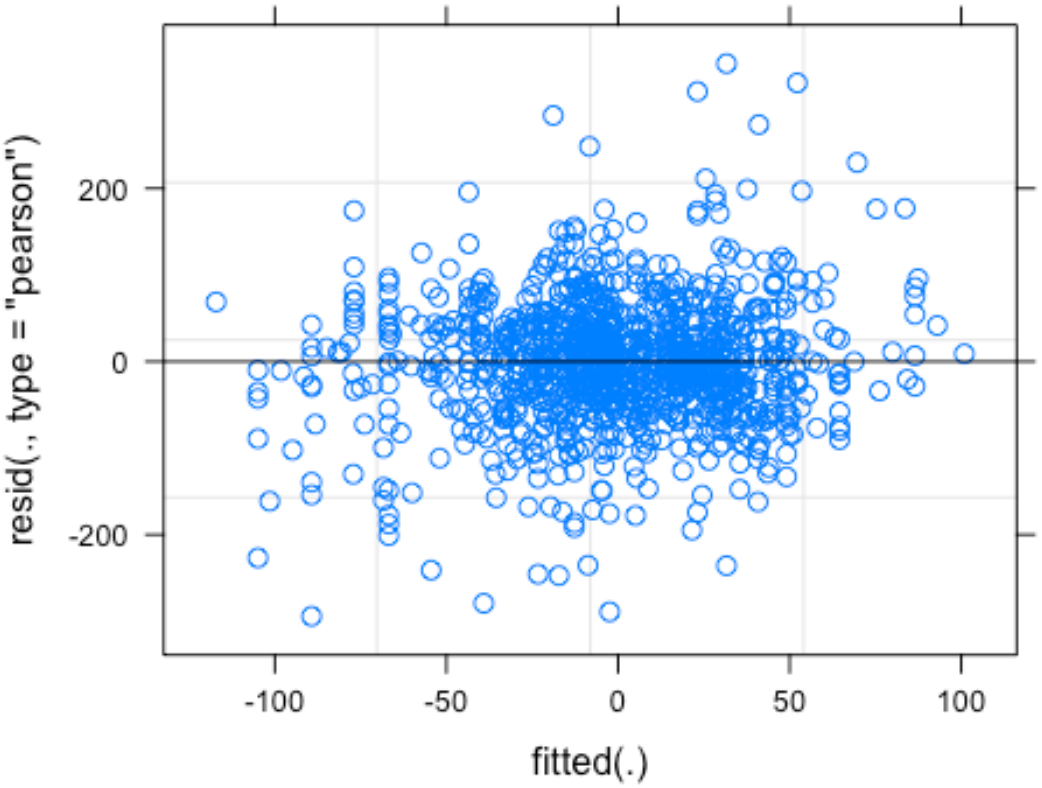

Hypothesis 4: Harvested Biomass

```
Linear mixed model fit by REML. t-tests use Satterthwaite's method [
lmerModLmerTest]
Formula: percent_delta ~ status + (1 | primary) + (1 | comparison)
   Data: h4_deltas

REML criterion at convergence: 19851.4

Scaled residuals:
    Min      1Q  Median      3Q     Max
-7.2428 -0.4164  0.0042  0.4912  4.9339
```

```
Random effects:
 Groups     Name        Variance Std.Dev.
 comparison (Intercept)  1649     40.61
 primary    (Intercept)  1767     42.03
 Residual                10814    103.99
Number of obs: 1629, groups:  comparison, 41; primary, 39

Fixed effects:
                             Estimate Std. Error       df t value Pr(>|t|)
(Intercept)                     8.100     10.279   59.194   0.788 0.433817
statusimplementation:control  -21.559      6.427 1595.703  -3.354 0.000814
statusrevision:control        -46.253      7.907 1611.422  -5.850 5.94e-09
statusreopened:control        -29.052      9.999 1615.663  -2.906 0.003716

(Intercept)
statusimplementation:control ***
statusrevision:control       ***
statusreopened:control       **
---
Signif. codes:  0 '***' 0.001 '**' 0.01 '*' 0.05 '.' 0.1 ' ' 1

Correlation of Fixed Effects:
            (Intr) sttsm: sttsrv:
sttsmplmnt: -0.249
```

```
sttsrvsn:cn -0.181  0.269

sttsrpnd:cn -0.161  0.310  0.110
```

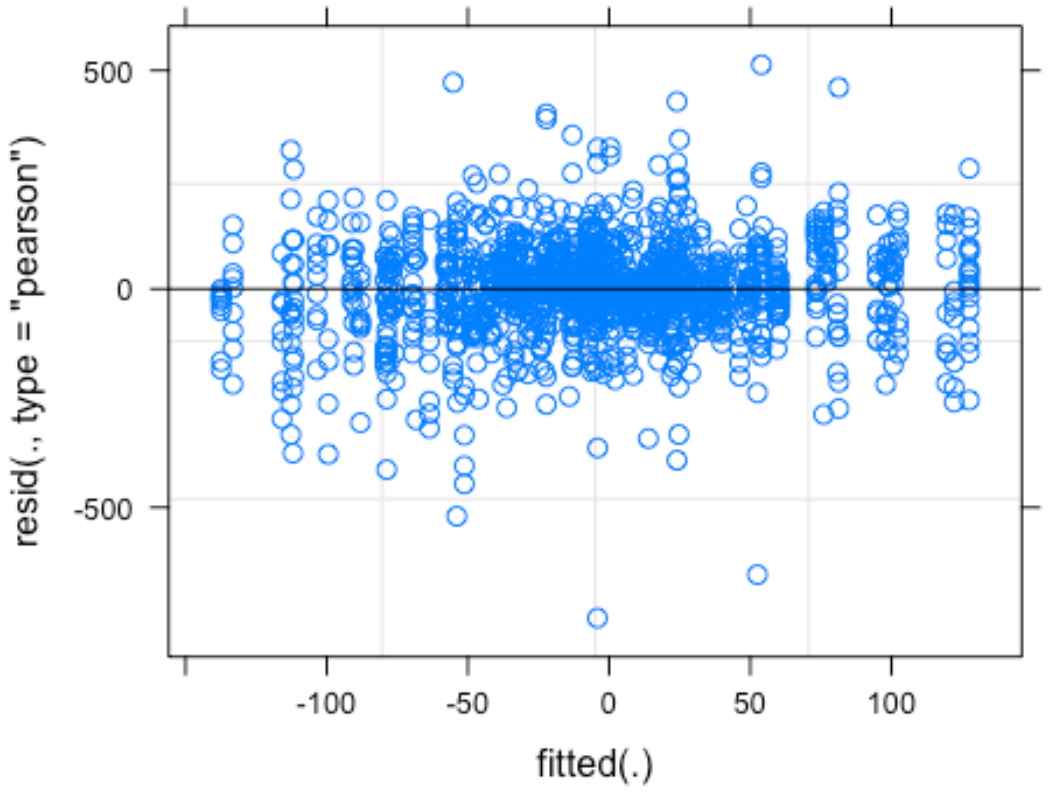

Hypothesis 5: Average Landings per Trip

(Mean of the Annual Median Pounds Per Trip per Fisher)

```
Linear mixed model fit by REML. t-tests use Satterthwaite's method [

lmerModLmerTest]

Formula: percent_delta ~ status + (1 | primary) + (1 | comparison)

   Data: h6_deltas_mean


REML criterion at convergence: 12605.4
```

```
Scaled residuals:
    Min      1Q  Median      3Q     Max
-5.4117 -0.3912 -0.0088  0.4119  7.8638

Random effects:
 Groups     Name        Variance Std.Dev.
 comparison (Intercept) 1305     36.12
 primary    (Intercept)  605     24.60
 Residual                6370     79.81
Number of obs: 1081, groups:  comparison, 41; primary, 39

Fixed effects:
                             Estimate Std. Error       df t value Pr(>|t|)
(Intercept)                    -1.846      8.068   42.284  -0.229  0.82012
statusimplementation:control  -15.120      6.275 1063.724  -2.409  0.01615
statusrevision:control        -23.696      7.408 1060.448  -3.199  0.00142
statusreopened:control        -27.094      9.598 1051.367  -2.823  0.00485

(Intercept)
statusimplementation:control *
statusrevision:control       **
statusreopened:control       **
---
Signif. codes:  0 '***' 0.001 '**' 0.01 '*' 0.05 '.' 0.1 ' ' 1
```

```
Correlation of Fixed Effects:
            (Intr) sttsm: sttsrv:
sttsmplmnt: -0.264
sttsrvsn:cn -0.195  0.252
sttsrpnd:cn -0.178  0.273  0.112
```

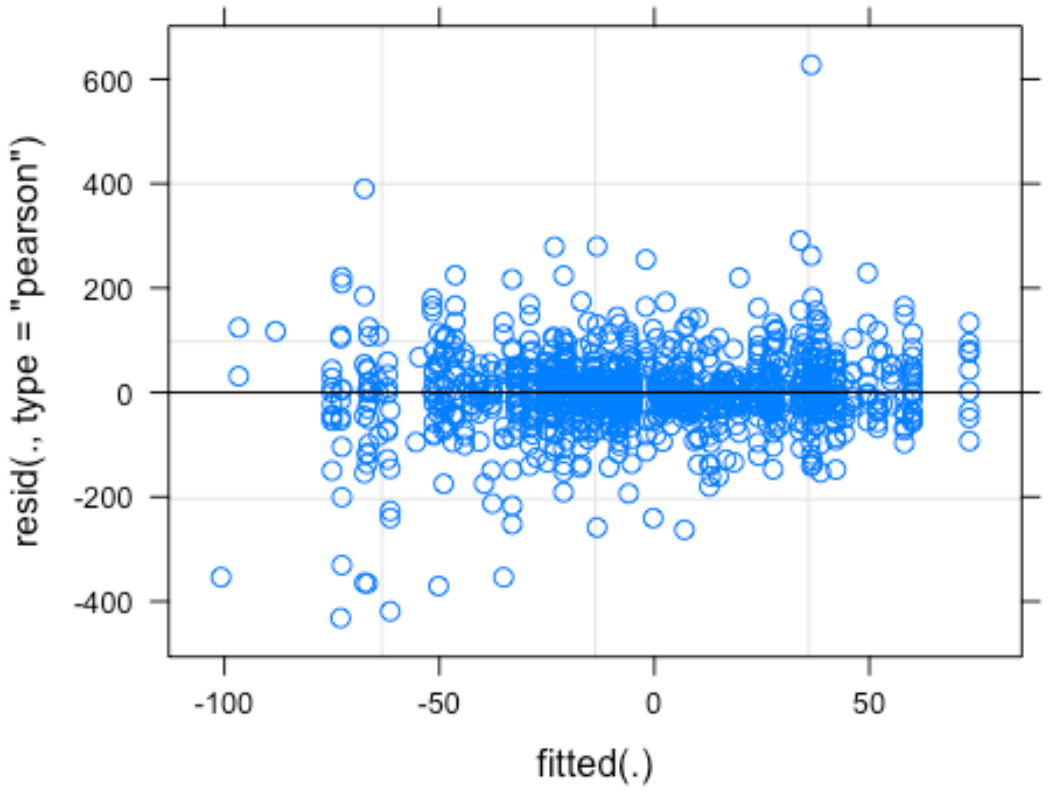

Appendix 5.1. JAGS code for Bayesian hierarchical growth model.

Model 1 incorporates both L_∞ and K individual variability; Model 2 incorporates L_∞ individual variability; Model 3 incorporates K individual variability; and Model 4 incorporates no individual variability. Methodology from Zhang et al. (2009).

```
# Model 1

model{
        for (i in 1:387)    {
                for (j in 2:n[i])   {
                        L[i, j] ~ dnorm(L_Exp[i, j], tau)
                        L_Exp[i, j] <- Linf[i] *(1.0 - exp(-k[i]*(A[i]+t[i, j -1])))
                        L.pred[i, j] ~ dnorm(L_Exp[i, j], tau)
                        p.value[i, j] <- step(L.pred[i, j] - L[i, j])
                }
                L[i, 1] ~ dnorm(L_Exp[i, 1], tau)
                L_Exp[i, 1] <-  Linf[i] *(1.0 - exp(-k[i]*A[i]))
                L.pred[i, 1] ~ dnorm(L_Exp[i, 1], tau)
                p.value[i, 1] <- step(L.pred[i, 1]- L[i, 1])
                Linf[i] ~ dnorm(Linf_mu, Linf_tau)
                k[i] ~ dnorm(k_mu, k_tau) I(0,1)
                A[i] ~ dgamma(shape, rate)
        }
        Linf_std <- sqrt(1/Linf_tau)
        k_std <- sqrt(1/k_tau)
        var <- 1/tau
        Linf_mu ~ dnorm(100, 0.0001)
        Linf_tau ~ dgamma(0.001, 0.0001)
        shape ~ dunif(0, 100)
        rate ~ dunif(0, 100)
        k_mu ~ dbeta(1, 1)
        k_tau ~ dgamma(0.001, 0.0001)
        tau ~ dgamma(0.001, 0.0001)
```

```
}

# Model 2
model{
        for (i in 1: 387)    {
                for (j in 2:n[i])    {
                        L[i, j] ~ dnorm(L_Exp[i, j], tau)
                        L_Exp[i, j] <- Linf[i] *(1.0 - exp(-k*(A[i]+t[i, j -1])))
                        L.pred[i, j] ~ dnorm(L_Exp[i, j], tau)
                        p.value[i, j] <- step(L.pred[i, j] - L[i, j])
                }
                L[i, 1] ~ dnorm(L_Exp[i, 1], tau)
                L_Exp[i, 1] <-  Linf[i] *(1.0 - exp(-k*A[i]))
                L.pred[i, 1] ~ dnorm(L_Exp[i, 1], tau)
                p.value[i, 1] <- step(L.pred[i, 1]- L[i, 1])
                Linf[i] ~ dnorm(Linf_mu, Linf_tau)
                A[i] ~ dgamma(shape, rate)
        }

        Linf_std <- sqrt(1/Linf_tau)
        k_std <- sqrt(1/k_tau)
        var <- 1/tau
        k ~ dnorm(k_mu, k_tau) I(0,1)
        Linf_mu ~ dnorm(100, 0.0001)
        Linf_tau ~ dgamma(0.001, 0.0001)
        shape ~ dunif(0, 100)
        rate ~ dunif(0, 100)
        k_mu ~ dbeta(1, 1)
```

```
        k_tau ~ dgamma(0.001, 0.0001)
        tau ~ dgamma(0.001, 0.0001)
}

# Model 3
model{
        for (i in 1: 387)    {
                for (j in 2:n[i])    {
                        L[i, j] ~ dnorm(L_Exp[i, j], tau)
                        L_Exp[i, j] <- Linf*(1.0 - exp(-k[i]*(A[i]+t[i, j -1])))
                        L.pred[i, j] ~ dnorm(L_Exp[i, j], tau)
                        p.value[i, j] <- step(L.pred[i, j] - L[i, j])
                }
                L[i, 1] ~ dnorm(L_Exp[i, 1], tau)
                L_Exp[i, 1] <-  Linf *(1.0 - exp(-k[i]*A[i]))
                L.pred[i, 1] ~ dnorm(L_Exp[i, 1], tau)
                p.value[i, 1] <- step(L.pred[i, 1]- L[i, 1])
                k[i] ~ dnorm(k_mu, k_tau) I(0,1)
                A[i] ~ dgamma(shape, rate)
        }
        Linf_std <- sqrt(1/Linf_tau)
        k_std <- sqrt(1/k_tau)
        var <- 1/tau
        Linf ~ dnorm(Linf_mu, Linf_tau)
        Linf_mu ~ dnorm(100, 0.0001)
        Linf_tau ~ dgamma(0.001, 0.0001)
        shape ~ dunif(0, 100)
        rate ~ dunif(0, 100)
```

```
        k_mu ~ dbeta(1, 1)
        k_tau ~ dgamma(0.001, 0.0001)
        tau ~ dgamma(0.001, 0.0001)
}

# Model 4
model{
        for (i in 1: 387)    {
                for (j in 2:n[i])    {
                        L[i, j] ~ dnorm(L_Exp[i, j], tau)
                        L_Exp[i, j] <- Linf*(1.0 - exp(-k*(A[i]+t[i, j -1])))
                        L.pred[i, j] ~ dnorm(L_Exp[i, j], tau)
                        p.value[i, j] <- step(L.pred[i, j] - L[i, j])
                }
                L[i, 1] ~ dnorm(L_Exp[i, 1], tau)
                L_Exp[i, 1] <-  Linf *(1.0 - exp(-k*A[i]))
                L.pred[i, 1] ~ dnorm(L_Exp[i, 1], tau)
                p.value[i, 1] <- step(L.pred[i, 1]- L[i, 1])
                A[i] ~ dgamma(shape, rate)
        }
        Linf_std <- sqrt(1/Linf_tau)
        k_std <- sqrt(1/k_tau)
        var <- 1/tau
        k ~ dnorm(k_mu, k_tau) I(0,1)
        Linf ~ dnorm(Linf_mu, Linf_tau)
        Linf_mu ~ dnorm(100, 0.0001)
        Linf_tau ~ dgamma(0.001, 0.0001)
        shape ~ dunif(0, 100)
```

```
        rate ~ dunif(0, 100)
        k_mu ~ dbeta(1, 1)
        k_tau ~ dgamma(0.001, 0.0001)
        tau ~ dgamma(0.001, 0.0001)
}
```

REFERENCES

Literature Cited

Abbot JK., Haynie AC. 2015. What are we protecting? Fisher behavior and the unintended consequences of spatial closures as a fishery management tool. *Ecological Applications* 22:762–777. DOI: https://doi.org/10.1890/11-1319.1.

Afonso P., Graça G., Berke G., Fontes J. 2012. First observations on seamount habitat use of blackspot seabream (Pagellus bogaraveo) using acoustic telemetry. *Journal of Experimental Marine Biology and Ecology* 436–437:1–10. DOI: 10.1016/j.jembe.2012.08.003.

Afonso P., McGinty N., Graça G., Fontes J., Inácio M., Totland A., Menezes G. 2014. Vertical migrations of a deep-sea fish and its prey. *PloS one* 9:1–10. DOI: 10.1371/journal.pone.0097884.

Allen GR. 1985. Fao Species Catalogue Vol . 6 . Snappers of the World. *FAO Fisheries Synopsis* 6:208. DOI: 10.1016/0025-326X(92)90600-B.

Alós J., Palmer M., Balle S., Arlinghaus R. 2016. Bayesian state-space modelling of conventional acoustic tracking provides accurate descriptors of home range behavior in a small-bodied coastal fish species. *Plos One* 11:1–23. DOI: 10.1371/journal.pone.0154089.

Amendment 14 to the fishery management plan for bottomfish and seamount groundfish fisheries of the Western Pacific region 2007. Honolulu, HI.

Andrews AH., DeMartini EE., Brodziak J., Nichols RS., Humphreys RL. 2012. A long-lived life history for a tropical, deepwater snapper (Pristipomoides filamentosus): bomb radiocarbon and lead-radium dating as extensions of daily increment analyses in otoliths. *Canadian Journal of Fisheries and Aquatic Sciences* 69:1850–1869. DOI: 10.1139/f2012-109.

Arnold G., Dewar H. 2001. Electronic tags in marine fisheries research: A 30-year perspective. In: *Electronic Tagging and Tracking in Marine Fisheries*. 7–64. DOI: 10.1007/978-94-017-1402-0_2.

Batista MI., Horta e Costa B., Goncalves L., Erzini K., Caselle JE., Goncalves EJ., Cabral HN. 2015. Assesssment of catches, landings and fishing effort as useful tools for MPA management. *Fisheries Research* 172:197–208.

Bellail R., Bertrand J., Pape O Le., Mahé J., Morin J., Poulard C., Rochet M., Schlaich I., Souplet A., Trenkel V. 2003. A multispecies dynamic indicator-based approach to the assessment of the impact of fishing on fish communities. *ICES CM* 2:1–12.

Benaglia T., Chauveau D., Hunter DR., Young D. 2009. Mixtools: An R package for analyzing finite mixture models. *Journal of Statistical Software* 32:1–29.

Beveridge I., Canals M., Rivera J., Sànchez A. 2012. *Cruise Report RV Ramon Margalef "Ocean Tracking Network-Gibraltar II" (OTN-GIBRALTAR II)*. Barcelona, Spain.

Bohnsack JA. 1998. Application of fishery reserves to reef fisheries management. *Austral Ecology* 23:298–304. DOI: 10.1111/j.1442-9993.1998.tb00734.x.

Börger L., Franconi N., De Michele G., Gantz A., Meschi F., Manica A., Lovari S., Coulson T. 2006. Effects of sampling regime on the mean and variance of home range size estimates. *Journal of Animal Ecology* 75:1393–1405. DOI: 10.1111/j.1365-2656.2006.01164.x.

Botsford LW., Micheli F., Hastings A. 2003. Principles for the design of fishery reserves. *Ecological Applications* 13:25–31. DOI: https://doi.org/10.1890/1051-0761(2003)013[0025:PFTDOM]2.0.CO;2.

Brodziak, J., D. Courtney, L. Wagatsuma, J. O'Malley, H-H. Lee, W. Walsh, A. Andrews, R. Humphreys, and G. DiNardo. 2011. Stock assessment of the main Hawaiian Islands Deep7 bottomfish complex through 2010. U.S. Dep. Commer., NOAA Tech. Memo., NOAA- TM-NMFS-PIFSC-29, 176 p. + Appendix.

Brodziak, J., R. Moffitt, and G. DiNardo. 2009. Hawaiian bottomfish assessment update for 2008. Pacific Islands Fish. Sci. Cent., Natl. Mar. Fish. Serv., NOAA, Honolulu, HI 96822-2396. Pacific Islands Fish. Sci. Cent. Admin. Rep. H-09- 02, 93 p.

Brodziak, J. A. Yau, J. O'Malley, A. Andrews, R. Humphreys, E. DeMartini, M. Pan, M. Parke, and E. Fletcher. 2014. Stock assessment update for the main Hawaiian Islands Deep 7 bottomfish complex through 2013 with projected annual catch limits through 2016. U.S. Dep. Commer., NOAA Tech. Memo., NOAA-TM-NMFS-PIFSC- 42, 61 p. doi:10.7289/V5T151M8

Burman P. 1989. A comparative study of ordinary cross-validation, v-fold cross-validation and the repeated learning-testing methods. *Biometrika* 76:503–514. DOI: 10.1093/biomet/76.3.503.

Cagua F. 2012. Factors Affecting Detection Probability of Acoustic Tags in Coral Reefs. King Abdullah University of Science and Technology. DOI: 10.25781/KAUST-X9EE5.

Cagua EF., Berumen ML., Tyler EHM. 2013. Topography and biological noise determine acoustic detectability on coral reefs. *Coral Reefs* 32:1123–1134. DOI: 10.1007/s00338-013-1069-2.

Cailliet G., Andrews A., Burton E., Watters D., Kline D., Ferry-Graham L. 2001. Age determination and validation studies of marine fishes: Do deep-dwellers live longer? *Experimental Gerontology* 36:739–764. DOI: 10.1016/S0531-5565(00)00239-4.

Christie P. 2004. Marine protected areas as biological successes and social failures in Southeast Asia. *American Fisheries Society Symposium* 42:155–164. DOI: 10.1016/S0002-9610(03)00290-3.

Clark M. 2001. Are deepwater fisheries sustainable? — the example of orange roughy (*Hoplostethus atlanticus*) in New Zealand. *Fisheries Research* 51:123–135. DOI: 10.1016/S0165-7836(01)00240-5.

Comfort CM., Weng K. 2014. Vertical habitat and behaviour of the bluntnose sixgill shark in Hawaii. *Deep-Sea Research Part II*:1–11. DOI: 10.1016/j.dsr2.2014.04.005.

Craig P., Ponwith B., Aitaoto F., Hamm D. 1993. The commercial, subsistence, and recreational fisheries of American Samoa. *Marine Fisheries Review* 55:109–116.

Crossin GT., Heupel MR., Holbrook CM., Hussey NE., Lowerre-Barbieri SK., Nguyen VM., Raby GD., Cooke SJ. 2017. Acoustic telemetry and fisheries management. *Ecological Applications* 27:1031–1049. DOI: 10.1002/eap.1533.

DeMartini EE., Landgraf KC., Ralston S. 1994. *A recharacterizatinon of the age-length and growth relationships of Hawaiian snapper Pristipomoides filamentosus*. Honolulu, HI: U.S. Department of Commerce, National Oceanic and Atmospheric Administration, National Marine Fisheries Service, Southwest Fisheries Science Center.

DeMartini EE., Parrish FA., Ellis DM. 1996. Barotrauma-associated regurgitation of food: Implications for diet studies of Hawaiian pink snapper, Pristipomoides filamentosus (family Lutjanidae). *Fishery Bulletin* 94:250–256.

Division of Aquatic Resources. 2019. *Commercial Marine Landing Database*. Honolulu, HI.

Drazen JC., Haedrich RL. 2012. A continuum of life histories in deep-sea demersal fishes. *Deep-Sea Research Part I: Oceanographic Research Papers* 61:34–42. DOI: 10.1016/j.dsr.2011.11.002.

Dwyer RG., Campbell HA., Irwin TR., Franklin CE. 2015. Does the telemetry technology matter? Comparing estimates of aquatic animal space-use generated from GPS-based and passive acoustic tracking. *Marine and Freshwater Research* 66:654–664. DOI: 10.1071/MF14042.

Edwards JE., Pratt J., Tress N., Hussey NE. 2019. Thinking deeper: Uncovering the mysteries of animal movement in the deep sea. *Deep-Sea Research Part I: Oceanographic Research Papers* 146:24–43. DOI: 10.1016/j.dsr.2019.02.006.

Erisman BE., Allen LG., Claisse JT., Pondella DJ., Miller EF., Murray JH. 2011. The illusion of plenty: Hyperstability masks collapses in two recreational fisheries that target fish spawning aggregations. *Canadian Journal of Fisheries and Aquatic Sciences* 68:1705–1716. DOI: 10.1139/f2011-090.

Eveson JP., Laslett GM., Polacheck T. 2004. An integrated model for growth incorporating tag–recapture, length–frequency, and direct aging data. *Canadian Journal of Fisheries and Aquatic Sciences* 61:292–306. DOI: 10.1139/f03-163.

Eveson JP., Polacheck T., Laslett GM. 2007. Consequences of assuming an incorrect error structure in von Bertalanffy growth models: a simulation study. *Canadian Journal of Fisheries and Aquatic Sciences* 64:602–617. DOI: 10.1139/f07-036.

Fabens AJ. 1965. Properties and fitting of the von Bertalanffy growth curve. *Growth* 29:265–289.

Fisheries in the Western Pacific; bottomfish and seamount groundfish fisheries; management measures in the Main Hawaiian Islands 2008. USA: https://www.federalregister.gov/documents/2008/04/04/08-1093/fisheries-in-the-western-pacific-bottomfish-and-seamount-groundfish-fisheries-management-measures-in.

Francini-Filho RB., Moura RL. 2008. Evidence for spillover of reef fishes from a no-take fishery reserve: An evaluation using the before-after control-impact (BACI) approach. *Fisheries Research* 93:346–356. DOI: 10.1016/j.fishres.2008.06.011.

Francis RICC. 1988. Maximum likelihood estimation of growth and growth variability from tagging data. *New Zealand Journal of Marine and Freshwater Research* 22:43–51. DOI: 10.1080/00288330.1988.9516276.

Friedlander AM., Parrish JD., DeFelice RC. 2002. Ecology of the introduced snapper Lutjanus kasmira (Forsskal) in the reef fish assemblage of a Hawaiian bay. *Journal of Fish Biology* 60:28–48. DOI: 10.1006/jfbi.2001.1808.

Friedlander AM., Stamoulis KA., Kittinger JN., Drazen JC., Tissot BN. 2014. Understanding the Scale of Marine Protection in Hawai'i: From Community-Based Management to the Remote Northwestern Hawaiian Islands. *Advances in Marine Biology* 69:153–203. DOI: 10.1016/B978-0-12-800214-8.00005-0.

Fry GC., Brewer DT., Venables WN. 2006. Vulnerability of deepwater demersal fishes to commercial fishing: Evidence from a study around a tropical volcanic seamount in Papua New Guinea. *Fisheries Research* 81:126–141. DOI: 10.1016/j.fishres.2006.08.002.

Gaines SD., White C., Carr MH., Palumbi SR. 2010. Designing fishery reserve networks for both conservation and fisheries management. *Proceedings of the National Academy of Sciences* 107:18286–18293. DOI: 10.1073/pnas.0906473107.

Gaither MR., Jones S a., Kelley C., Newman SJ., Sorenson L., Bowen BW. 2011. High connectivity in the deepwater snapper Pristipomoides filamentosus (lutjanidae) across the indo-pacific with isolation of the Hawaiian archipelago. *PLoS ONE* 6:1–13. DOI: 10.1371/journal.pone.0028913.

Gaither MR., Toonen RJ., Sorenson L., Bowen BW. 2010. Isolation and characterization of microsatellite markers for the crimson jobfish, pristipomoides filamentosus (Lutjanidae). *Conservation Genetics Resources* 2:169–172. DOI: 10.1007/s12686-009-9119-3.

Gell FR., Roberts CM. 2003. Benefits beyond boundaries: The fishery effects of fishery reserves. *Trends in Ecology and Evolution* 18:448–455. DOI: 10.1016/S0169-5347(03)00189-7.

Gelman A., Rubin DB. 1992. lnference from iterative simulation using multiple sequences. *Statistical Science* 7:457–472. DOI: 10.2307/2246093.

Gillett R. 2011. *Fisheries of the Pacific Islands: Regional and national information*. Bangkok, Thailand.

Gjelland KO., Hedger RD. 2013. Environmental influence on transmitter detection probability in biotelemetry: Developing a general model of acoustic transmission. *Methods in Ecology and Evolution* 4:665–674. DOI: 10.1111/2041-210X.12057.

Glazier, E. 2007. Hawai`i pelagic handline fisheries: History, trends and current status. Impact Assessment, Inc., Pacific Islands Office. Honolulu, HI. 96813. http://www.wpcouncil.org/pelagic/Documents/FinalHandlineBackgroundDocumentCouncil3808.pdf

Gordon JDM., Merrett NR., Haedrich RL. 1995. Environmental and biological aspects of slope dwelling fishes of the North Atlantic slope. In: *Proceedings of NATO Advanced Workshop on deepwater fisheries of the north Atlantic Slope*. DOI: 10.1007/978-94-015-8414-2_1.

Grafton RQ., Kompas T. 2005. Uncertainty and the active adaptive management of fishery reserves. *Marine Policy* 29:471–479. DOI: 10.1016/j.marpol.2004.07.006.

Gray AE. 2016. Fine scale movement of the lustrous pomfret (Eumegistus illustris) at Cross Seamount. University of Hawaii.

Grothues TM. 2009. A review of acoustic telemetry technology and a perspective on its diversification relative to coastal tracking arrays. In: *Tagging and Tracking of Marine Animals with Electronic Devices*. Dordrecht: Springer, 77–90. DOI: 10.1007/978-1-4020-9640-2_5.

Haedrich RL., Merrett NR., Dea NRO. 2001. Can ecological knowledge catch up with deep-water fishing ? A North Atlantic perspective. *Fisheries Research* 51:113–122. DOI: 10.1016/S0165-7836(01)00239-9.

Haight WR. 1989. Trophic relationships, density and habitat associations of deepwater snappers (Lutjanidae) from Penguin Bank, Hawaii. University of Hawaii at Manoa.

Haight WR., Kobayashi DR., Kawamoto KE. 1993. Biology and management of deepwater snappers of the Hawaiian a rchipelago. *Marine Fisheries Review* 55:20–27.

Halpern BS. 2003. The impact of fishery reserves: Do reserves work and does reserve size matter? *Ecological Applications* 13. DOI: 10.1890/1051-0761(2003)013[0117:tiomrd]2.0.co;2.

Hannah RW., Matteson KM. 2007. Behavior of nine species of Pacific rockfish after hook-and-line capture, recompression, and release. *Transactions of the American Fisheries Society* 136:24–33. DOI: 10.1577/T06-022.1.

Hannesson R. 1998. Fishery reserves: What would they accomplish? *Marine Resource Economics* 13:159–170. DOI: 10.1086/mre.13.3.42629231.

Harding K. 2019. Four bottomfish restricted fishing areas (BRFA) to open. *Hawaii Division of Aquatic Resources Bottomfish News* 21:8.

Hardman-Mountford NJ., Polunin NVC., Boulle D. 1997. Can the age of the tropical species be determined by otolith measurement?: a study using Pristipomoides filamentosus (Pisces: Lutjanidae) from the Mahe Plateau, Seychelles. *Naga, The ICLARM Quarterly* 20:27–31.

Hawaii Administrative Rules § 189-3 - License and permit provisions and fees for fishing, fish, and fish products 2015.

Hawaii Administrative Rules §13-261 - Kaho`olawe Island Reserve 2002.

Hawaii Administrative Rules §13-74-20 - Commercial marine license 1998.

Hawaii Reported Landing Tables 2016. *Available at https://www.pifsc.noaa.gov/wpacfin/hi/dar/Pages/hi_data_3.php* (accessed March 23, 2018).

Heupel MR., Semmens JM., Hobday AJ. 2006. Automated acoustic tracking of aquatic animals: Scales, design and deployment of listening station arrays. *Marine and Freshwater Research* 57:113. DOI: 10.1071/MF05091.

Heupel M., Simpfendorfer C., Lowe C. 2005. *Passive acoustic telemetry technology: current applications and future directions*. Sarasota, FL.

Heupel MR., Webber DM. 2012. Trends in acoustic tracking: where are the fish going and how will we follow them? *American Fisheries Society Symposium*:219–231.

Hilborn R., Stokes K., Maguire JJ., Smith T., Botsford LW., Mangel M., Orensanz J., Parma A., Rice J., Bell J., Cochrane KL., Garcia S., Hall SJ., Kirkwood GP., Sainsbury K., Stefansson G., Walters C. 2004. When can fishery reserves improve fisheries management? *Ocean and Coastal Management* 47:197–205. DOI: 10.1016/j.ocecoaman.2004.04.001.

Hixon MA., Johnson DW., Sogard SM. 2014. BOFFFFs: on the importance of conserving old-growth age structure in fishery populations Mark. *ICES Journal of Marine Science* 71:2171–2185. DOI: 10.1093/icesjms/fst200.

Hobday AJ., Pincock D. 2011. Estimating detection probabilities for linear acoustic monitoring arrays. *American Fisheries Society Symposium* 76:1–22.

Hochhalter SJ., Reed DJ. 2011. The effectiveness of deepwater release at improving the survival of discarded yelloweye rockfish. *North American Journal of Fisheries Management* 31:852–860. DOI: 10.1080/02755947.2011.629718.

Horta e Costa B., Batista MI., Gonçalves L., Erzini K., Caselle JE., Cabral HN., Gonçalves EJ. 2013. Fishers' Behaviour in Response to the Implementation of a Marine Protected Area. *PLoS ONE* 8:e65057. DOI: 10.1371/journal.pone.0065057.

Hospital, J., and C. Beavers. 2011. Management of the main Hawaiian Islands bottomfish fishery: fishers' attitudes, perceptions, and comments. Pacific Islands Fish. Sci. Cent., Natl. Mar. Fish. Serv., NOAA, Honolulu, HI 96822-2396. Pacific Islands Fish. Sci. Cent. Admin. Rep. H-11-06, 46 p. + Appendices.

How JR., De Lestang S. 2012. Acoustic tracking: Issues affecting design, analysis and interpretation of data from movement studies. *Marine and Freshwater Research* 63:312–324. DOI: 10.1071/MF11194.

Huvenne VAI., Bett BJ., Masson DG., Le Bas TP., Wheeler AJ. 2016. Effectiveness of a deep-sea cold-water coral Marine Protected Area, following eight years of fisheries closure. *Biological Conservation* 200:60–69. DOI: 10.1016/j.biocon.2016.05.030.

Ikehara WN. 2006. Bottomfish management and monitoring in the main Hawaiian islands. In: *Deep Sea 2003: Conference on the governance and management of deep-sea fisheries. Part 2: Conference poster papers and workshop papers*. 289–300. Available at http://www.fao.org/3/a0337e/A0337E10.htm#ch2.2.8.

James IR. 1991. Estimation of von Bertalanffy growth curve parameters from recapture data. *Biometrics* 47:1519–1530. DOI: 10.2307/2532403.

Jarvis ET., Lowe CG. 2008. The effects of barotrauma on the catch-and-release survival of southern California nearshore and shelf rockfish (Scorpaenidae, Sebastes spp.). *Canadian Journal of Fisheries and Aquatic Sciences* 65:1286–1296. DOI: 10.1139/F08-071.

Jensen AL. 1996. Beverton and Holt life history invariants result from optimal trade-off of reproduction and survival. *Canadian Journal of Fisheries and Aquatic Sciences* 53:820–822. DOI: 10.1139/f95-233.

Johnson P., Potemra J. 2011. Main Hawaiian Islands Multibeam Bathymetry Synthesis: 50-m Bathymetry and Topography.

Kami HT. 1972. The Pristipomoides (Pisces: Lutjanidae) of Guam with notes on their biology and fisheries aspects.

Kelley CD., Ikehara W. 2006. The impacts of bottomfishing on Raita and west St. Rogatien banks in the Northwestern Hawaiian Islands. *Atoll Research Bulletin*:305–318.

Kelley CD., Moffitt R., Smith JR. 2006. Mega- to micro-scale classification and description of bottomfish essential fish habitat on four banks in the Northwestern Hawaiian Islands. *Atoll Research Bulletin*:319–332.

Kelley, C.D., and Moriwake, V.N. 2012. Appendix 3: Essential fish habitat descriptions, Part 1: Hawaiian bottomfish. WPRFMC Final Fish. Manag. plan coral reef Ecosyst. West. 596 Pacific Reg. Vol. III, Essent. Fish Habitat Manag. ment Unit Species 597

Kessel ST., Cooke SJ., Heupel MR., Hussey NE., Simpfendorfer CA., Vagle S., Fisk AT. 2013. A review of detection range testing in aquatic passive acoustic telemetry studies. *Reviews in Fish Biology and Fisheries* 24:199–218. DOI: 10.1007/s11160-013-9328-4.

Kessel ST., Hussey NE., Webber DM., Gruber SH., Young JM., Smale MJ., Fisk AT. 2015. Close proximity detection interference with acoustic telemetry: the importance of considering tag power output in low ambient noise environments. *Animal Biotelemetry* 3:5. DOI: 10.1186/s40317-015-0023-1.

Kikkawa BS. 1984. Maturation, spawning, and fecundity of Opakapaka, Pristipomoides filamentosus, in the Northwest Hawaiian Islands. *Proceedings of the Second Symposium on Resource Investigations in the Northwestern Hawaiian Islands* 2:149–160.

Kimura DK., Shimada AM., Lowe SA. 1993. Estimating von Bertalanffy growth parameters of sablefish Anoplopoma fimbria and Pacific cod Gadus macrocephalus using tag-recapture data. *Fishery Bulletin* 91:271–280.

Kobayashi DR. 2008. Spatial connectivity of Pacific insular species: Insights from modeling and tagging. University of Technology, Sydney, Australia.

Kobayashi DR., Okamoto HY., Oishi FG. 2008. Movement of the deepwater snapper opakapaka, Pristipomoides filamentosus, in Hawaii: Insights from a large-scale tagging program and computer simulation. University of Technology, Sydney, Australia.

Kramer DL., Chapman MR. 1999. Implications of fish home range size and relocation for fishery reserve function. *Environmental Biology of Fishes* 55:65–79. DOI: 10.1023/A:1007481206399.

Kulbicki M., Sarramégna S., Letourneur Y., Wantiez L., Galzin R., Mou-Tham G., Chauvet C., Thollot P. 2007. Opening of an MPA to fishing: Natural variations in the structure of a coral reef fish assemblage obscure changes due to fishing. *Journal of Experimental Marine Biology and Ecology* 353:145–163. DOI: 10.1016/j.jembe.2007.02.021.

Kuznetsova A., Brockhoff PB., Christensen RHB. 2017. lmerTest Package: Tests in Linear Mixed Effects Models . *Journal of Statistical Software* 82. DOI: 10.18637/jss.v082.i13.

Langseth B., Syslo J.,Yau A., Kapur M., and Brodziak J. 2018. Stock assessment for the main Hawaiian Islands deep 7 bottomfish complex in 2018, with catch projections through 2022. NOAA Tech. Memo. NMFS-PIFSC-69, 217 p.

Laslett GM., Eveson JP., Polacheck T. 2002. A flexible maximum likelihood approach for fitting growth curves to tag-recapture data. *Canadian Journal of Fisheries and Aquatic Sciences* 59:976–986. DOI: 10.1139/f02-069.

Lauck T., Clark CW., Mangel M., Munro GR. 1998. Implementing the precautionary principle in fisheries management through fishery reserves. *Ecological Applications* 8:72–78.

Lincoln-Smith MP., Pitt KA., Bell JD., Mapstone BD. 2006. Using impact assessment methods to determine the effects of a fishery reserve on abundances and sizes of valuable tropical invertebrates. *Canadian Journal of Fisheries and Aquatic Sciences* 63:1251–1266. DOI: 10.1139/F06-033.

Lockwood DR., Hastings A., Botsford LW. 2002. The effects of dispersal patterns on fishery reserves: Does the tail wag the dog? *Theoretical Population Biology* 61:297–309. DOI: 10.1006/tpbi.2002.1572.

Luers MA., DeMartini EE., Humphreys RLJ. 2017. Seasonality, sex ratio, spawning frequency and sexual maturity of the opakapaka Pristipomoides filamentosus (Perciformes: Lutjanidae) from the Main Hawaiian Islands: fundamental input to size-at-retention regulations. *Marine and Freshwater Research* 69:325–335. DOI: 10.1071/MF17195.

Lundquist CJ., Granek EF. 2005. Strategies for successful marine conservation: Integrating socioeconomic, political, and scientific factors. *Conservation Biology* 19:1771–1778. DOI: 10.1111/j.1523-1739.2005.00279.x.

Lurton X. 2010. *An Introduction to Underwater Acoustics*. Springer-Verlag Berlin Heidelberg.

Maller RA., Deboer ES. 1988. An analysis of two methods of fitting the von Bertalanffy curve to capture-recapture data. *Marine and Freshwater Research* 39:459–466. DOI: 10.1071/MF9880459.

Mangel M. 2000. Irreducible uncertainties, sustainable fisheries and fishery reserves. *Evolutionary Ecology Research* 2:547–557.

Mateos-Molina D., Schärer-Umpierre MT., Appeldoorn RS., García-Charton JA. 2014. Measuring the effectiveness of a Caribbean oceanic island no-take zone with an asymmetrical BACI approach. *Fisheries Research* 150:1–10. DOI: 10.1016/j.fishres.2013.09.017.

Mathies NH., Ogburn MB., McFall G., Fangman S. 2014. Environmental interference factors affecting detection range in acoustic telemetry studies using fixed receiver arrays. *Marine Ecology Progress Series* 495:27–38. DOI: 10.3354/meps10582.

McFadden D. 1974. Conditional logit analysis of qualitative choice behavior. In: P. Zarembka ed. *Frontiers in Econometrics*. New York: Academic Press, 105–142. DOI: 10.1108/eb028592.

Mclennan MF., Campbell MJ., Sumpton WD. 2014. Surviving the effects of barotrauma: Assessing treatment options and a "natural" remedy to enhance the release survival of line caught pink snapper (Pagrus auratus). *Fisheries Management and Ecology* 21:330–337. DOI: 10.1111/fme.12083.

Medved RJ. 1985. Gastric evacuation in the sandbar shark, Carcharhinus plumbeus. *Journal of Fish Biology* 26:239–253. DOI: 10.1111/j.1095-8649.1985.tb04263.x.

Medwin H., Clay CS. 1998. *Fundementals of Acoustical Oceanography*. San Diego, CA: Academic Press.

Mees CC. 1993. Population biology and stock assessment of Pristopomoides filamentosus. *Journal of Fish Biology* 43:695–708.

Mees CC., Rousseau JA. 1997. The potential yield of the lutjanid fish Pristipomoides filamentosus from the Mahe Plateau, Seychelles: Managing with uncertainty. *Fisheries Research* 33:73–87. DOI: 10.1016/S0165-7836(97)00069-6.

Merritt D., Donovan MK., Kelley C., Waterhouse L., Parke M., Wong K., Drazen JC. 2011. BotCam: A baited camera system for nonextractive monitoring of bottomfish species. *Fishery Bulletin* 109:56–67.

Meyer CG. 2003. An empirical evaluation of the design and function of a small fishery reserve (Waikīkī marine life conservation district). University of Hawaii.

Meyer CG., Papastamatiou YP., Holland KN. 2007. Seasonal, diel, and tidal movements of green jobfish (Aprion virescens, Lutjanidae) at remote Hawaiian atolls: Implications for marine protected area design. *Marine Biology* 151:2133–2143. DOI: 10.1007/s00227-007-0647-7.

Miller KI., Russ GR. 2014. Studies of no-take fishery reserves: Methods for differentiating reserve and habitat effects. *Ocean & Coastal Management* 96:51–60. DOI: 10.1016/j.ocecoaman.2014.05.003.

Minutes of the 158th meeting of the Western Pacific Regional Fishery Management council 2013. Honolulu, HI. Available at: http://www.wpcouncil.org/wp-content/uploads/2013/07/158-CM-Minutes-with-signed-cover-page.pdf

Misa WFXE., Drazen JC., Kelley CD., Moriwake VN. 2013. Establishing species-habitat associations for 4 eteline snappers with the use of a baited stereo-video camera system. *Fishery Bulletin* 111:293–308. DOI: 10.7755/FB.111.4.1.

Moffitt RB. 1993. Deepwater Demersal Fish. In: Wright A, Hill L eds. *Nearshore marine resources of the South Pacific: Information for fisheries development and management*. Canada: Honiara [Solomon Islands], Suva [Fiji]: Forum Fisheries Agency, Institute of Pacific Studies, 73–95.

Moffitt RB., Dinardo G., Brodziak J., Kawamoto K., Quach M., Pan M., Brookins K., Kokubun R., Tam C. 2011. *Bottomfish CPUE standardization workshop*.

Moffitt RB., Kobayashi DR., and Dinardo GT. 2006. Status of the Hawaiian bottomfish stocks, 2004. Pacific Islands Fish. Sci. Cent., Natl. Mar. Fish. Serv., NOAA, Honolulu, HI 96822-2396. Pacific Islands Fish. Sci. Cent. Admin. Rep. H-06-01

Moffitt RB., Parrish FA. 1996. Habitat and life history of juvenile Hawaiian pink snapper, Pristipomoides filamentosus. *Pacific Science* 50:371–381.

Moore C., Drazen J., Kelley C., Misa W. 2013. Deepwater marine protected areas of the main Hawaiian Islands: establishing baselines for commercially valuable bottomfish populations. *Marine Ecology Progress Series* 476:167–183. DOI: 10.3354/meps10132.

Moore C., Drazen JC., Radford BT., Kelley C., Newman SJ. 2016. Improving essential fish habitat designation to support sustainable ecosystem-based fisheries management. *Marine Policy* 69:32–41. DOI: 10.1016/j.marpol.2016.03.021.

Morato T., Watson R., Pitcher TJ., Pauly D. 2006. Fishing down the deep. *Fish and Fisheries* 7:24–34. DOI: 10.1111/j.1467-2979.2006.00205.x.

Murphy HM., Jenkins GP. 2010. Observational methods used in marine spatial monitoring of fishes and associated habitats: a review. *Marine and Freshwater Research* 61:236. DOI: 10.1071/mf09068.

National Marine Fisheries Service. 2005. *Final Environmental Impact Statement - Seamount and Groundfish Fisheries in the Western Pacific Region - Chapter 3 Affected Enviornment*. Honolulu, HI.

Newman SJ., Cappo M., Williams DMB. 2000. Age, growth and mortality of the stripey, Lutjanus carponotatus (Richardson) and the brown-stripe snapper, L. vitta (Quoy and Gaimard) from the central Great Barrier Reef, Australia. *Fisheries Research* 48:263–275. DOI: 10.1016/S0165-7836(00)00184-3.

Newman SJ., Dunk IJ. 2002. Growth, age validation, mortality, and other population characteristics of the red emperor snapper, Lutjanus sebae (Cuvier, 1828), off the Kimberley coast of north-western Australia. *Estuarine, Coastal and Shelf Science* 55:67–80. DOI: 10.1006/ecss.2001.0887.

Newman SJ., Wakefield CB., Williams AJ., O'Malley JM., Nicol SJ., DeMartini EE., Halafihi T., Kaltavara J., Humphreys RL., Taylor BM., Andrews AH., Nichols RS. 2015. International workshop on methodological evolution to improve estimates of life history parameters and fisheries management of data-poor deep-water snappers and groupers. *Marine Policy* 60:182–185. DOI: 10.1016/j.marpol.2015.06.020.

Newman SJ., Williams AJ., Wakefield CB., Nicol SJ., Taylor BM., O'Malley JM. 2016. Review of the life history characteristics, ecology and fisheries for deep-water tropical demersal fish in the Indo-Pacific region. *Reviews in Fish Biology and Fisheries* 26:537–562. DOI: 10.1007/s11160-016-9442-1.

Nichols RS. 2019. Sex-specific growth and longevity of "Ehu", Etelis carbunculus (Family lutjanidae) within the Hawaiian archipelago. University of Hawaii.

Norse EA., Brooke S., Cheung WWL., Clark MR., Ekeland I., Froese R., Gjerde KM., Haedrich RL., Heppell SS., Morato T., Morgan LE., Pauly D., Sumaila R., Watson R. 2012. Sustainability of deep-sea fisheries. *Marine Policy* 36:307–320. DOI: 10.1016/j.marpol.2011.06.008.

O'Dor R., Lindholm J., Oxenford H., Parsons D. 2004. Acoustic Tracking of Fish : How Continuous Data on Fish Movement Could Change the Planning of MPAs. *MPA news* 5:1–6.

O'Malley J. 2015. A Review of the Cooperative Hawaiian Bottomfish Tagging Program of the Pacific Islands Fisheries Science Center and the Pacific Islands Fisheries Group. Pacific Islands Fish. Sci. Cent., Natl. Mar. Fish. Serv., NOAA, Honolulu, HI 96818-5007. Pacific Islands Fish. Sci. Cent. Admin. Rep. H-15-05, 36 p. doi:10.7289/V59W0CF7

Oishi FG. 1994. *Opakapaka Resource Assessment 1993 to 1994*. Honolulu, HI.

Oishi FG. 1995. *Opakapaka Resource Assessment 1994 to 1995*. Honolulu, HI.

Okamoto HY. 1993. *Develop opakapaka (pink snapper) tagging techniques to assess movement behavior*. Honolulu, HI.

Osenberg CW., Schmitt RJ., Holbrook SJ., Abu-Saba KE., Flegal AR. 1994. Detection of environmental impacts: Natural variability, effect size, and power analysis. *Ecological Applications* 4:16–30. DOI: 10.2307/1942111.

Otis D., Burnham, Kenneth., White, Gary., Anderson, David. 1978. Statistical inference from capture data on closed animal populations. *Wildlife Monographs* 62:3–135.

Oyafuso ZS., Drazen JC., Moore CH., Franklin EC. 2017. Habitat-based species distribution modelling of the Hawaiian deepwater snapper-grouper complex. *Fisheries Research* 195:19–27. DOI: 10.1016/j.fishres.2017.06.011.

Oyafuso ZS., Leung PS., Franklin EC. 2019. Evaluating bioeconomic tradeoffs of fishing reserves via spatial optimization. *Marine Policy* 100:163–172. DOI: 10.1016/j.marpol.2018.11.016.

Palmer MJ., Phillips BF., Smith GT. 1991. Application of nonlinear models with random coefficients to growth data. *Biometrics* 47:623–635. DOI: 10.2307/2532151.

Palumbi SR. 2001. The ecology of marine protected areas. In: *Marine community ecology*. 509–530.

Palumbi SR. 2004. Fishery reserves and ocean neighborhoods: The spatial scale of marine populations and their management. *Annual Review of Environment and Resources* 29:31–68. DOI: 10.1146/annurev.energy.29.062403.102254.

Pante E., Simon-Bouhet B. 2013. Marmap: A package for importing, plotting and analyzing bathymetric and topographic data in R. *PLoS ONE* 8:e73051. DOI: 10.1371/journal.pone.0073051.

Parke M. 2007. Linking Hawaii Fisherman Reported Commercial Bottomfish Catch Data to Potential Bottomfish Habitat and Proposed Restricted Fishing Areas using GIS and Spatial Analysis, NOAA Technical Memorandum NMFS-PIFSC-11. Honolulu, HI.

Parker SJ., McElderry HI., Rankin PS., Hannah RW. 2006. Buoyancy Regulation and Barotrauma in Two Species of Nearshore Rockfish. *Transactions of the American Fisheries Society* 135:1213–1223. DOI: 10.1577/T06-014.1.

Parrish FA., Hayman NT., Kelley C., Boland RC. 2015. Acoustic tagging and monitoring of cultured and wild juvenile crimson jobfish (Pristipomoides filamentosus) in a nursery habitat. *Fishery Bulletin* 113:231–241. DOI: 10.7755/FB.113.3.1.

Pedersen MW., Burgess G., Weng KC. 2014. A quantitative approach to static sensor network design. *Methods in Ecology and Evolution* 5:1043–1051. DOI: 10.1111/2041-210X.12255.

Pedersen MW., Weng KC. 2013. Estimating individual animal movement from observation networks supplemental. *Methods in Ecology and Evolution* 4:920–929. DOI: 10.1111/2041-210X.12086.

Pelletier D., Claudet J., Ferraris J., Benedetti-Cecchi L., Garcìa-Charton JA. 2008. Models and indicators for assessing conservation and fisheries-related effects of marine protected areas. *Canadian Journal of Fisheries and Aquatic Sciences* 65:765–779. DOI: 10.1139/f08-026.

Pilling GM. 2000. Validation of annual growth increments in the otoliths of the lethrinid Lethrinus mahsena and the lutjanid Aprion virescens from sites in the tropical Indian Ocean, with notes on the nature of growth increments in Pristipomoides filamentosus. *Fishery Bulletin* 98:600–611.

Pincock D. 2008. *Understanding the Performance of VEMCO 69 kHz Single Frequency Acoustic Telemetry*. Halifax, Nova Scotia, Canada.

Pincock DG. 2012. *Application Note False Detections : What They Are and How to Remove Them from Detection Data*. Halifax, Nova Scotia, Canada.

Piraino MN., Szedlmayer ST. 2014. Fine-scale movements and home ranges of red snapper around artificial reefs in the Northern Gulf of Mexico. *Transactions of the American Fisheries Society* 143:988–998. DOI: 10.1080/00028487.2014.901249.

Planes S., Jones GP., Thorrold SR. 2009. Larval dispersal connects fish populations in a network of marine protected areas. *Proceedings of the National Academy of Sciences of the United States of America* 106:5693–5697. DOI: 10.1073/pnas.0808007106.

Plummer M. 2003. JAGS: A program for analysis of Bayesian graphical models using Gibbs sampling. In Proceedings of the 3rd international workshop on distributed statistical computing. In: *Proceedings of the 3rd international workshop on distributed statistical computing. Vol. 124.*

Polovina JJ. 1987. Assessment and management of deepwater bottom fishes in Hawaii and the Marianas. *Tropical snappers and groupers: Biology and fisheries management*:505–532.

Pomeroy RS., Watson LM., Parks JE., Cid GA. 2005. How is your MPA doing? A methodology for evaluating the management effectiveness of marine protected areas. *Ocean and Coastal Management* 48:485–502. DOI: 10.1016/j.ocecoaman.2005.05.004.

Pooley SG. 1993. Economics and Hawaii's marine fisheries. *Marine Fisheries Review* 55:93–101.

Pribyl AL., Schreck CB., Parker SJ., Weis VM. 2012. Identification of biomarkers indicative of barotrauma and recovery in black rockfish Sebastes melanops. *Journal of Fish Biology* 81:181–196. DOI: 10.1111/j.1095-8649.2012.03322.x.

R Core Team. 2014. R: A Language and Environment for Statistical Computing.

Radtke RL. 1987. Age and growth information available from the otoliths of the Hawaiian snapper, Pristipomoides filamentosus. *Coral Reefs* 6:19–25. DOI: 10.1007/BF00302208.

Ralston S. 1987. Mortality Rates of Snappers and Groupers. In: Polovina JJ, Ralston S V. eds. *Tropical Snappers and Groupers: Biology and Fisheries Management*. Boulder, Colorado: Westview Press, 375–404.

Ralston S., Miyamoto GT. 1983. Analyzing the width of daily otolith increments to age the Hawaiian snapper, Pristipomoides filamentosus. *Fishery Bulletin* 81:523–535.

Ralston SVD., Polovina J. 1982. A multispecies analyis of the commercial deep-sea handline fishery in Hawaii. *Fishery Bulletin* 80:435–448.

Ralston S V., Williams HA. 1988. *Depth distributions, growth, and mortality of deep slope fishes from the Mariana archipelago*.

Rankin PS., Hannah RW., Blume MTO., Miller-Morgan TJ., Heidel JR. 2017. Delayed effects of capture-induced barotrauma on physical condition and behavioral competency of recompressed yelloweye rockfish, Sebastes ruberrimus. *Fisheries Research* 186:258–268. DOI: 10.1016/j.fishres.2016.09.004.

Richards BL., Smith SG., Ault JS., DiNardo GT., Kobayashi DR., Domokos R., Anderson J., Taylor J., Misa W., Giuseffi L., Rollo A., Merritt D., Drazen JC., Clarke ME., and Tam C. 2016. Design and Implementation of a Bottomfish Fishery-independent Survey in the Main Hawaiian Islands. U.S. Dep. Commer., NOAA Tech. Memo., NOAA-TM-NMFS-PIFSC-53, 54p. doi:10.7289/V5RR1W87.

Richards BL, Smith JR, Smith SG, Ault JS, Kelley CD, Moriwake VN. 2017. A five-meter resolution multi-beam bathymetric and backscatter synthesis for the Main Hawaiian Islands. Available at http://www.soest.hawaii.edu/HMRG/multibeam/index.php

Rife AN., Aburto-Oropeza O., Hastings PA., Erisman B., Ballantyne F., Wielgus J., Sala E., Gerber L. 2013. Long-term effectiveness of a multi-use marine protected area on reef fish assemblages and fisheries landings. *Journal of Environmental Management* 117:276–283. DOI: 10.1016/j.jenvman.2012.12.029.

Roach JP., Hall KC., Broadhurst MK. 2011. Effects of barotrauma and mitigation methods on released Australian bass Macquaria novemaculeata. *Journal of Fish Biology* 79:1130–1145. DOI: 10.1111/j.1095-8649.2011.03096.x.

Roberts CM., Branch G., Bustamante RH., Castilla JC., Dugan J., Halpern BS., Lafferty KD., Leslie H., Lubchenco J., Mcardle D., Ruckelshaus M., Warner RR. 2014. Application of ecological criteria in selecting fishery reserves and developing reserve networks. *Ecological Society of America* 13.

Rochet M-J., Trenkel VM. 2003. Which community indicators can measure the impact of fishing? A review and proposals. *Canadian Journal of Fisheries and Aquatic Sciences* 60:86–99. DOI: 10.1139/f02-164.

Rogers BL., Lowe CG., Fernández-Juricic E. 2011. Recovery of visual performance in rosy rockfish (Sebastes rosaceus) following exophthalmia resulting from barotrauma. *Fisheries Research* 112:1–7. DOI: 10.1016/j.fishres.2011.08.001.

Rossiter JS., Levine A. 2014. What makes a "successful" marine protected area? The unique context of Hawaii's fish replenishment areas. *Marine Policy* 44:196–203. DOI: 10.1016/j.marpol.2013.08.022.

Russ GR. 2002. Yet Another Review of Fishery reserves as Reef Fishery Management Tools. In: *Coral Reef Fishes*. Elsevier, 421–443. DOI: 10.1016/B978-012615185-5/50024-4.

Russell ES. 1931. Some theoretical considerations on the "overfishing" problem. *ICES Journal of Marine Science* 6:3–20. DOI: 10.2118/941216-g.

Russell ES. 1942. *The overfishing problem*. London: Cambridge University Press.

Sackett DK., Drazen JC., Moriwake VN., Kelley CD., Schumacher BD., Misa WFXE. 2014. Marine protected areas for deepwater fish populations: An evaluation of their effects in Hawai'i. *Marine Biology* 161:411–425. DOI: 10.1007/s00227-013-2347-9.

Sackett DK., Kelley CD., Drazen JC. 2017. Spilling over deepwater boundaries: Evidence of spillover from two deepwater restricted fishing areas in Hawaii. *Marine Ecology Progress Series* 568:175–190. DOI: 10.3354/meps12049.

Sale PF., Cowen RK., Danilowicz BS., Jones GP., Kritzer JP., Lindeman KC., Planes S., Polunin NVC., Russ GR., Sadovy YJ., Steneck RS. 2005. Critical science gaps impede use of no-take fishery reserves. *Trends in Ecology and Evolution* 20:74–80. DOI: 10.1016/j.tree.2004.11.007.

Schadt S., Knauer F., Kaczensky P., Revilla E., Wiegand T., Trepl L. 2002. Rule-based assessment of suitable habitat and patch connectivity for the Eurasian lynx. *Ecological Applications* 12:1469–1483. DOI: 10.1890/1051-0761(2002)012[1469:RBAOSH]2.0.CO;2.

Scherrer SR., Rideout BP., Giorli G., Nosal E-M., Weng KC. 2018. Depth- and range-dependent variation in the performance of aquatic telemetry systems: understanding and predicting the susceptibility of acoustic tag–receiver pairs to close proximity detection interference. *PeerJ* 6:e4249. DOI: 10.7717/peerj.4249.

Shaklee JB., Samollow PB. 1984. Genetic variation and population structure in a deepwater snapper, Pristipomoides filamentosus, in the Hawaiian Archipelago. *Fishery Bulletin* 82:703–713.

Simpfendorfer CA., Heupel MR., Collins AB. 2008. Variation in the performance of acoustic receivers and its implication for positioning algorithms in a riverine setting. *Canadian Journal of Fisheries and Aquatic Sciences* 65:482–492. DOI: 10.1139/f07-180.

Slijkerman D., Tamis J. 2015. Fisheries displacement effects related to closed areas: a literature review of relevant aspects. *IMARES report* C170/15:52.

Smith JR. 2016. *Multibeam backscatter and bathymetry synthesis for the Main Hawaiian Islands, Final Technical Report*.

Smith MD., Zhang J., Coleman FC. 2006. Effectiveness of fishery reserves for large-scale fisheries management. *Canadian Journal of Fisheries and Aquatic Sciences* 63:153–164. DOI: 10.1139/f05-205.

Spalding S. 2006. History of the Hawaii bottomfish fishery. *Hawaii Fishing News*:16–18.

Starr R., Heine JN., Johnson K a. 2000. Techniques for tagging and tracking deepwater rockfishes. *North American Journal of Fisheries Management* 20:597–609. DOI: 10.1577/1548-8675(2000)020<0597:TFTATD>2.3.CO;2.

Stevenson TC., Tissot BN., Walsh WJ. 2013. Socioeconomic consequences of fishing displacement from marine protected areas in Hawaii. *Biological Conservation* 160:50–58. DOI: 10.1016/j.biocon.2012.11.031.

Stickel LF. 1954. A comparison of certain methods of measuring ranges of small mammals. *Journal of Mammalogy* 35:1–15. DOI: 10.2307/1376067.

Stumpf WA., Mohr CO. 1962. Linearity of home ranges of California mice and other animals. *The Journal of Wildlife Management* 26:149–154.

Su Y., Yajima M. 2012. R2jags: A Package for Running JAGS from R.

Thiault L., Osenberg CW., Claudet J. 2017. Progressive-Change BACIPS: a flexible approach for environmental impact assessment. DOI: 10.1111/2041-210X.12655.

Thorson JT., Munch SB., Cope JM., Gao J. 2017. Predicting life history parameters for all fishes worldwide. *Ecological Applications* 27:2262–2276. DOI: 10.1002/eap.1606.

Tinhan T., Erisman B., Aburto-Oropeza O., Weaver A., Vázquez-Arce D., Lowe CG. 2014. Residency and seasonal movements in Lutjanus argentiventris and Mycteroperca rosacea at Los Islotes Reserve, Gulf of California. *Marine Ecology Progress Series* 501:191–206. DOI: 10.3354/meps10711.

Tsuchiya T., Futa K., Goto S., Yamamoto F., Shimizu E. 2015. Analysis of long-distance propagation characteristic by an air gun source. In: *Proceedings of Symposium on Ultrasonic Electronics*. Tokyo, Japan, 2–3.

Uchiyama JH., Tagami DT. 1984. Life history, distribution, and abundance of bottomfishes in the Northwestern Hawaiian Islands. In: Grigg RW, Tanoue KY eds. *Proceedings of the Second Symposium on Resource Investigations in the Northwestern Hawaiian Islands*. 229–247.

Uehara M., Ebisawa A., Ohta I., Aomuma Y. 2019. Effectiveness of deepwater marine protected areas: Implication for Okinawan demersal fisheries management. *Fisheries Research* 215:123–130. DOI: 10.1016/j.fishres.2019.03.018.

Underwood AJ. 1992. Beyond BACI: the detection of environmental impacts on populations in the real, but variable, world. *Journal of Experimental Marine Biology and Ecology* 161:145–178. DOI: 10.1016/0022-0981(92)90094-Q.

Urick RJ. 1967. *Principles of Underwater Sound for Engineers*. Tata McGraw-Hill Education. DOI: 10.1029/2003JD004173.Aires.

Vandeperre F., Higgins RM., Sánchez-Meca J., Maynou F., Goñi R., Martín-Sosa P., Pérez-Ruzafa A., Afonso P., Bertocci I., Crec'hriou R., D'Anna G., Dimech M., Dorta C., Esparza O., Falcón JM., Forcada A., Guala I., Le Direach L., Marcos C., Ojeda-Martínez C., Pipitone C., Schembri PJ., Stelzenmüller V., Stobart B., Santos RS. 2011. Effects of no-take area size and age of marine protected areas on fisheries yields: A meta-analytical approach. *Fish and Fisheries* 12:412–426. DOI: 10.1111/j.1467-2979.2010.00401.x.

Vaz AC. 2012. Here today, gone tomorrow: flow variability, larval dispersal and fisheries management in Hawai`i. University of Hawaii.

Vemco. 2015.About VEMCO. *Available at http://vemco.com/about/* (accessed June 24, 2015).

Vemco. 2017. Collision Calculator. *Available at https://vemco.com/collision-calculator/* (accessed October 20, 2017).

Wakefield CB., O'Malley JM., Williams AJ., Taylor BM., Nichols RS., Halafihi T., Humphreys RL., Kaltavara J., Nicol SJ., Newman SJ. 2017. Ageing bias and precision for deep-water snappers: Evaluating nascent otolith preparation methods using novel multivariate comparisons among readers and growth parameter estimates. *ICES Journal of Marine Science* 74:193–203. DOI: 10.1093/icesjms/fsw162.

Wang Y-G., Thomas MR., Somers IF. 1995. A maximum likelihood approach for estimating growth from tag–recapture data. *Canadian Journal of Fisheries and Aquatic Sciences* 52:252–259. DOI: 10.1139/f95-025.

Weng KC. 2013. A pilot study of deepwater fish movement with respect to fishery reserves. *Animal Biotelemetry* 1:17. DOI: 10.1186/2050-3385-1-17.

Western Pacific Regional Fishery Management Council. 2009. *Fishery Ecosystem Plan for the Hawaii Archipelago*. Honolulu, HI.

Western Pacific Regional Fishery Management Council. 2014. *WPRFMC Five-year Research Priorities under the MSRA 2014-2019*. Honolulu, HI.

Williams A., Bax NJ., Kloser RJ., Althaus F., Barker B., Keith G. 2009. Australia's deep-water reserve network: Implications of false homogeneity for classifying abiotic surrogates of biodiversity. *ICES Journal of Marine Science* 66:214–224. DOI: 10.1093/icesjms/fsn189.

Williams, A.J., Nicol, S.J., Bentley, N., Starr, P.J., Newman, S.J., McCoy, M.A., Kinch, J., Williams, P.G., Magron, F., Pilling, G.M., Bertram, I., and Batty, M. 2012. International workshop on developing strategies for monitoring data-limited deepwater demersal line fisheries in the Pacific Ocean. Rev. Fish Biol. Fish. 22:527–531. https://doi.org/10.1007/s11160-011-9234-6.

Wood SN. 2011. Fast stable restricted maximum likelihood and marginal likelihood estimation of semiparametric generalized linear models. *Journal of the Royal Statistical Society* 73:3–36.

WPRFMC five-year research priorities under the MSRA 2014-2019. 2014.Western Pacific Regional Fishery Management Council, Honolulu, HI. 12 p.

Wright S. 1931. Evolution in Mendelian populations. *Genetics* 16:97–159.

Zeller D., Darcy M., Booth S., Lowe MK., Martell S. 2008. What about recreational catch? Potential impact on stock assessment for Hawaii's bottomfish fisheries. *Fisheries Research* 91:88–97. DOI: 10.1016/j.fishres.2007.11.010.

Zhang Z., Lessard J., Campbell A. 2009. Use of Bayesian hierarchical models to estimate northern abalone, Haliotis kamtschatkana, growth parameters from tag-recapture data. *Fisheries Research* 95:289–295. DOI: 10.1016/j.fishres.2008.09.035.

Ziemann DA., Kelley C. 2004. *Detection and Documentation of Bottomfish Spillover*. Oceanic Institute, Waimanalo, HI

Ziemann DA., Kelley CD. 2007. *Detection and Documentation of Bottomfish Spillover from the Kahoolawe Island Reserve*. Oceanic Institute, Waimanalo, HI

Ziemann DA., Kelley CD. 2008. *Detection and Documentation of Bottomfish Spillover from the Kahoolawe Island Reserve, Phase III*. Oceanic Institute, Waimanalo, HI